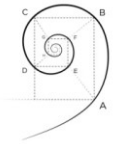

DOTTORATO DI MEDICINA MOLECOLARE E TRASLAZIONALE

CICLO XXXII

Anno Accademico 2018/2019

MED/04

CHARACTERIZATION AND SPATIAL LOCALIZATION OF T-REGULATORY SUBSETS IN HUMAN TUMORS

Dottoranda : Martina MARTINOVIC

Matricola N° : R11805

TUTORE : prof. Sergio ABRIGNANI

COORDINATORE DEL DOTTORATO: prof. Michele SAMAJA

Dichiarazione **di integrità della ricerca**

Il seguente lavoro è stato svolto nel rispetto dei principi su cui si fonda l'integrità della ricerca, redatti nel Codice di condotta europeo per l'integrità della ricerca, da ALLEA - All European Academies.

I principi sono i seguenti:

• Affidabilità nel garantire la qualità della ricerca: si riflette nella progettazione, nella metodologia, nell'analisi e nell'uso delle risorse.

• Onestà nello sviluppare, condurre, rivedere, riferire e comunicare la ricerca in maniera trasparente, equa, completa e obiettiva.

• Rispetto per i colleghi, i partecipanti alla ricerca, la società, gli ecosistemi, il patrimonio culturale e l'ambiente.

• Responsabilità per la ricerca dall'idea iniziale alla pubblicazione, per la sua gestione e organizzazione, per la formazione, la supervisione e il tutoraggio, e infine per i suoi impatti più ampi.

INDEX

SOMMARIO

È ormai evidente che il ruolo del microambiente tumorale è di cruciale importanza nella progressione tumorale. In questo contesto i linfociti T hanno attirato notevole attenione da parte degli scienziati, poiché essendo in grado di infiltrare i tumori, possono esercitare le proprie funzioni all'interno dei tumori stessi, promuovendone l'eradicazione, oppure, in determinate circostanze, favorendone l'espansione, tramite l'istituzione di un ambiente immunosoppressivo.

Le cellule $CD8^+$ T sono da sempre state considerate come la componente principale infiltrante i tumori, in grado di reprimerne la proliferazione tramite il rilascio di molecole citotossiche. Per questa ragione sono stati condotti diversi studi sulle $CD8^+$ infiltranti, con l'obiettivo finale di promuovere le funzioni finalizzate all'eliminazione delle cellule tumorali.

Al contrario il ruolo delle cellule $CD4^+$ T è stato per un lungo periodo sottovalutato nel contesto dell'immunologia dei tumori. È risaputo che cellule $CD4^+$ sono in grado di produrre segnali verso le altre componenti cellulari del sistema immunitario, che a loro volta portano all'attivazione di risposte anti-tumorali; tuttavia esistono sottoclassi delle cellule $CD4^+$, le cellule T regolatorie, il cui ruolo sembra essere quello di promuovere la crescita tumorale.

Le cellule del sistema immunitario localizzate nei pressi della massa tumorale, sono continuamente esposte a innumerevoli segnali, provenienti da cellule tumorali, tessuti circostanti e perfino dalle diverse componenti del sistema immunitario stesso.

Tutti questi segnali molecolari, possono causare cambiamenti nell'identità e differenziamento delle cellule presenti nel microambiente tumorale, specialmente in quelle appartenenti al sistema immunitario.

La plasticità cellulare è una peculiarità delle cellule $CD4^+$, è noto infatti che esse sono in grado di plasmarsi e adattare il loro fenotipo in base agli stimoli a cui vengono esposte. Questo fenomeno, unito alla loro capacità di interazione con altre cellule, può drasticamente influenzare la progressione tumorale.

Per questo motivo la caratterizzazione di cellule $CD4^+$ intratumorali potrebbe essere fondamentale per la comprensione dei fenomeni che determinano l'insorgenza e la progressione dei tumori. In questo lavoro, abbiamo eseguito un sequenziamento di RNA a singola cellula, da cellule $CD4^+$ T isolate da pazienti di cancro al colon-retto, tumore al polmone non a piccole cellule e le loro rispettive parti di tessuto adiacente non tumorale. Dalla nostra analisi emerge l'arricchimento di due sottoclassi di $CD4^+$ T, le cellule T regolatorie (Treg) e le cellule T regolatorie di tipo 1 (Tr1). Vista la scarsa conoscenza nella letteratura del ruolo delle Tr1 all'interno di un contesto tumorale, ci siamo concentrati sulla loro caratterizzazione. Abbiamo verificato l'espressione di *EOMES* nelle Tr1 intratumorali, il fattore di trascrizione che ne guida il differenziamento di recente identificato in modelli murini e in cellule Tr1 isolate da sangue periferico di donatori sani umani. Abbiamo inoltre verifcato che, come riportato in letteratura, le cellule Tr1 producono IL-10 e GZMK. Inoltre, volendo correlare la presenza di Tr1 intratumorali con la prognosi del paziente, abbiamo identificato un trascritto specifico delle Tr1, *CHI3L2*, la cui espressione correla con una peggiore prognosi del paziente.

I nostri dati suggeriscono quindi che le cellule $CD4^+$ T intratumorali, sono arricchite per la componente regolatoria, e che le Tr1, insieme alle Treg, contribuiscono all'istituzione di un microambiente tumorale immunosoppressivo, che inibisce le risposte anti-tumorali, rendendole perciò dei potenziali futuri bersagli di immunoterapie.

ABSTRACT

It is becoming increasingly clear that tumor immune microenvironment (TIME) plays a crucial role in cancer progression. In this contest T lymphocytes gained remarkable attention since they are often found to infiltrate tumors where they exert their functions to eradicate nascent tumor, but also in certain circumstances to promote its progression with the establishment of an immunosuppressive environment.

$CD8^+$ T cells were considered the predominant immune cellular component to infiltrate tumors, able to repress their proliferation through the release of cytotoxic molecules. Therefore several studies have been undertaken with the final goal to boost their activity against tumor cells.

On the contrary, the role of $CD4^+$ T cells has been largely underestimated in cancer immunity. They are known to provide helper signals to other immune subsets that lead to anti-tumoral responses, but also other subsets as regulatory T cells, have been described to promote the tumor growth by impairing effector cells activities.

The immune cells that are found in tumor bed are continuously exposed to a plethora of signals, given by cancer cells, surrounding tissues or even by components of the immune system itself. All those different signals can affect cells identity, especially from the immune compartment. Cell plasticity is a peculiar feature of $CD4^+$ T cells, which are known to shape and to adapt their phenotype in response to the different stimuli they are exposed to. This, together with their ability to interact with other cells from the immune system, can drastically affect tumor progression.

Therefore the characterization of intratumoral $CD4^+$ T cells could be fundamental in understanding the mechanisms leading to immunosurveillance failure. With this aim we performed single cell-RNAseq on $CD4^+$ T cells isolated from Colorectal Cancer (CRC) and Non small cell lung cancer (NSCLC) and their respective adjacent healthy tissues. Our analysis revealed the enrichment of two subsets of $CD4^+$ T cells in tumoral samples, T regulatory cells (Treg) and Type-1 regulatory T cells (Tr1). Since little is known about Tr1 cells' role in cancer immunology, we focused on their characterization. We checked for

the production of IL-10, GMZK and for the expression of EOMES, the lineage transcription factor that has been recently identified in mouse and human peripheral Tr1 cells. Moreover, we sought to establish a correlation between Tr1 infiltration and patients' outcome. We identified CHI3L2 as a specific Tr1 transcript and found that its expression correlates with a worse prognosis. All together, our data suggest that the $CD4^+$ T regulatory cells are enriched in tumors and that Tr1 cells could largely contribute to the establishment of an immunosuppressive microenvironment that inhibits anti-tumor responses, making them suitable targets for novel immunotherapies.

INTRODUCTION

1. Cancer Immunity

The immune system, a complex network of cells, tissues and organs, is responsible for host defense, guaranteeing the elimination of endogenous and exogenous pathogens promoting state of health of individuals. A dysfunction in its activity may lead to infections, tumor development and immunodeficiency related diseases. The immune system counts on several components, able to recognize and eliminate pathogens from different sources and with different kinetics.

The first defense against pathogens occurs through the innate immunity, which include anatomical and physical barriers, but also cellular subsets as neutrophils, monocytes and macrophages.

The adaptive immune system is involved in the latter phases of infection, through the activity of lymphocytes, which are antigen specific effector cells able to recognize pathogens through interaction with Antigen Presenting Cells, responsible for the protection against the same pathogen through memory[1].

It is now well established that immune system plays a crucial role in cancer development and patients' outcome[2]. Starting from the early 1900, it took almost a century to demonstrate that immune system was responsible of controlling and potentially eradicating the events leading to the development of malignances.

It took several years and appropriate mouse models to get to the comprehension of the mechanisms allowing the recognition of nascent tumors. In fact, it was predominantly believed that tumors, as arising from *self* cells, were not detectable from the immune cells.

Thomas and Burnet independently, by immunizing mice against syngeneic transplants, demonstrated the capability of the immune system to recognize *self* cells which underwent aberrant proliferation rate after chemical treatments, through the recognition of specific molecules, the Tumor Specific Antigens [3, 4].

In the following years several studies have been made to characterize tumor specific antigens and to prove their existence also in humans. Thanks to the acquired knowledge

circa T lymphocytes, and the conditions required to culture them *in vitro*, it became possible to isolate Cytotoxic T Lymphocytes (CTL) from melanoma patients and to produce stable CTL clones, whose molecular characterization, allowed the identification of different human tumor antigens [5].

Tumor specific antigens are subdivided into two classes, high tumoral specific antigens include antigens produced after viral infection, gene mutations and cancer germline gene expression, whereas low tumoral specific antigens include differentiation antigens and proteins that are overexpressed in tumors[6].

Finally, genetic engineering advancements gave researchers the possibility to modulate specific compartments of the immune system, to better assess the interplay between cancer and immune cells. The generation of a mouse lacking recombination activation gene 1 ($RAG1^{-/-}$ or $RAG2^{-/-}$), which is not capable of rearrange lymphocyte antigen receptors, thus not able to develop Natural Killer T cells, T cells and B cells[7] put a milestone in the Cancer Immunology field and the role of adaptive immunity in tumor elimination. Mice carrying those mutations develop tumors more frequently after syngenic transplantation, but also the number of spontaneous tumors were increased compared to wild type mice.

These last experiments carried in the 90's provided the proof of principle of the concept of Immunosurveillance, firstly conceived by Paul Erlich at the beginning of the XX^{th} century [8].

Since then great effort by the scientists worldwide has been put into investigating the mechanisms through which the immune system recognize, regulate and possibly eradicate arising tumors, in order to understand what causes the failure of the immune system, allowing tumor progression.

The concept of Immunosurveillance has evolved in Immunoediting in the early 90s, thanks to the group of Robert Schreiber, who proposed a new model of possible outcomes after cell proliferation disruption: The three Es of cancer Immunoediting (Figure 1).

This model proposes three possible scenarios after the tumor recognition: elimination, equilibrium and escape.

Elimination resembles the concept of Immunosurveillance: the immune cells successfully individuate and eliminate aberrant cells, which is the best possible outcome for the individual.

There are several events that together contribute to the elimination of the nascent tumor; the growth of the tumor makes necessary to provide nutrients through the formation of new vessels, in a process known as tumor angiogenesis[9]. This event not only provides all the metabolites useful for the tumor cells to proliferate, but also allows the infiltration of immune cells in the tumor compartment. The expansion of the tumor may damage the surrounding healthy tissues, thus providing inflammatory signals able to recruit elements from the innate immunity as Natural Killer (NK), Natural Killer T cells (NKT), macrophages and Dendritic Cells (DCs). The production of IFNγ as a result leads to a cascade of events that include the induction of angiostatic chemokines and apoptosis in cancer cells. Finally DCs that ingest tumor cells traffic to the drain lymphnodes, allowing the differentiation of tumor specific $CD4^+$ and $CD8^+$ T cells.

Equilibrium is the most dynamic and crucial phase of the interplay between the immune system and cancer cells: there is a continuous recognition of malignant cells, and at the same time aberrant cells continue to proliferate and to accumulate mutations, sometimes producing less immunogenic variants, that are able to bypass the elimination process. The immune system is thus able to control, but not to fully eradicate the nascent tumor.

A lot of studies have been carried on in order to address the populations mostly involved in the equilibrium phase, to understand which is the one most determinant in tumor outcome.

It is now been established that a major contribute to this phase is given by T lymphocytes, that exert their function through the recognition of Tumor Specific Antigens presented by the major histocompatibility complex (MHC)[10].

In particular the interaction between the effector and regulatory T cell compartments is a crucial event in defining the malignant cell fate. In fact, anti-tumor T cell responses that

take place in cancer patients can be disabled by suppressive mechanisms triggered by the interplay between malignant cells and the tumor microenvironment[11].

Escape is the most unwanted scenario of the Immunoediting: the immune system fails to eliminate and to contain cancer expansion.

There are several mechanisms exploited by malignant cells to elude the Immunosurveillance, such as the accumulation of genetic and epigenetic mutations that determinate the generation of neoantigens that can be missed by the immune cells, the downregulation of the MHC that causes an impairment of T lymphocytes activity[12]; the overexpression of genes such as *BCL2,* which leads to an increase in aberrant cell survival[13].

In the past years it has also been demonstrate that the inhibition of the effector T cell compartment and the recruitment of regulatory T cells is another fundamental mechanism of tumor escape. In this contest, T regulatory cells play a crucial role[14, 15].

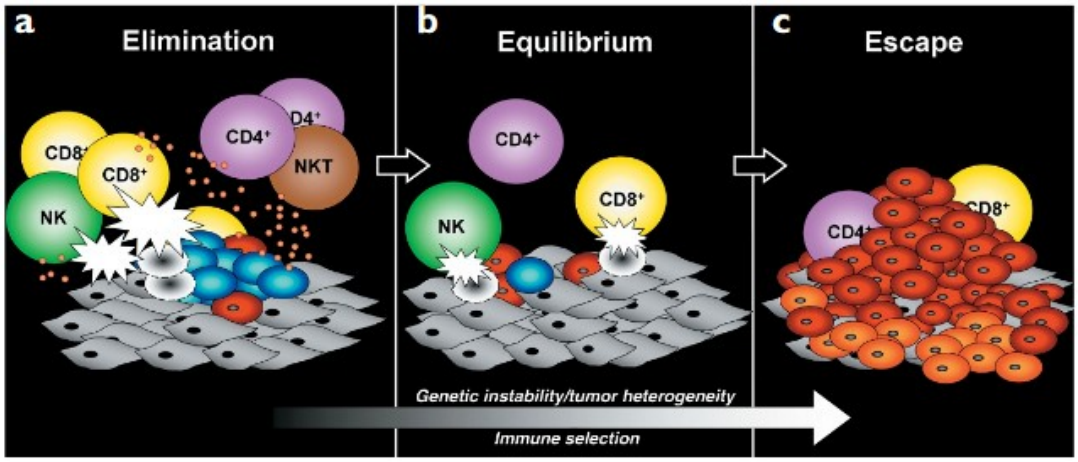

Figure 1
Cancer immunoediting
a. Elimination. The immune system recognizes aberrant cells and eliminate the tumor through the release of effector molecules **b.** Equilibrium. The balance between T effector cells and regulatory T cells determinates tumor progression **c**. Escape. Tumor cells proliferate due to accumulation of genetic instability. Tumor cells are depicted in blue, in red other tumor variants, stroma and healthy cells are in grey.

(Dunn et al.; 2002)

1.1. Tumor immune microenvironment

Cancer is a systemic disease, whose progression is driven not only by the aberrant proliferation of mutated cells, but also by the surrounding elements that together compose the tumor microenvironment (TME).[16]

TME comprises a variety of cells, ranging from stromal cells as fibroblasts and pericytes, to mesenchymal and epithelial cells, blood cells and also immune cells. The tumorigenesis process is the result of the interactions between all the cells mentioned above, in particularly by the interaction of immune cells and stroma cells.[17]

The stroma component together with extracellular matrix (ECM) is normally fundamental in the maintenance of physiological homeostasis, but after the initiation of the carcinogenesis process, it adapts to cancer cells in order to provide all the necessary elements for their survival, thus allowing cancer progression[15]. Among the signals provided by stroma cells there are also inflammatory cytokines, through which the immune cells are recruited from periphery to the tumor site. It has become increasingly clear that infiltration of immune cells is crucial for the determination of tumor outcome and the response of patients to therapies. Indeed a classification of tumors based on their tumor immune microenvironment (TIME) composition has been proposed.

Infiltrate excluded (I-E) TIME do not display infiltration by cytotoxic T cells, which are found at tumor margins, whereas components from innate immunity as macrophages are founded at tumor core.

Infiltrated inflamed (I-I) TIME on the contrary are infiltrated by a high percentage of cytotoxic cells and often referred as hot tumors. Finally a sub-class of I-E TIME has been proposed, which is characterized by the presence of tertiary lymphoid structures, and so renamed TLS-TIME, in which can be found several aggregates of immune cells, as B cells, T cells and Dendritic cells, (Figure 2).

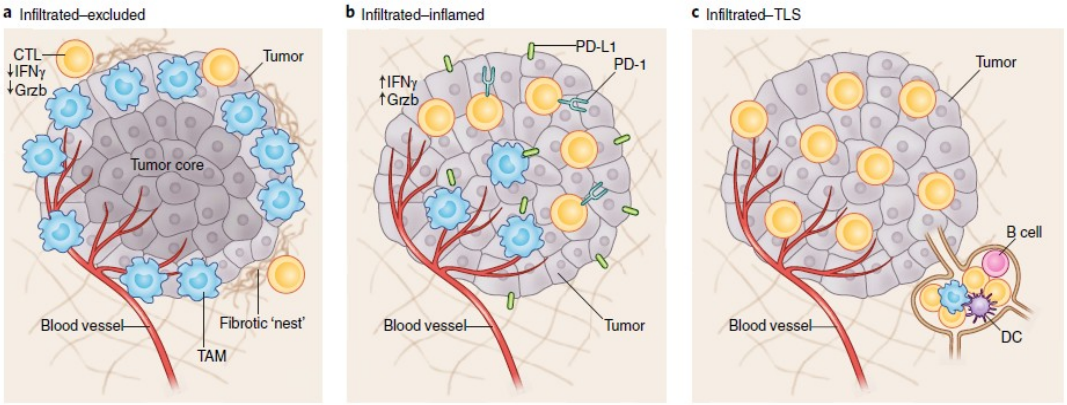

Figure 2
Classification of TIME.
a. I–E TIME, characterized by infiltration of macrophages (TAM) and the localization of cytotoxic T cells (CTL) at the margins of the tumor. **b**. I–I TIME, characterized by the infiltration of CTL at tumor core with high expression of checkpoint receptors as PD-1, and GzmB and IFNγ. **c**. TLS-TIME, which differ from I-I TIME for the presence of tertiary lymphoid structures composed by T cells, B cells and DC. (Binnewies et al.; 2018)

2. Adaptive Immune system in cancer development: the balance between effector and regulatory T cells

The critical contribution of adaptive immunity in a tumoral context is now a well established concept. T lymphocytes have been found to infiltrate several tumors, and a lot of correlation studies have been made to infer their presence with the prognosis of the patient. The involvement of the adaptive immune cells takes place thanks to the recognition of tumor specific antigens, which are presented by the major histocompatibility complex (MHC), thus allowing an initiation of the immune response mediated by $CD4^+$ and $CD8^+$ T cells, which include their activation and clonal expansion, secretion of cytokines and recruitment of other immune cells within the tumor bed.[18]
It has been shown that the balance and the interplay between the components of the adaptive immunity, the effector and regulatory T cells, is crucial in tumor development.[19] The effector T cells, through the secretion of cytotoxic molecules, counteract the action of the regulatory T cells, which are the ones responsible for the

establishment of an immunosuppressive microenvironment, that eventually favors the tumor escape.

The major players in the effector compartment are the $CD8^+$ T cells and the $CD4^+$ T cells, whereas the regulatory compartment is composed by different subsets of $CD4^+$ T cells.

2.1. Effector T cell compartment

2.1.1. $CD8^+$ effector T cells

$CD8^+$ T cells are a subset of T cells that origin in the thymus and detect antigens through the presentation by the major histocompatibility complex class-I (MHC-I)[20] (Dranhoff et al.; 2004). Once a $CD8^+$ Tcell recognizes a presented antigen, it becomes an effector cell with cytotoxic properties (CTL) [21].

CTLs cells are involved in tumor elimination phase[22] (Borst et al., 2018) and their presence within tumors has been correlated with a better prognosis in different cancer types as breast cancer, lung cancer, colorectal cancer and hepatocellular carcinoma[23]. Indeed a correlation between CTLs and reduction in tumor size has been reported[24].

Typically a Naïve $CD8^+$ T cell is recruited to the tumor site thanks to the formation of new vessels promoted by aberrant angiogenesis and by attractant chemokines secreted in the TME[25, 26]. Once arrived in tumor proximity it can differentiate into a CTL or into a memory $CD8^+$ T cell.

The mechanisms through which CTLs are able to kill target cells comprise the release of perforin and sub sequentially granzymes A and B (GzmA and GzmB); they are also able to induce apoptosis by activation of caspases through activation of Fas ligand (FasL). Moreover CTLs are able to secret different inflammatory cytokines as IFN-γ and tumor necrosis factor α (TNF-α)[27].

Despite their cytoxic properties, CTLs often fail to eliminate arising tumors. This event is still under investigation, but several reasons have been proposed.

First of all, a continuous antigen exposure could drive an exhausted or dysfunctional phenotype in CTLs already in the early state of tumorigenesis[28] (Figure3).

Second an upregulation of inhibitory receptors, as PD1, LAG3, 41-BB, TIM3 and CTLA-4 leads both to an impaired proliferation and altered granzymes and pro-inflammatory cytokines production[29-31].

The mechanisms underlying the acquisition of a dysfunctional phenotype still need to be fully elucidated. It is clear that tumor microenvironment plays a crucial role, especially when immunosuppressive conditions are predominant. In particularly, the presence of T regulatory cells, TAMs and myeloid derived suppressor cells can induce a suppression of $CD8^+$ effector T cells, and the ratio between CTLs and Treg cells is often considered a prognostic marker for patients. Finally, physiological changes in tumor bed as hypoxia and metabolic alterations may lead to an impairment of cytotoxic properties, as well as cytokines release as IL-10, TGF-β and indoleamine-2,3 dioxygenase (IDO).

2.1.2. $CD4^+$ effector T cells

$CD4^+$ effector T cells comprise different subsets, whose contribution in cancer immunity for a long time was believed to be exerted by providing help to CTLs, to enhance their cytotoxic activities[32] (Pardoll &Topalian; 1998). In the past years evidences in melanoma mouse models have shown their role also in directly inhibiting tumor growth[33].

After the recognition of a tumor antigen through the presentation of MHC class-II (MHC-II), the $CD4^+$ Naïve T cells differentiate into different effector $CD4^+$ subsets, with different cytokine secreting profiles [34, 35]. Th1 cells are the most characterized effector $CD4^+$ T cells, whose differentiation is guided by the transcription factor *T-bet* [36], which is also responsible for the upregulation of the IL-12 receptor, the chemokine receptor CXCR3 and the induction of IFN-γ production [37].

Th2 cells have been originally described in humoral immunity and anti-inflammatory responses. They are characterized by the expression of the transcription factor *GATA-3*, which drives their differentiation from $CD4^+$ Naïve T cells through the activation of *STAT6* [38-41].

More recently other T-helper subtypes have been identified; Th17 cells are characterized by the expression of IL-17, and the transcription factor *ROR-γt*, whose role is critical in their differentiation and the upregulation of IL-17. Finally Th9 cells, with distinctive production of IL-9 and whose differentiation is driven by the transcription factors *STAT6*, interferon regulatory factor 4(*IRF4*), and *PU.1* [42] have been recently described.

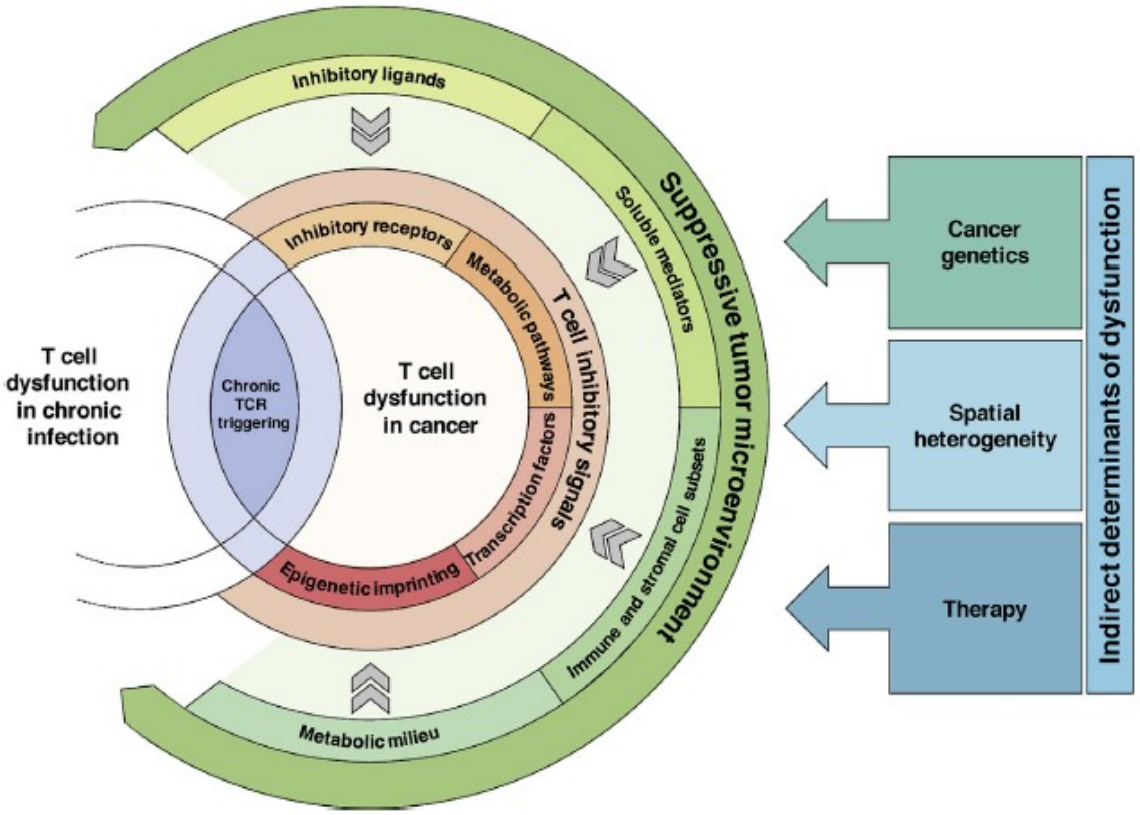

Figure 3
Induction of T cell dysfunction
The acquisition of a dysfunctional phenotype is driven by chronic TCR stimulation as happens in chronic infection. Moreover tumor microenvironment provides inhibitory stimuli as suppressive soluble mediators, metabolic factors, suppressive cell populations. In addition, cancer mutations, spatial cell localization and therapies can induce a suppressive microenvironment that promotes the acquisition of a dysfunctional phenotype.

(Thommen & Schumacher; 2018).

2.2. Regulatory T cell compartment

2.2.1. $CD4^+$ Regulatory T cells

Regulatory T cells (Treg) were firstly described as a $CD4^+$ $CD25^+$ population of T lymphocytes whose role was to mediate immunological *self* tolerance[43].

Since then several studies had been made to characterize Treg cells, and the identification of their master transcriptional factor *Foxp3* came in the early 2000. Rudensky and Sakaguchi's laboratories independently demonstrated that the expression of forkhead box P3 (*foxp3)* was restricted to $CD4^+$ $CD25^+$ T lymphocytes and that its expression was essential for Treg differentiation.[44, 45]. Functional experiments were carried out to address *foxp3* role in Treg cell; mouse models lacking *foxp3* develop severe lymphoproliferative disease with multiorgan inflammation, especially in skin, lung and liver[46] (sHarma et al.; 2009); in humans, the absence of *FOXP3* expression is related to the IPEX (immune dysregulation, polyendocrinopathy, enter-opathy, X-linked) syndrome[47].

As far as concern Treg cell identity the expression of *FOXP3* is crucial for the maintenance of their function and activities. FOXP3 was found to interact with multiple transcription factors involved in activation, differentiation and response to TCR stimulation, such as NFAT[48], nuclear factor kappa-B (NF-kB)[49], runt-related transcription factor 1 (RUNX1)[50], RORs[51], IFN regulatory factor 4 (IRF4)[52], signal transducer activator of transcription 3 (STAT3)[53] and Jun[54]. Genome wide analyses have shown that *FOXP3* binds the promoter region of many genes associated with TCR signaling. A large number of FOXP3 bound genes were upregulated or downregulated in $FOXP3^+$ T cells, indicating that the protein can act both as a transcriptional activator and repressor[55]. Many transcriptional targets of human and murine FOXP3 protein were discovered, including genes whose expression is up-regulated like *CD25*, *CTLA-4* and *GITR*, or repressed as *IL-2* and *PTPN22[52]*. Finally, constitutive expression of *FOXP3* was demonstrate to be fundamental for the maintenance of Treg cells suppressive function, in fact $CD4^+$ $CD25^+$ cells lacking its expression, fail to exert their suppressive functions and its ectopic

expression in peripheral $CD4^+$ $CD25^-$ cells is sufficient to activate a suppression program[44].

Treg suppressive activity

Treg cells are able to maintain immune homeostasis by exploiting their suppressive functions.

A lot of effort has been put into deciphering the mechanisms of Treg mediated suppression, mostly by performing *in vitro* experiments; so far, several mechanisms of suppression have been identified (Figure 4).

Suppression by inhibitory cytokines

Treg cells are known to produce inhibitory cytokines as IL-10, IL-35 and TGF-β.

IL-10 is able to inhibit the production of specific pro-inflammatory cytokines such as IL-12, moreover after the binding to its receptor IL-10R, it blocks the proliferation of effector T cells and Dendritic cells. Similar to IL-10, the multifunctional cytokine TGF-β is able to inhibit the production of IL-12, resulting in the suppression of effector T cells differentiation and proliferation.

IL-35 is an immune-modulatory cytokine predominantly expressed by Treg cells. It is able to suppress the proliferation of helper T cells and to promote the conversion of Naive T cells into Treg suppressive cells[56, 57].

Suppression by cytolysis

It has been shown that many $CD4^+$ cells exert cytotoxic activity. Indeed, similar to NK and $CD8^+$ lymphocytes, also Treg cells are able to produce granzyme A or B and to exert a perforin dependent cytotoxicity against target cells [58, 59].

Suppression by modulation of dendritic cell (DC)

Studies *in vivo* have revealed direct interactions between Treg cells and Dendritic Cells (DCs) in a

process that involve CTLA-4, which is constitutively expressed by Treg cells [60].

CTLA-4 competes with the co-stimulatory molecule CD28 for the binding to CD80 and CD86, inducing cell cycle arrest, preventing IL-2 secretion and limiting T cell contact with APCs [61]. Moreover, CTLA-4 interactions with APCs has been demonstrated to induce secretion of indoleamine 2,3-dioxygenase (IDO), that catalyzes degradation of tryptophan, resulting in metabolic disruption and starvation of effector T lymphocytes[62]. Furthermore, the adhesion molecule LAG-3 (or CD-223) expressed on Treg cells surface, can inhibit DCs maturation and activation upon interaction with MHC-II molecules on these cells[63].

Suppression by modulation of intracellular cAMP levels

Treg cells can exert suppressive functions by the elevation of intracellular cAMP levels in responder cells, which is globally accepted to be a potent suppressor. Two scenarios have been proposed regarding the mechanisms of cAMP modulation: Treg cells are able to convey cAMP molecules directly through tight junctions established once there is a contact with an effector T cell. Alternatively they can act as a source of adenosine, which can trigger adenylate cyclases into target cells, thus drastically increasing cAMP levels[64].

Suppression by metabolic disruption

Another mechanism described to suppress effector T-cells occurs through metabolic disruption. The high expression of CD25 empowers Treg cells to consume local IL-2 and could starve actively dividing effector T cells by depleting the IL-2 they need to survive[65]. IL-2 receptor is expressed by T lymphocytes, NK cells, B cells, macrophages, and monocytes; however, only T lymphocytes are capable of producing this cytokine[66].

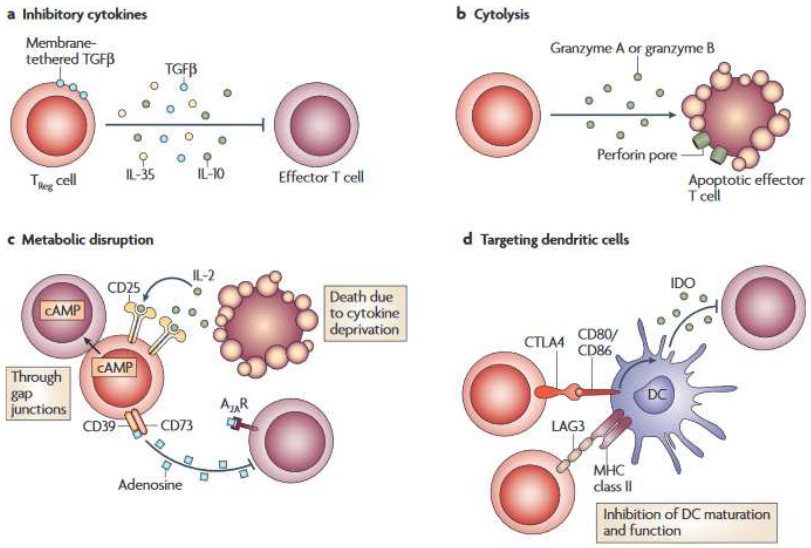

Figure 4

Mechanisms of Treg cells suppressive function

Schematic representation of four different mechanisms of Treg suppressive function: a.Inhibitory cytokine production such as TGF- β; **b.** Cytolysis through granzyme release; **c.** Metabolic disruption such as deprivation of IL-2 and release of inhibitory molecule like adenosine; **d.** Inhibition of DC maturation and function through IDO release and expression of inhibitory receptor LAG3.

(Vignali, Collison, & Workman, 2009).

2.2.2. Type 1 regulatory T cells

Type 1 regulatory T cells (Tr1) are a distinctive T lymphocyte population exerting regulatory functions. Tr1 cells were initially described as $CD4^{+}CD25^{-}$ T cells with a remarkable IL-10 production[67].

The correlation between IL-10 production and tolerance mechanisms, was initially made in a severe combined immunodeficiency (SCID) tolerant patient, who was successfully treated with hematopoietic stem cell transplantation (HSCT) and displayed increased levels of IL-10, which correlated with hypo-responsive $CD4^{+}$ T cells[68]. Some years later, it has been shown that the administration of IL-10 to $CD4^{+}$ T cells allows the differentiation of IL-10 producing cells which do not produce IL-2 nor IL-4, after renamed Tr1 cells[67]. It has been shown also that IL-27 is a driver of Tr1 differentiation[69] , and that CD49b and LAG-3 are markers of Tr1 phenotype[70] . However none of those

markers is univocally expressed by Tr1 cells; LAG-3 is also known to be expressed by Treg cells and more generally on activated T cells, whereas CD49b is expressed by memory T cells[71, 72].

Moreover, Tr1 cells express checkpoint receptors, as PD1, TIM3 and CTLA-4 [70].

It took over two decades after Tr1 discovery to identify the transcriptional factor involved in their differentiation and maintenance. Indeed in 2017 *Eomesodermin* (*Eomes*), a Tbox transcription factor that has been reported to control cytotoxic functions of $CD8^+$T cells and NK cells[73] was identified as Tr1 master transcriptional factor in mice, required for Tr1 differentiation, acting together with *Blimp-1* to activate *IL-10* transcription, at the same time repressing differentiation into other Th lineages[74]. *EOMES* was also recently identified as a lineage defining transcription factor in human pheripheral Tr1 cells [75]. A wide genome analysis performed on $CD4^+CD127^-$ cells secreting IL-10, revelead *EOMES* to be the most upregulated gene in Tr1 cells, together with Granzyme A (*GZMA*), Granzyme K (*GZMK*), surface receptors as CD27 and others already reported in literature as LAG3, TIM3, and 4-1BB (Figure 5).

GMZK has gained remarkable attention, because besides from the Natural Killer (NK) and the $CD8^+$ T cell compartment, its expression in $CD4^+$ correlated only with Tr1 cells, while was not detected in other $CD4^+$ T cell subsets known to express *EOMES* and to exhibit cytotoxic activities ($CD4^+$ CTLs)[76].

Moreover Gruarin et colleagues demonstrated the role of *EOMES* in driving the cytotoxic properties of human Tr1 cells, indeed the induction of *EOMES* in $CD4^+$ Naïve T cells, leads to an increase in IFN-γ and GZMK levels; in addition the downregulation of *EOMES* through specific siRNA in isolated Tr1 cells, leads to an impaired production of the same molecules, thus demonstrating that EOMES is necessary for their transcription. Finally ChIP analysis showed that EOMES binds to the promoter regions of IFN-γ and GzmK[75].

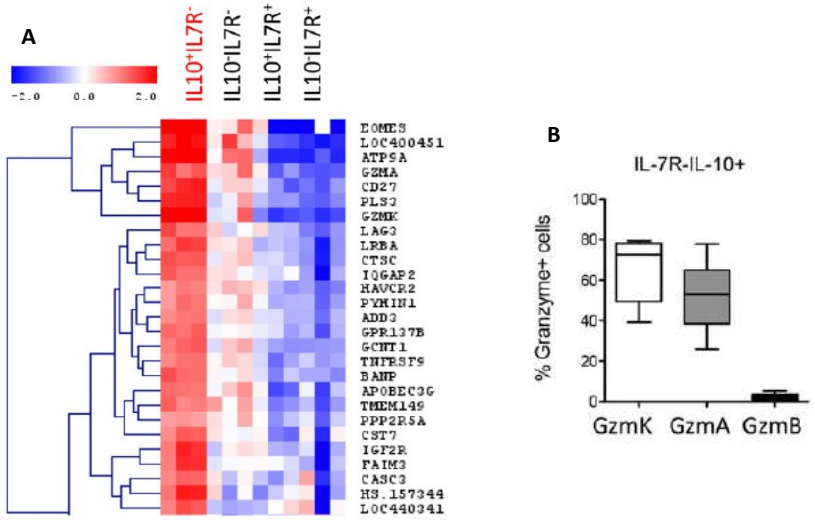

Figure 5

A. Gene expression analysis of $CD4^+IL\text{-}7R^+$ and $IL\text{-}7R^-CD25^-$T-cell subsets purified from human peripheral blood. Upregulated genes are shown in red, downregulated in blue. **B.** Intracellular levels of GzmK, A, and B in

$CD4^+IL\text{-}7R^-$ $IL\text{-}10^+$ T cells. Data from different experiments were pooled and shown as mean + SEM, **/***$p < 0.005/0.00005$.

(Adapted from Gruarin et al.; 2018)

Tr1 suppressive activity

Suppression by inhibitory cytokines

The mostly characterized mechanism of suppression mediated by Tr1 cells is the secretion of the inhibitory cytokine IL-10.

IL-10 inhibits T cell responses and proliferation by blocking INF-γ, IL-2 and GM-CSF. Moreover IL-10 is known to interfere with several molecules expressed on antigen presenting cells (APC), thus compromising adaptive immunity[77] (Roncarolo et al.; 2006).

Those molecules include major histocompatibility complex (MHC), costimulatory molecules and pro-inflammatory cytokines[78-80].

Similarly to IL-10, also TGF-β is an inhibitory molecule known to inhibit cell proliferation and activation.

Suppression by cell-contact dependent mechanisms

CTLA-4 is expressed by Tr1 cells and it has been characterized as a checkpoint inhibitory receptor also in Treg cells. It is known that CTLA-4 blocks T cell activation and it has been demonstrate that its expression on Tr1 cells mediates allergic responses in cooperation with IL-10 and TGF-β[81].

Similar to what happens for CTLA-4, also PD-1 is expressed on Tr1 cells and it is critical for the regulation of T cell activation and function during immunity and tolerance. Blocking PD-1 on Tr1 cells leads to an impairment of suppression mechanism in allergic diseases, suggesting its role in Tr1's suppressive capability [81].

Suppression by cytotoxic activities

Tr1 cells are able to produce several granzymes, GZMA, GZMB and GZMK[75].

It has been demonstrated that the release of GZMB specifically targets myeloid origin cells, in an antigen-independent manner, that requires activation via HLA class I molecules [82], (Figure 6).

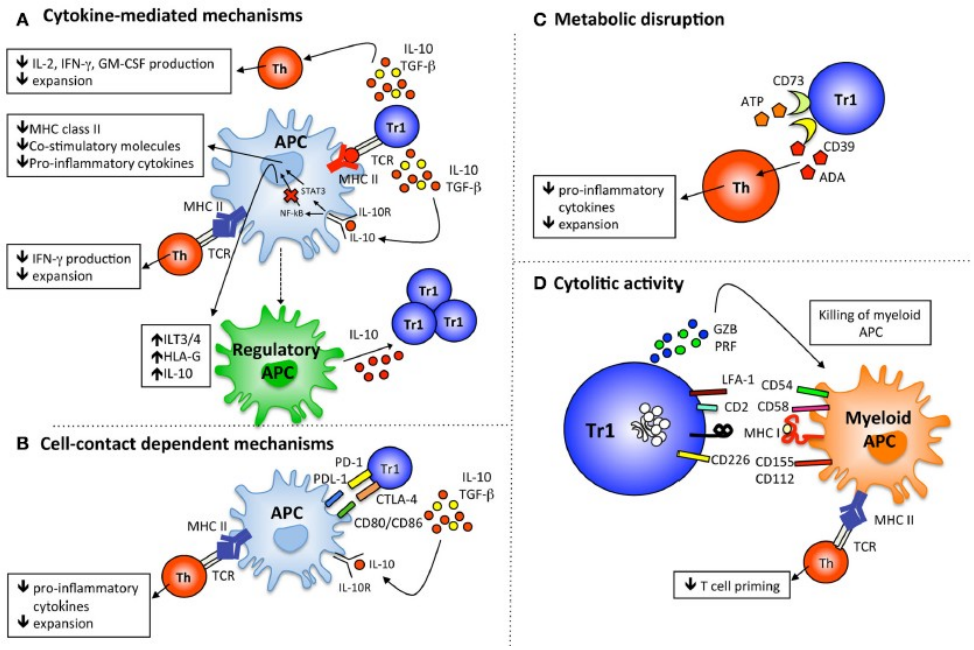

Figure 6

Mechanisms of Tr1 cells suppressive function

A. Suppression through cytokine release as IL-10 and TGF-β. IL-10 release induces the expression of tolerogenic genes as ILT3, ILT4 and HLA-G, and regulate APC's capability to produce IL-10. Moreover IL-10 release limits T effector cells production of granzymes and cytokines. **B.** Suppression through cell-contact mechanisms: expression of inhibitory receptors as CTLA-4 and PD-1 leads to downregulation of MHC-II on APC cells, thus limiting antigen presentation to effector cells. **C.** Metabolic disruption mediated by surface receptors CD73 and CD39, that inhibit ATP degradation thus limiting its consumption by effector T cells.

D. Cytolitic disruption of myeloid origin cells occurs through secretion of granzymes (A and B).

(Magnani et al.; 2011)

3. The establishment of an immunosuppressive microenvironment mediated by $CD4^+$ T regulatory cells favors cancer progression

It is now well established that T regulatory cells play a pivotal role in tumor progression.

In the last years a great effort has been put into investigating tumor infiltrating T regulatory cells, in order to assess their contribution in shaping tumor and other immune cells, thus playing a critical role in determining the tumor outcome. While it is clear that effector cells are involved in directly killing tumor cells, initially the assessment of Treg cells role in cancer immunity has been more controversial. Treg cells in fact have been shown to trigger the suppressive mechanisms that lead to an impaired activity of other immune cells compartments, but still in some cancer types their presence within tumor bed was shown to correlate with a better prognosis for patients[83] .

Because of their important role in orchestrating the immune response in TME, the elucidation of the mechanisms leading to T regulatory cells infiltration and activity is still a matter of first concern.

It has been reported that Treg can be found in almost all tumors, e.g. head and neck[84] , lung[85], liver[86], gastrointestinal tract[87], breast, pancreas[88] and ovary[89].

A high percentage of Treg cells in the tumor microenvironment (TME) is usually associated with a poor prognosis for patients[90]. In fact, the abundance of the regulatory T cell compartment leads to the perturbation of the equilibrium phase of the tumor, in favor of the suppression of the effector T cells, thus allowing malignant cell proliferation and expansion[91].

Therefore, the molecular characterization of tumor infiltrating Treg cells has become a priority issue in tumor immunology.

Unlike Treg cells, little is known about the molecular features and the clinical relevance of intratumoral Tr1 cells. Tr1 cells could be involved in melanoma in antitumor immune responses where tumor associated macrophages (TAMs) represent the most abundant immune cell type, whose activity is correlated with poor prognosis and response to therapies[92]. Taking advantage of the Tr1 capability to suppress myeloid origins cells through the release of GZMB and perforin, in 2017 Yan and colleagues demonstrated an

antitumor function of Tr1 cells through the elimination of tumor-promoting macrophages, which was not shared by conventional Tregs. Moreover they have reported a decrease in GZMB and perforin downregulation in tumor infiltrating Tr1 cells, thus suggesting a possible modulation of cytotoxic activities mediated by the tumor microenvironment[93].

Also in colorectal cancer it has been reported the presence of Tr1 cells, referred as $CD4^{+}LAG\text{-}3^{+}$ $CD49b^{-}$, whose presence together with $IL\text{-}17^{+}$ cells, correlates with disease progression [94]. Still, their molecular features in the tumor microenvironment and their clinical relevance need to be deeply investigated.

4. $CD4^{+}$ T regulatory cells as novel therapeutic tools for cancer treatment

Immunotherapies have become a breakthrough in cancer treatments. Unlike other treatments as surgery, chemotherapy and radiation, which target directly malignant cells or tumor site, immunotherapies are designed to boost anti tumor responses and at the same time to block the regulatory compartment that promotes tumor escape by suppressing cytotoxic activities mediated by effector T cells.

In this contest Treg cells emerged as primary targets, since they were found in several tumors and have been negative correlated with patient survival.

Whereas *in vivo* depletion of Treg cells in mice have shown reduction in tumor size and prolonged survival[95] , first attempts in modulation of human Treg cells, have been made by targeting their surface molecules.

The development of monoclonal antibodies (mABs) targeting Treg surface molecules such as CD25 or CTLA-4, led to an improvement of patient survival [96].

Cytotoxic T-lymphocyte-associated antigen (CTLA-4) was first discovered in 1987[97]. It is an inhibitory costimulatory receptor, whose inhibition augments adaptive immune responses[98]. Its correlation with Treg cells was firstly inferred after the generation of

Ctla4$^{-/-}$ mice that display early and fatal impairment of self tolerance, similarly to what happens in *foxp3*$^{-/-}$ mice[99] . It is constitutively expressed in Treg cells where its physiological role is to enhance their immunosuppressive activity [100], whereas in conventional T cells it is induced upon TCR stimulation[101]. Indeed targeting intratumoral Treg cells through the development of monoclonal antibodies against CTLA-4, gained remarkable results in preclinical models and also in melanoma patients.

Programmed death 1 (PD-1) is another inhibitory receptor expressed by activated T cells. Its ligand PD-L1 is expressed by tissues during inflammatory processes, and the binding to PD1 leads to immune tolerance, even in the presence of harmful antigens[102]. In certain tumors as melanoma, it has been reported an overexpression of PD-L1, that favors tumor escape by boosting immune tolerance mechanisms against malignant cells [103].

The inhibition of CTLA-4 and PD-1, also known as checkpoint receptors, have drastically changed the treatment for melanoma and other cancer types[104, 105] , indeed the Food and Drug Administration (FDA) approved the anti–CTLA-4 antibody Ipilimumab (Yervoy®) for the treatment of metastatic melanoma patients, as well as anti-PD1/PDL1 inhibitors: nivolumab (Opdivo®), pembrolizumab (Keytruda®), cemiplimab (Libtayo®), atezolizumab (Tecentriq®), durvalumab (Imfinzi®), and avelumab (Bavencio®) [106].

Unfortunately, despite of relevant clinical success, still a large number of patients do not respond to therapies, or at least do not exhibit long term benefits[107]. The unsuccessful rate of checkpoint inhibitors is due to their lack of specificity for tumor infiltrating lymphocytes, targeting also other cells sharing the inhibitory receptors. In fact, adverse events were observed in up to 60% of patients, mostly inflammatory processes that arise in the gastrointestinal tract, skin and endocrine glands [108] underlying their importance in the maintenance of tolerance.

Further studies are needed to asses peculiar features of tumor infiltrating lymphocytes, in order to effectively target the T regulatory compartment without affecting the periphery and so the overall immune homeostasis. To this aim in 2016 in our laboratory we performed a comprehensive transcriptome analysis of human $CD4^+$ Treg cells infiltrating two different tumor types, non small cell lung cancer and colorectal cancer (NSCLC and

CRC). A unique molecular signature of tumor-infiltrating Treg cells was identified. Among the upregulated genes, some regulatory checkpoints have been found, as *GITR, OX40* and *CTLA-4* which are also known to be associated with increased suppressor activity. Other well characterized genes as *TIGIT, LAG-3, TIM-3, MAGEH1, LAYN, CCR8*, *PD-1* and its ligand *PD-L1* were also found to be upregulated in infiltrating Treg cells [11], (Figure 7). All these data suggest a modulation of Treg cells that occurs in tumor microenvironment, but also underlie the importance of characterizing infiltrating T lymphocytes, which display different characteristics from the ones found in the peripheral blood or healthy tissues, hopefully to find exclusive markers that could be exploited as targets of immunotherapies.

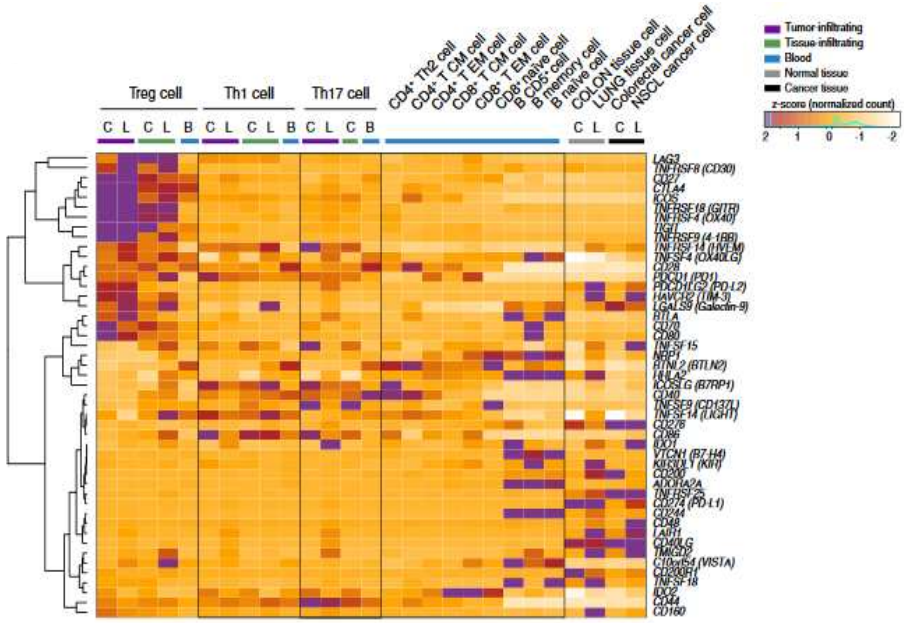

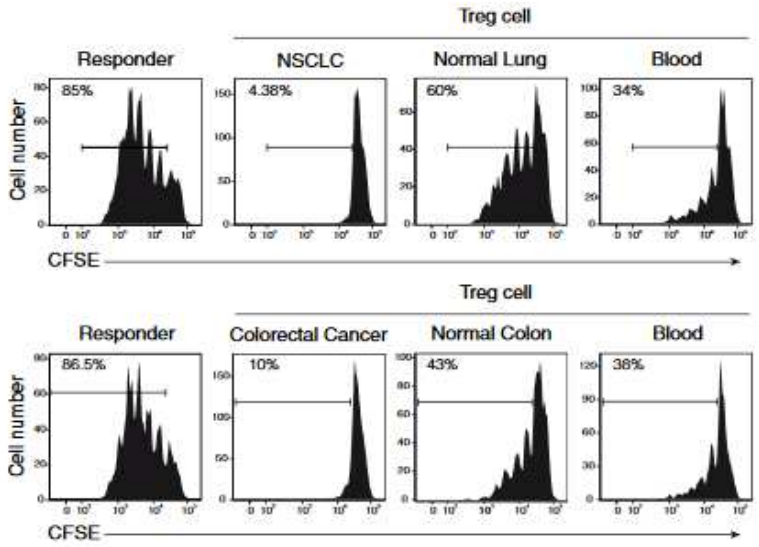

Figure 7

Intratumoral Treg cells are characterized by a unique molecular signature and are highly suppressive

A. *Z*-score normalized RNA-seq expression values of immune checkpoints genes are represented as a heatmap. Cell populations are reported as a color code in the upper part of the graph, while gene names have been assigned to heatmap rows. Colon tissues are indicated as C, lung tissues as L, and peripheral blood as B

B. Representative flow cytometry plots showing suppressive activity of Treg cells isolated from tumor (NSCLC or CRC), normal tissue and blood of the same patient.

Percentage of proliferating cells is indicated. Data are representative of three independent experiments.

(De Simone et al.; 2016)

5. Colorectal cancer

Colorectal cancer (CRC) is the third most common cancer worldwide and the second cause of cancer related mortality [109]. Despite the increasing knowledge in the mechanisms driving CRC development and its treatments, still the overall survival does not exceed 30 months in most of the patients [110].

CRC is an heterogeneous disease, characterized by different molecular pathways are involved in its initiation and progression.

First distinction in CRCs relies on their somatic mutations and genetic instability. 15-20% of CRCs display high mutation burden and defects in the mismatch repair system (MMR) thus presenting an instability in the microsatellite regions (MSI). These CRC patients are the ones who better respond to immunotherapies and with better prognosis, as opposed to CRCs with microsatellite stability (MSS)[111].

Recently a molecular classification of CRC has been proposed, based on gene expression profiles of tumor and stroma cells, leading to the establishment of a Consensus Molecular Subtype (CMS) classification.

The CMS classification subdivide CRCs in four major groups: CMS1, which comprises hypermutated cancers, with high microsatellite instability (MSI-H) and high percentages of immune infiltrates. CMS2 consist of all the CRCs in which it has been reported a mutation in Myc and Wnt pathways, CMS3 include tumors exhibiting KRAS mutations and disruption in metabolic pathways; finally CMS4, comprise cancers with activated TGFβ pathways, increased angiogenesis and also presence of immune infiltrates [112].

The CMS classification turned out to be very helpful in defining therapies for CRC patients. In fact, by cataloguing each tumor based on its consensus molecular subtype, it is easier to provide more targeted treatments to patients. Indeed immunotherapies with checkpoint inhibitors work fine for CMS1 patients (MSI), while do not have any effect in CMS3 or CMS4 subtypes, because of their lack of immune infiltrates. Further studies are needed to asses new therapeutic strategies to treat all the CRCs, by exploiting novel pathways as well as the acquired knowledge on tumor infiltrating lymphocytes in order to

render immunogenic CMS2 and CMS3 patients, to be able to treat them successfully with immunotherapies.

6. Non small cell lung cancer

Non small cell lung cancer (NSCLC), which accounts the 85% of lung cancers, is the third most common cancer and the first cause of cancer related mortality[113].

Several mutations have been identified as responsible for the initiation of the tumor: Kirsten rat sarcoma (KRAS) and epidermal growth factor receptor (EGFR) are the most common mutated genes together with their related pathways, thus representing targets for therapeutic intervention [114, 115].

As it happens for other cancers types, the tumor microenvironment (TME) also plays a role in promoting tumor progression. It has been established that NSCLC has a high somatic mutation burden, which turns out in the generation of neoantigens that can be recognized by the effector compartments of the immune system, but it can also be the cause of the upregulation of inhibitory checkpoint receptors as PD-1 and LAG-3[116].

Besides from canonical cytotoxic therapies and targeted therapies against mutated genes, checkpoint inhibitors have gained promising results in NSCLC cure.

Immune checkpoint inhibitors against PD-1 have gained promising results in patients with NSCLC, which display a longer overall survival compared to canonical treatments. Unfortunately not all the patients respond to therapy, often developing resistance to the therapy itself, due to the downregulation of the major histocompatibility complex, to defects in IFN-γ signaling and an alteration of IDO expression, an enzyme fundamental for T cell metabolism[117, 118].

AIM OF THE PROJECT

The role of intratumoral $CD4^+$ T cells has been largely underestimated in the past years. Besides the knowledge in providing help to other immune subsets, little was known about their physiological role in a tumoral context, especially until the discovery of $CD4^+$ Treg cells. Indeed, the identification of Treg cells within tumors, their negative correlation with patients' survival has caught the attention of scientist worldwide, a lot of studies have been performed toward their functional modulation as a therapeutic tool. Our laboratory published a comprehensive transcriptome analysis on Treg cells from CRC and NSCLC, identifying a specific intratumoral Treg signature which is different from Treg cells found in healthy tissues and peripheral blood. Our results confirmed a plasticity of Treg cells, that is a peculiar feature of overall $CD4^+$ T cells, which adapt and shape their phenotype in response to the environment they are found in. Indeed, the characterization of intratumoral $CD4^+$ T cells, which are constantly exposed to different stimuli provided by the tumor microenvironment is needed to better assess their heterogeneity and function. To this aim we performed a transcriptome analysis by single cell RNA sequencing of $CD4^+$ T cells isolated from NSCLC and CRC and their respective adjacent healthy tissues.

METHODS

Human primary tissues

Primary human lung or colorectal tumors and non-neoplastic counterparts were obtained from 50 and 31 patients, respectively. Patients' records clinicopathological staging, tumor histotype and grade are listed in Table S1. Informed consent was obtained from all patients, and the study was approved by the Institutional Review Board of the San Gerardo Hospital, San Paolo Hospital, Grande Ospedale Metropolitano Niguarda and Ospedale Humanitas Research Hospital. No patients received palliative surgery or neoadjuvant chemo- and/or radiotherapy. NSCLC specimens and the adjacent tumor-free tissues were cut into pieces and single-cell suspensions were prepared by using the Tumor Dissociation Kit, human and the gentleMACS™ Dissociator (Miltenyi Biotech cat. 130-095-929). Cell suspensions were than resuspended in DMSO with 10% fetal bovine serum (FBS) and stored in liquid nitrogen until flow cytometry, or further processed by ficoll-hypaque density-gradient centrifugation (Amersham Bioscience). CRC specimens were cut into pieces, incubated in 1 mM EDTA (Sigma-Aldrich) for 50 min at 37 °C and then incubated in type D collagenase solution 0.5 mg/mL (Roche Diagnostic) for 4 h at 37°C.

Cell preparation

Mononuclear cells were isolated from these cell suspensions by ficoll-hypaque density-gradient centrifugation (Amersham Bioscience). T cell fractions were recovered after fractionation on a four-step gradient consisting of 100%, 60% and 40% and 30% Percoll solutions (Pharmacia). Tr1 cells were purified by flow cytometry sorting using the following fluorochrome conjugated antibodies: anti-CD4 APC/Cy7 (clone OKT4 Biolegend), anti-IL7R PE (clone MB15-18C9 Miltenyi) anti-CD25 VioBright FITC (clone 4E3 Miltenyi) anti-CD27 VioBlue (clone M-T271 Miltenyi) anti-CD195 PEcy7 (clonej418F1 Biolegend) using a FACSAria II (BD) as CD4+IL-7R-CCR5+CD27+ [119, 120]. Fresh cells were harvested,

washed with 1 PBS and re-suspended in PBS supplemented with 0.04% bovine serum albumin. Cell were then counted using an automated counter (Countess II Thermo Fisher) and cell viability was assessed by Trypan blue exclusion. Samples were selected according to cell viability and for the analysis samples with a viability above 85% were used.

Flow Cytometry

Cytokine production was assessed by intracellular staining after stimulation with 0.1µM phorbol ester (PMA) and 1µg/ml ionomycin (Sigma-Aldrich) in the presence of 10 µg/ml Brefeldin A (Sigma). Intracellular staining was performed using eBioscience FOXP3 staining kit according to the manufacturer protocol (eBioscience cat 00-5523-00). Briefly cells were harvested and fixed for 30 min in fixation/permeabilization buffer at 4 °C, and then stained with anti-EOMES antibody efluor660 (eBioscience, clone WD1928) and anti-IL10PE (JES-19F1, Biolegend) anti-IFN-γ Pecy5 (clone 4S.B3) anti- granzyme K Fitc (clone GM6C3 Santa Cruz Biotechnology) in permeabilization buffer for 30 min at 4 °C. Cells were then washed two times, resuspended in FACS washing buffer and analyzed by flow cytometry.

Sequencing library construction using the Chromium 10X platform

Cellular suspensions (5000 cells per sample) were loaded on a Chromium 10X Instrument (10x Genomics, Pleasanton, CA, USA) to generate single-cell GEMs. Single-cell RNA-Seq libraries were prepared using Chromium™ Single Cell 3' Library & Gel Bead Kit v2 (16 rxns PN-120237; 10x Genomics). GEM-RT was performed in a Veriti© 96-Well Thermal Cycler (Thermo Fisher; PN-4375786): 55 C for 2 h, 85 C for 5 min; held at 4 C. After RT, GEMs were broken and the single-strand cDNA was cleaned up with DynaBeads MyOne Silane Beads (Thermo Fisher Scientific; P/N 37002D) and SPRIselect Reagent Kit (0.6 SPRI; Beckman Coulter; P/N B23318). cDNA was amplified using the Veriti© 96-Well Thermal Cycler: 98 C for 3 min; cycled 14 : 98 C for 15 s, 67 C for 20 s, and 72 C for 1 min; 72 C for 1 min; held at 4 C. Amplified cDNA product was cleaned up with the SPRIselect Reagent Kit (0.6 SPRI). Indexed sequencing libraries were constructed using the reagents in the

Chromium™ Single Cell 3' Library Kit, following these steps: (1) fragmentation, end repair and A-tailing; (2) adapter ligation; (3) post-ligation cleanup with SPRIselect; (4) sample index PCR and cleanup. The barcode sequencing libraries were quantified by quantitative PCR (KAPA Biosystems Library Quantification Kit for Illumina platforms P/N KK4824). Sequencing libraries were loaded on an Illumina HiSeq2500 platform and sequenced using the following read length: 26bp Read1, 8 bp I7 Index and 98 bp Read2.

Single-cell RNA-seq data processing and quality control

The fastq files of $CD4^+$ cells infiltrating tumor and adjacent CRC and NSCLC tissues were processed by Cell Ranger software pipeline (version 2.0.1) provided by 10X Genomics. Alignment with STAR (human genome GRCh38), barcodes, UMIs and cell filtering as well as downsampling of the reads for the aggregation of different samples were performed using default parameters. Four different counts matrices were created: one with three biological replicates for $CD4^+$ infiltrating CRC (21115 genes across 10230 cells), one with 2 biological replicates for $CD4^+$ infiltrating NSCLC (21047 genes across 9497 cells), one that combines $CD4^+$ infiltrating CRC samples and three CD4+ replicates infiltrating adjacent tissues (23638 genes across 21356 cells) and finally a matrix with $CD4^+$ infiltrating NSCLC samples and adjacent tissue counterparts (23073 genes across 17340 cells).

These matrices were then processed using the R package Seurat. First of all, we removed genes detected in less than 0.1% of the total data and cells with fewer than 200 expressed genes. Then, we evaluated the portions of genes related to mitochondrial and riboprotein fractions, discarding those cells with a % of MT and %RP counts higher than 5% and 50% respectively. Moreover, we filtered out cells with a number of detected genes > 2500 to avoid the inclusion of doublets. Overall we filtered out 853 and 1003 cells for individual CRC and NSCLC tumor related analyses and 2745 and 2504 cells respectively for combined analyses. The number of cells for the downstream analyses was 9230 and 8644 for CRC and NSCLC $CD4^+$ lymphocytes and 18852 and 14613 for both CRC and NSCLC combined analyses. Finally, log-normalization method considering a scaling factor of 10^4 was used on the filtered matrices to obtain normalized values.

Dimensionality reduction and clustering

To capture the variability related to the biology of the system, we restricted the counts matrices to a subset of genes associated with high dispersion (x.low.cutoff = 0.05 or 0.1, x.high.cutoff = 3, y.cutoff = 0.5) for each specific analysis. We then checked if these High Variable Genes (HVG), about 500 for all the analyses, included mitochondrial or riboprotein genes to remove all the unwanted/technical source of variation. Then, the values were centered and scaled before inputting them into Principal Component Analysis (PCA). In particular, to minimize the technical noise, we selected all the statistically significant PCs looking at the associated standard deviation. 10 or 9 principal components were identified with PCElbowPlot function (9 PCs only in CD4+ combined tumor-adjacent NSCLC analysis). We then grouped the cells according to graph-based clustering approach, indicating the number of PCs selected in the previous step. Initially, a KNN (K-Nearest Neighbor) graph was constructed based on euclidean distance in PCA space, thus refining the weight of the edges between two cells using Jaccard similarity. Finally, Louvain algorithm was used to cluster the cells together, optimizing the modularity function. A key aspect of the clustering is the definition of the number of clusters in which the cells are partitioned: with the “resolution” parameter we investigated the best value to asses the granularity of our data. In particular, we selected 0.7 for all the analyses. Finally, a Barnes-hut t-SNE was employed using cell loadings for the significant principal components as input, allowing a better division of the cells into isolated clusters.

Identification of Differential expression Genes and Unique markers

Differentially expressed genes for each cluster were identified using FindAllMarkers implemented by Seurat. Each cluster was compared to the cluster made by all the other cells and genes that are detected in a minimum fraction of 20% cells in either of the two groups were tested by running a Wilcoxon rank-sum test; we kept the genes that were upregulated and with an average log fold change of 0.5.

Unique marker genes were identified using at base the FindMarker functionality provided by Seurat using the Wilcoxon rank-sum test; the minimum fraction of cells in which a gene is detected in at least one of the two comparing group at 10%; and the average log fold change set to 0.25, retaining only the upregulated genes. Each cluster of interest were compared with all the other clusters iteratively and only the genes common to all the comparisons were classified as unique markers for that cluster.

Clustering comparison

In order to assess the degree of conservation between the clusters identified by the independent analyses of tumor CRC and tumor NSCLC datasets, a Jaccard index was calculated on the lists of differentially expressed genes for all the clusters in both tumors.

Gene Set Enrichment Analysis (GSEA)

GSEA was performed by pre-ranked GSEA [121] using custom genes modules we previously generated [11]. Pre-ranked genes for the cluster of interest were computed using the FindMarkers functionality by Seurat using the default parameters and the resulting gene list was ranked in descending order by the average log fold change.

Total RNA isolation and RT-qPCR

Total RNA was isolated using TRIzol Reagent (Thermo Fisher Scientific), according to manufacturer's instructions. Residual contaminating genomic DNA was removed from the total RNA fraction using DNA-free Kit (Thermo Fisher Scientific). The RNA yields were quantified using the QuantiFluor RNA System (Promega) with Quantus Fluorometer (Promega) and the RNA quality was assessed by the Agilent 2100 Bioanalyzer (Agilent Technologies. For reverse transcription, equal amounts of DNA-free RNA (200 ng) were reverse-transcribed with SuperScript IV First-Strand Synthesis System (LifeTechnologies) in the conditions suggested by the manufacturer. Quantitative RT-PCR was performed to assess the expression of CHI3L2 (Hs00970220_m1), EOMES (Hs 00172872_m1), GZMK (Hs 00157878_m1), CD4 (Hs 01058407_m1), CD8A (Hs 00233520_m1), NCAM1 (Hs

00941830_m1), MS4A1 (Hs 00544819_m1), with 1 ng of diluted cDNA and TaqMan 2X Universal PCR Master Mix (Thermo Fischer Scientific). Gene expression levels were calculated using DCt method and 18s FAM (Hs 99999901_s1) as normaliser. Reverse transcription and qRT-PCR analysis were performed in biological triplicates.

Suppression assay

(CFSE)-labelled responders $CD4^+$ $Naive^+$ T cells from healthy donors were cocultured with different effector to target (Responder/suppressor) ratios with unlabelled $CD127^-CD25^-$ $CCR5^+CD27^+$CD4Tr1 cells sorted from TILs of CRC or NSCLC patients using FACS Aria II (BD Biosciences), in the presence of Dynabeads T-Activator CD3/CD28 (Life Technologies, Carlsbad, CA cod 11131D) at a bead to cell ratio of 1:10. Proliferation of CFSE-labeled cells was assessed after 96 hours.

smRNA FISH

CRC and the relative non-neoplastic counterpart tissues were treated in a sucrose gradient and then embedded in OCT (Calbiochem). RNA smFISH was carried out as previously described (La Manno et al.;2016) with minor modifications. In details, 5-µm thick sections of CRC and the relative non-neoplastic counterpart tissues were mounted on coverglasses, post-fixed with 4% paraformaldehyde for 10 min at room temperature and permeabilized with Protease III (Advanced Cell Diagnostic). Samples were incubated for 10 min at 70°C in Tris-EDTA (pH 8.0). The sections were then washed twice with SSC 2X and incubated with hybridization buffer containing labelled probes (LGC Biosearch Technologies) O/N at 38.5°C. After three rinses in 20% formamide-SSC 2X, the un-mounted sections were imaged in 10%Glycerol-PBS1X employing a multifunctional HCA-automated Nikon Ti-E inverted widefield microscope, equipped with CREST Optics VideoConfocal SuperResolution and 16-LED excitation device (PE-4000; Cool-Led) for multi parametric fluorescence detection. High resolution 100x TIRF oil immersion objective (NA 1.46; Nikon Instruments) was employed for single molecule visualization. After smRNA fish detection, sections were counterstained with DAPI and Phalloidin

(Thermofisher) for nuclear and cytoskeleton labeling and further re-acquired employing the same XYZ coordinates. Low magnification images were acquired using a 40x air objective (NA 0.9; Nikon Instruments) in large-scanning field modality to detect whole sections. Sequentially acquired images were channel-aligned, processed and segmented using NIS-Elements v5.02 (Nikon Instruments, Lim softwares) specific modules. In details, single molecule detection and morphological parameters were evaluated for correct cell segmentation and in-cell particle tracking.

Immunofluorescence

CRC and the relative non-neoplastic counterpart tissues were treated in a sucrose gradient and then embedded in OCT (Calbiochem). Sections were washed in PBS and incubated in blocking solution, PBS plus 10% normal goat serum (Vector Laboratories). Sections were incubated overnight at 4°C with the following primary antibodies: α-CD4, 5 µg/µl, IgG2a mouse VIT4 (from MiltenyBiotec 130-094-153); α -GZMK, 4,5 µg/µl, IgG2b mouse GM6C3 (from Santa Cruz Biotechnology, sc-56125); α -EOMES, 10 µg/µl, IgG1 mouse WD1928 (from Thermo-Fisher Scientific 14-4877-82). Sections were then washed and secondary stained with isotype specific secondary antibodies conjugated with AlexaFluor dyes (AF488 goat α-mouse IgG1, AF594 goat α-mouse IgG2a, AF647 goat α-mouse IgG2b) (Invitrogen Molecular Probes; Thermo-Fisher Scientific) for 1hr at RT, followed by nuclear counterstaining with DAPI (Thermo-Fisher Scientific). Sections were mounted in DABCO mounting media (Sigma-Merk) and imaged using a multifunctional HCA-automated Nikon Ti-E inverted widefield microscope, equipped with CREST Optics VideoConfocal SuperResolution and 16-LED excitation device (PE-4000; Cool-Led) for multi parametric fluorescence detection. At least n=4 fields of view were acquired for each sample using a 100x TIRF oil immersion objective (NA 1.46) and a 40x air objective (NA 0.9) (both from Nikon Instruments) in large-scanning field modality to detect whole sections. Acquired images were processed and segmented using NIS-Elements v5.02 (Nikon Instruments, Lim softwares) specific modules. In details, mean fluorescence

intensities of protein labellings and morphological parameters were evaluated for correct cell segmentation and in-cell protein detection.

High dimensional flow cytometry

Frozen samples were thawed in RPMI-1640 supplemented with 10% FBS (Sigma-Aldrich) and 1% penicillin-streptomycin, and 1% Ultra-glutamine (both from Lonza) and 20 µg/ml Deoxyribonuclease I from bovine pancreas (Sigma-Aldrich). After extensive washing with

PBS (Sigma-Aldrich), the cells were stained immediately with the Zombie Aqua Fixable Viability Kit (BioLegend) for 15 minutes at room temperature (RT). Then, the cells were washed and stained with the combination of mAbs purchased from either BD Biosciences, BioLegend or eBioscience. mAbs were previously titrated to define the optimal concentration, as described [122]. Chemokine receptors were stained for 20 minutes at 37°C, while all other surface markers (except CD3) were stained for 20 minutes at RT. Intracellular molecules (including CD3) were detected following fixation of cells with the FOXP3/transcription factor staining buffer set (eBioscience) according to manufacturer's instructions, and by incubating with specific mAbs for 30 min at 4°C.

Samples were acquired on a FACS Symphony A5 flow cytometer (BD Biosciences) equipped with 5 lasers (UV, 350 nm; violet, 405 nm; blue, 488; yellow/green, 561 nm; red, 640 nm; all tuned at 100 mW, except UV tuned at 60 mW) and capable to detect 30 parameters. Flow cytometry data were compensated in FlowJo by using single stained controls (BD Compbeads incubated with fluorescently-conjugated antibodies), as described [122].

Kaplan-Meier and multivariate analysis

Log-rank test and Kaplan-Meier survival plot were used to evaluate the correlation (association of) between patient survival time and expression of *CHI3L2* gene. Transcriptional profiles and clinical parameters for CRC (GSE17536, n=177) and NSCLC (GSE41271, n=80, squamo) patients were downloaded from GEO data portal. For study

GSE41271 five patients were excluded due to incomplete or inaccurate annotation (GSM1012883, GSM1012884, GSM1012885, GSM1013100, GSM1012888), retaining a total of two hundred and sixty three patients. Melanoma data set and corresponding clinical data was downloaded from the publicly TCGA database (SKCM, n=103). To correct the effect of T cell levels within each sample, the expression of the selected gene was normalized to the CD3 level genes (geometric mean of *CD3D*, *CD3E* and *CD3G*). In order to analyze the prognostic value of *CHI3L2*, the cohorts were dichotomized into higher (gene level higher than the cut-off point, upper extreme) and lower groups (gene level lower than the cut-off point, lower extreme) whereas patients with the relative expression between the two extremes were excluded from survival analysis. The median of relative expression plus (minus) 5% Median Absolute Deviation (MAD) was used as a cut-off point for the dichotomization of patients into the two groups.

In addition, we performed multivariate cox proportional hazards analysis to determine whether *CHI3L2* was an independent predictor of patient survival. For each dataset, a model with gene expression group and other covariates including sex, age and grade was built. The hazard ratio (HR) and 95% confidence interval were estimated and only covariates with $p \leq 0.05$ were marked as statistically significant in relation to patient survival. Statistical analysis was performed by using the R “survival” package.

RESULTS

1. Definition of $CD4^+$ T cell transcriptional landscape in human NSCLC and CRC by single-cell RNA-sequencing

In order to obtain a characterization of $CD4^+$ T cell expression signatures and heterogeneity in the tumor microenvironment, we performed single-cell RNA sequencing of $CD4^+$ T cells isolated from NSCLC, CRC and the adjacent non-tumoral tissues (Figure 1A). After sequencing, we explored our data using a graph-based clustering approach. The analysis was based on the identification of high variable genes (HVGs) across the single cells, data dimensionality reduction by principal component analysis (PCA) and t-distributed stochastic neighbor embedding (t-SNE) for the visualization of high-dimensional single cell data in 2D.

In details, first we identified highly variable genes (HGVs) across the single cells; those are genes that strongly contribute to the expression profile, and their identification allowed us to exclude from the analysis all the genes that are variable due to technical reasons.

Then we used the Principal Component Analysis (PCA) on HVGs, a statistical procedure that is used for the reduction of the dimensionality of a dataset. The algorithm works to find the principal components (PC) that represent the overall variance coming from each sample. In fact, single cell RNAseq data are composed of a large number of variables that need to be compressed to be evaluated simultaneously, while retaining the maximum amount of variance and minimizing the information loss.

Finally for a better visualization of high-dimensional single cell data we performed a t-distributed stochastic neighbor embedding (t-SNE). This method allows to map all the data in two dimensions, ideally keeping close to each other the close neighbours and maintaining distant the others. The result is a 2D visualization of the dataset, which is organized in isolated clusters. This analysis on our samples defined nine clusters for $CD4^+$ T cells infiltrating NSCLC and eight clusters for CRC (Figure 1B).

We then sought to determine the identity of each cluster, so we performed a differential gene expression analysis, to look for quantitative changes in expression levels between

different clusters. To this aim, we used FindAllMarkers by Seurat, which identifies positive and negative markers for cells of each cluster. We found 230 and 175 upregulated genes for NSCLC and CRC respectively (Figure 1C). Through this analysis we were not able to unequivocally define the canonical cell subsets which are described within CD4+ T cell compartment (e.g. Th1 and Th17 cells). This is due on the one hand to a technical limitation of single-cell transcriptome analysis which fails to detect low abundant mRNAs such as lineage defining transcription factors. On the other hand it reflects the biology of the system at tumor sites where cell subset boundaries are not well defined and are likely continuously shaped by changes in the tumor microenvironment (e.g., growth factors, chemokines and cytokines concentration, hypoxia).

We then asked if some of these clusters were conserved among the two tumors, so we compared the differentially expressed genes of the different CD4+ T cell clusters using the Jaccard index (Figure 1D), which allows to evaluate the similarity between two datasets, and found that clusters 1 and 4 of both tumors display the highest similarity.

Through single-cell analysis and clustering we assessed the transcriptional landscape of CD4+ T cells in the human tumor microenvironment, identified the genes that best describe the different CD4+ T cell clusters, and assessed their degree of conservation in two tumor types.

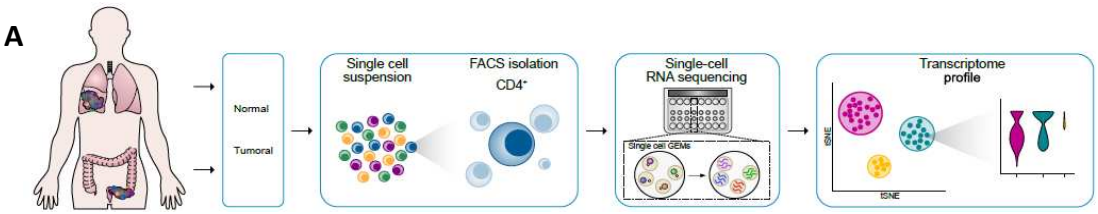

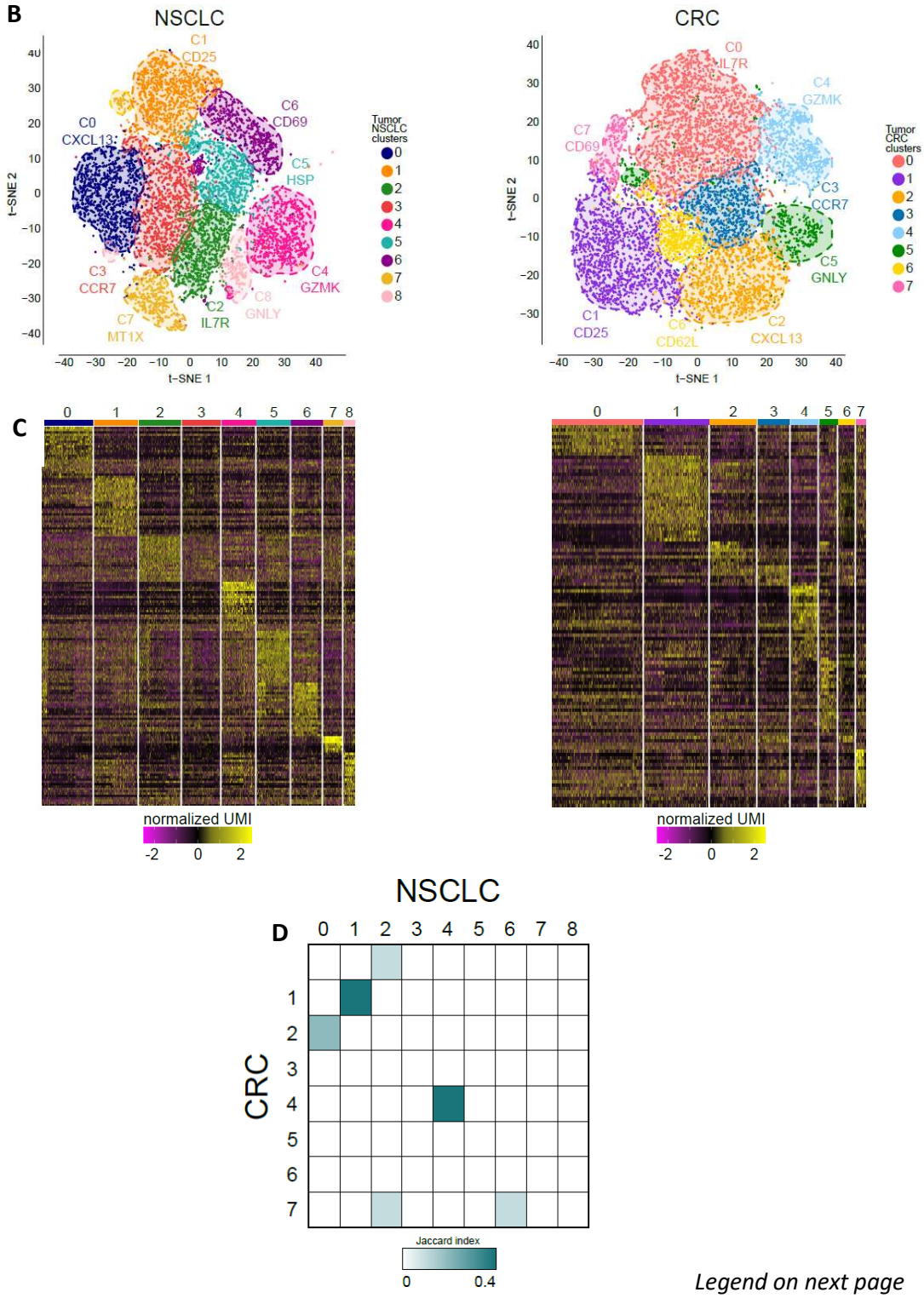

Legend on next page

Figure 1. Single-cell RNA-seq of $CD4^+$T cells isolated from tumors and non-tumoral adjacent tissues

A. Schematic representation of the experimental workflow for isolation of $CD4^+$ T cells and preparation for single-cell analysis.
B. Major tumor infiltrating $CD4^+$ T cell populations identified in NSCLC and CRC tumors through unsupervised clustering. t-SNE projection is used for data visualization. Each point depicts a single cell, colored according to 9 and 8 clusters designated in NSCLC and CRC respectively.
C. Heatmaps represent z-score distribution of the top 25 differentially expressed genes with an average log fold change > 0.5, for each cluster defined in Figure1B. Cluster identity is reported in the upper bar color coded as in Figure1B
D. Heatmap represents the Jaccard similarity index calculated on the differentially expressed genes of each NSCLC and CRC cluster. Jaccard Index = (the number in both sets) / (the number in either set) * 100

2. Specific $CD4^+$ T cell subsets are enriched in tumor tissues compared to adjacent normal tissues

To identify specific tumor infiltrating $CD4^+$ T cell subsets, we then performed a novel graph-based clustering analysis on the combined single-cell datasets of $CD4^+$ T cells infiltrating non-tumoral and tumor tissues. We identified twelve clusters of $CD4^+$ T cells in the combined analyses of NSCLC and lung tissue and twelve in CRC and colon tissue (Figure 2A). The different clusters contain cells derived preferentially from non-tumoral (in white in the combined t-SNE visualization) or tumor tissue (in red) (Figure 2B).

To identify clusters exclusively expressed by the tumors and not their corresponding healthy tissues, we looked for clusters highly enriched in $CD4^+$ T lymphocytes, and then we checked if the cells belonging to those clusters mostly (at least 75%) populate unique clusters defined in the analysis of tumor tissues alone (Figure2B). We found that clusters 1 and 4 of both tumors are specifically enriched in tumors, and corresponded to the ones we identified in the above analysis of tumor tissues alone as displaying the highest degree of similarity (Figure 1D).

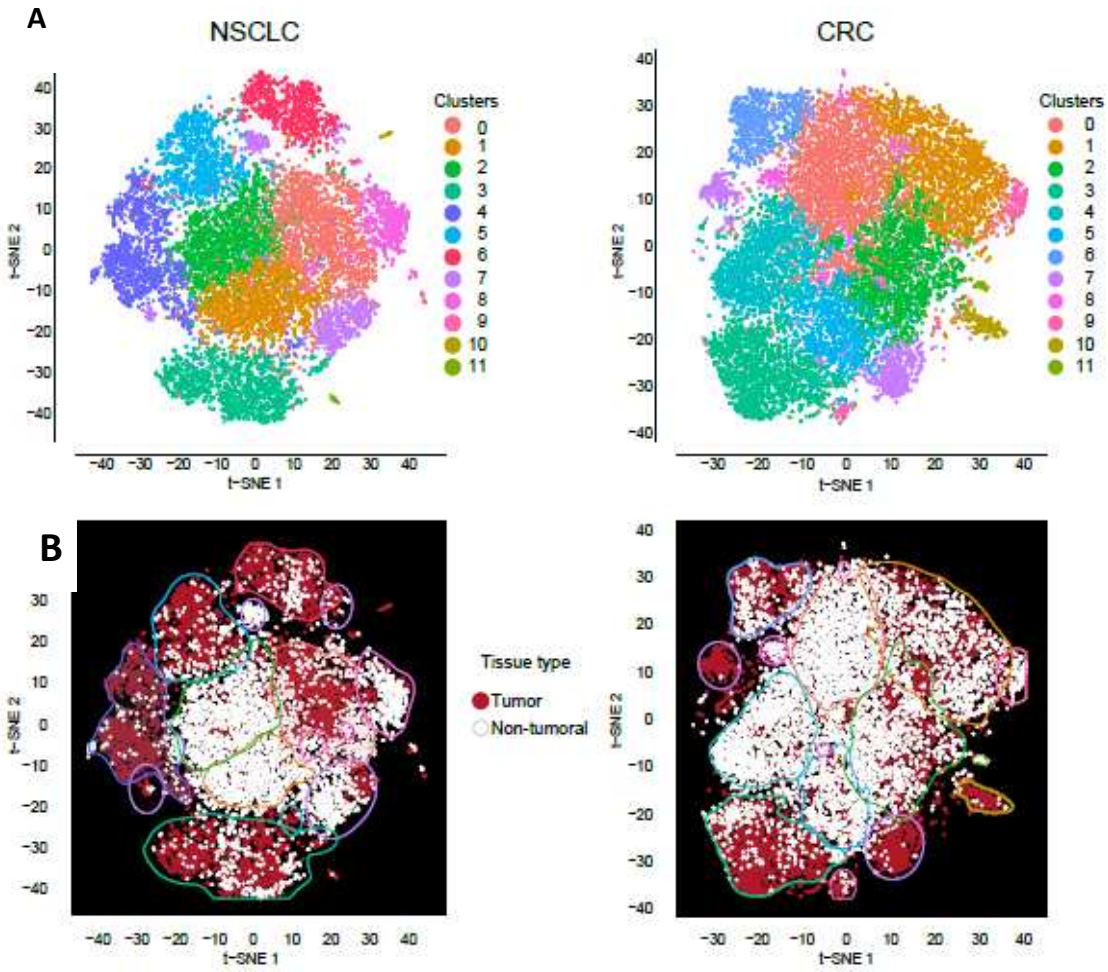

Figure 2. Identification CD4+ T cell subsets enriched in the tumor microenvironment

A. tSNE visualization of $CD4^+$ T cells data combined from tumor and non-tumoral adjacent tissue.
B. tSNE visualization highlighting the tissue of origin. Red dots represent $CD4^+$ T cells isolated from the tumors and white dots cells isolated from the adjacent tissues. Contour color refers to clusters as defined in Fig 2A.

3. Immuno-suppressive $CD4^+$ T cell subsets are enriched both in CRC and NSCLC

We then investigated in more details the nature of the conserved clusters, so we performed a Gene Set Enrichment Analysis (GSEA) using reference gene sets that had been generated in our laboratory on human $CD4^+$ T cell subsets from both peripheral blood of healthy donors and tumor infiltrating cells.[11]

GSEA is a powerful statistical method that allows the identification of genes that are over-represented in a large set of genes that may share common features (e.g. belonging to the same pathway, the same pathology, the same chromosomal location, etc.). This approach consists in ranking a list of genes according to the significance of the differentially expressed genes between different conditions, and evaluating whether members of a given gene set are overrepresented at the top (or bottom) of the ranked list of genes. The Enrichment Plot resulting from a GSEA shows the running-sum statistics with a green curve, where the x axis represents the ranked list of genes and the y axis represents the score produced walking down the ranked list. The maximum deviation from zero encountered in walking the list will give rise to the Enrichment Score (ES). Positive and negative ESs indicate enrichment at the top and bottom of the ranked list, respectively. We performed GSEA analysis on our single cell RNA data and found that Cluster 1 in NSCLC and CRC is enriched for $CD4^+$ regulatory T cells (Treg) specific genes, particularly FOXP3, the Treg cell master transcription factor, and CD25, the specific surface marker that encodes for IL2R (Figure 3A). Moreover, cells belonging to cluster 1 express high levels of the tumor Treg signature genes (MAGEH1; TIGIT; OX40 and GITR) previously identified by bulk RNA-sequencing analysis in several primary and metastatic tumors [11, 123] (Figure 3A).

Interestingly GSEA on cluster 4 of both tumors classified these cells as Type 1 regulatory T cells (Tr1) (Figure 3B), a subset of regulatory cells that do not express FOXP3 but display several mechanisms of immune suppression, involved in tolerance mechanisms and so far poorly associated with tumoral tissues (Roncarolo et al.; 2006). We found also that tumor

infiltrating Tr1 cells express EOMES, recently identified as Tr1 lineage-defining transcription factor[74], IFN-γ and high levels of several granzymes (GZM), in particular GZMK.

Through the combined analysis of single-cell transcriptomic datasets of $CD4^+$ T cells infiltrating NSCLC and CRC and the adjacent non-tumoral tissues, we found that Treg and Tr1, two $CD4^+$ T cell subsets defined by their suppressive activity towards effector T cells, are highly represented and specifically enriched in tumors (Figure 3C).

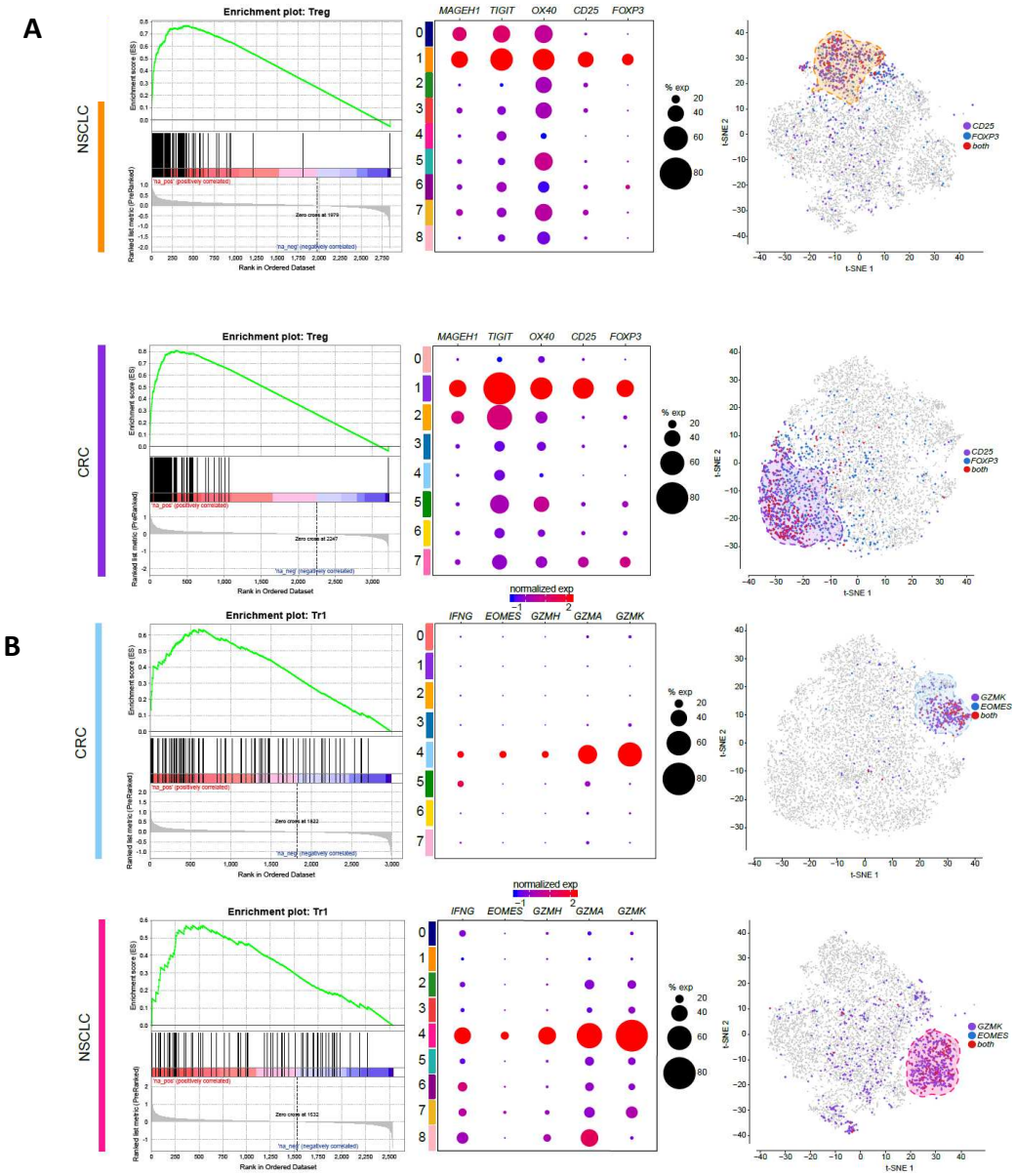
A
NSCLC
Enrichment plot: Treg
MAGEH1 TIGIT OX40 CD25 FOXP3
% exp
20
40
60
80
CD25
FOXP3
both
t-SNE 1
t-SNE 2
CRC
Enrichment plot: Treg
normalized exp
B
CRC
Enrichment plot: Tr1
IFNG EOMES GZMH GZMA GZMK
GZMK
EOMES
both
NSCLC
Enrichment plot: Tr1
Rank in Ordered Dataset

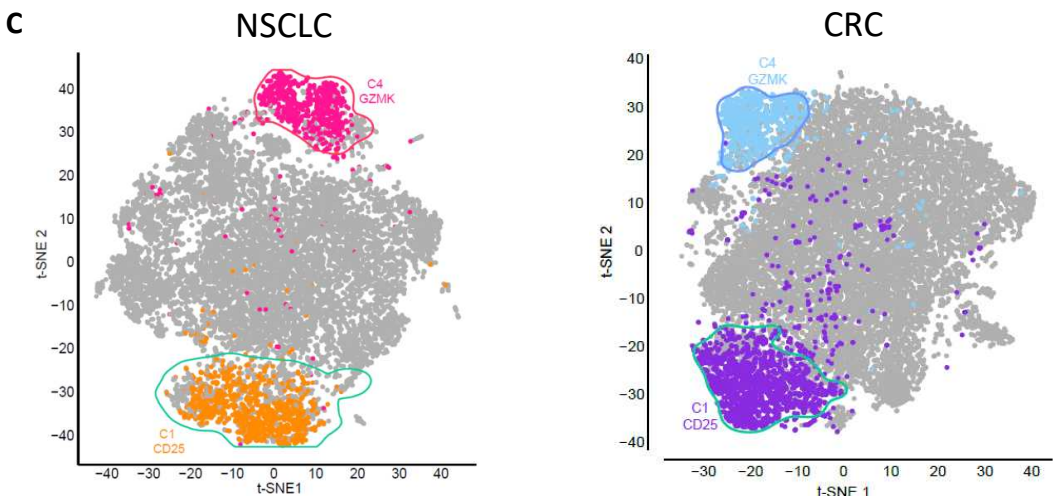

Figure 3. Definition of CD4$^+$ T cell subset identity by GSEA analysis.

A. *Left panels:* Gene set–enrichment analyses are presented as enrichment score profiles for genes in clusters 1 and 4 in NSCLC and CRC, with CD4$^+$ Treg cells as reference gene set. Nominal $P < 0.05$. *Center panels*: Expression of selected cell-type-specific genes in the CD4$^+$ T cell clusters. Individual dot size and color reflect the percentage of expression of each marker gene and the mean expression value of the gene across all cells. *Right panels:* Expression of CD25 and FOXP3 in CD4$^+$ Treg cell clusters.
B. *Left panels:* Gene set–enrichment analyses are presented as enrichment score profiles for genes in clusters 1 and 4 in NSCLC and CRC with CD4$^+$ Tr1 cells as reference gene set. Nominal $P < 0.05$. *Center panels:* Expression of selected cell-type-specific genes in CD4$^+$ T cell clusters. Individual dot size and color reflects the percentage of expression of each marker gene and the mean expression of the gene across all cells. *Right panels:* Expression of GZMK and EOMES in CD4$^+$ Tr1 cell clusters.
C. Selected clusters of Treg (C1) and Tr1 (C4) of the the combined analysis are highlighted and coloured as their cluster of origin in Figure 1B.

4. Human NSCLC and CRC are infiltrated by functional Type 1 Regulatory $CD4^+$ T cells

Little is known on the the role of Tr1 cells at tumor sites, so we decided to focus on the characterization of the localization, the phenotype and function of the intratumoral Tr1 cells. First, we assessed GZMK and EOMES co-expression in tumor and non-tumoral tissues by single molecule RNA-FISH and by immunofluorescence. We used specific RNA probes to detect CD4, GZMK and EOMES transcripts or antibodies to detect their protein products (Fig 4A). To confirm and extend our findings, we investigated the expression of the Tr1 signature protein GZMK by tumor-infiltrating $CD4^+$ T cells from 48 NSCLC and 28 CRC patients using flow cytometry. We identified a $CD4^+$ subset expressing GZMK while lacking the canonical CD25 and FOXP3 Treg markers, as well as GNLY, a cytotoxic molecule typical for CTL. These cells co-expressed CCR5 and PD-1, as previously reported for Tr1 in non-tumoral tissues [119, 120]. Moreover, the $GZMK^+$ cells express EOMES, the master transcription factor of Tr1 cells, while the $GZMK^-$ cells do not (Figure 4B).

Since IL-10 production is one of the distinctive features of Tr1 cells along with their ability to suppress antigen-specific effector T-cell responses [77], we assessed the capability of the $GZMK^+$ $CD4^+$ T cells to produce IL-10 as well as IFN-γ compared to effector $GZMK^-$ $CD4^+$ T cells. We observed that only $EOMES^+$ $GZMK^+$ cells showed high IL-10 and IFN-γ production (Figure 4C). Finally in order to address Tr1 cells suppressive functions, we performed a suppression assay as described by Venken et al. In 2007: briefly after the isolation of intratumoral Tr1 T cells, we cocoltured them *in vitro* with Naive $CD4^+$ T cells previously labeled with 5,6-carboxyfluorescein diacetate succinimidylester (CSFE) and activated in vitro with anti-CD3/CD28 beads. We followed the proliferation rate of Naive $CD4^+$ T cells that loose half of the CFSE labelling upon each cell division, and found that Tr1 cells from both tumor types suppressed the proliferation of Naive $CD4^+$ T cells (Figure 4D).

Overall, these results show that GZMK^{+} EOMES^{+} cells are Tr1 cells as defined by their signature genes, the production of IL-10 and by their ability to suppress proliferation of effector T-cells.

A

Single molecule RNAfish

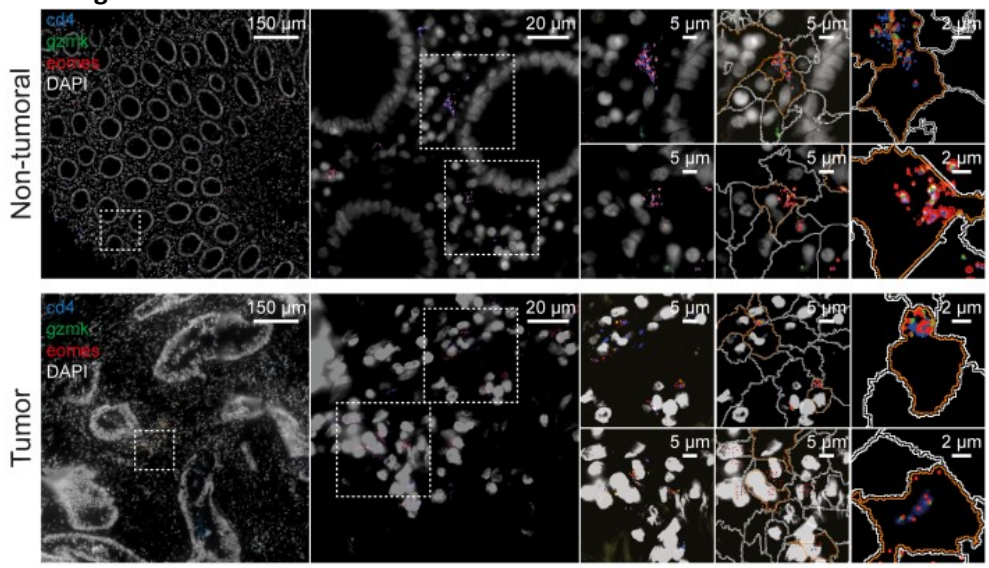

Immunofluorescence

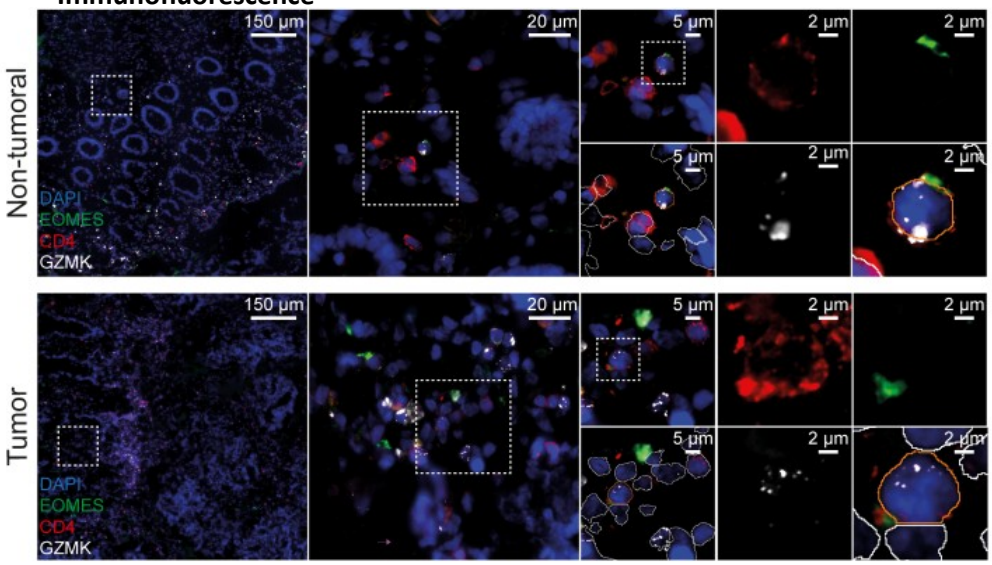

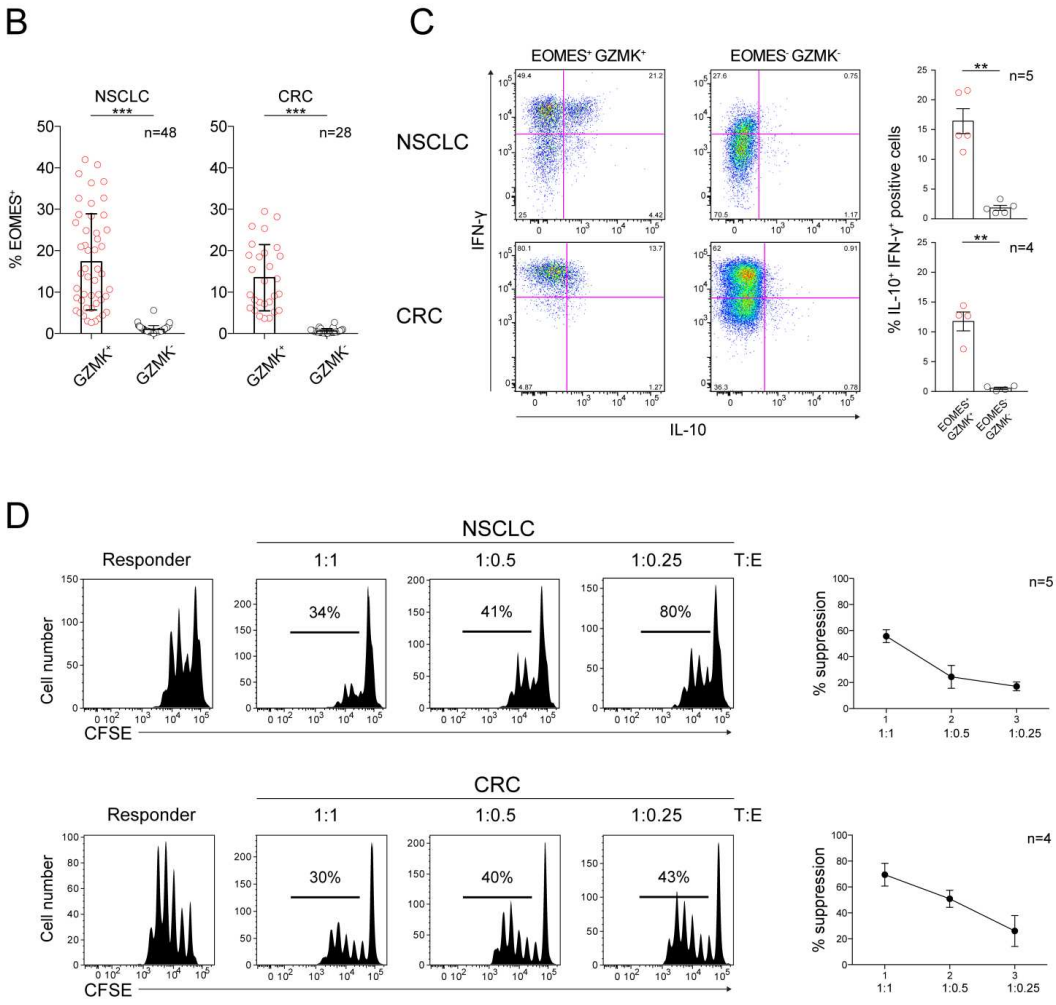
B
NSCLC
CRC
***
n=48
n=28
% EOMES+
GZMK+
GZMK-
C
EOMES+ GZMK+
EOMES- GZMK-
NSCLC
CRC
IFN-γ
IL-10
**
n=5
n=4
% IL-10+ IFN-γ+ positive cells
D
NSCLC
Responder
1:1
1:0.5
1:0.25
T:E
34%
41%
80%
Cell number
CFSE
% suppression
n=5
CRC
30%
40%
43%
n=4

Figure 4. Functional chacarterization of EOMES^{+} GRZK^{+} tumor infiltrating Tr1 cells

A . *Upper Panels:* RNA single molecule FISH analysis of non-tumoral adjacent colon (top) and CRC (bottom) samples.Images show different magnification specified by in-image overimposed scale bar. Nuclei are shown in grey, CD4 smRNA-FISH probe in blue, GZMK probe in green, EOMES probe in red. Dotted rectangular areas highlight the area used for higher magnification assessment. For better visualization, images overimposed with cellular segmentation for Tr1 cells are depicted with orange-labelled cell contour, whereas other segmented cells are shown with white-labelled cell contour. *Lower Panels:* Multiple immunofluorescence labelling for CD4 (red), GZMK (white) and EOMES (green) in non-tumoral adjacent colon (top) and CRC (bottom) samples. Representative images at different magnification are shown. Dotted rectangular areas highlight the area used for higher magnification assessment. Zoomed-in focused areas on single Tr1 cells (defined as triple positive for CD4, GZMK and EOMES protein labellings) were split into single-channel visualization for better evaluation of triple positivity. Cellular segmentation is shown highlighting orange-labelled cell contours for Tr1 cells versus white-labelled cell contours for all other segmented cells.
B. Bar plots (± SEM) show the percentage of EOMES^{+} cells amongst either GZMK $^{+}$ or GZMK $^{-}$ CD4^{+} T cells that infiltrate NSCLC (n= 48 patients) and CRC (n= 28 patients) and were analyzed by high dimensional flow cytometry. Paired t-test *** p<0.001.
C. *Left panels:* The representative experiment shows, for one sample of NSCLC derived T cells and one sample of CRC derived T cells, intracellular staining for IL-10 and IFN-γ in EOMES^{+}GZMK^{+} CD4^{+} Tr1 and EOMES^{-}GZMK^{-} CD4^{+} effector cells stimulated with PMA and ionomycin. Numbers in quadrants indicate cell percentages. *Right panels* Bar plots (± SEM) show the percentage of IL-10^{+} IFN-γ $^{+}$ amongst activated EOMES^{+}GZMK^{+} CD4^{+} Tr1 and EOMES^{-}GZMK^{-} CD4^{+} Tr1 and Teff control cells derived from NSCLC (n= 5 patients) and CRC (n= 4 patients). **p<0.01; t-test.
D. *Left panels*: Representative flow cytometry plots showing suppressive activity of Tr1 cells isolated from tumor samples (NSCLC or CRC). Carboxyfluorescein diacetate succinimidyl ester (CFSE)-labeled CD4^{+} naive T cells were cocultured with an equal number of Tr1 cells for 4 days with CD3/CD28 beads *Right panels*: Capacity of Tr1 cells to suppress proliferation at varying Tr1/Tnaive ratios. Data are representative of n = 5 and n = 4 (± SEM) experiments performed with NSCLC and CRC infiltrating Tr1 cells.

5. Tr1 cells are highly enriched at tumor sites and negatively correlate with patient survival

After the identification of Tr1 cells at transcript level and their functional characterization, we wanted to assess their enrichment in tumors also at protein level. We thus quantified by flow cytometry the Tr1 cell subset within the $CD4^+$ T cell population isolated from tumors, adjacent non-tumoral tissues, and the peripheral blood of NSCLC and CRC patients. We found that the percentage of Tr1 cells is significantly increased in tumors with respect to both the peripheral blood and the non-tumoral tissue (Figure 5A). Furthermore, in both tumors the percentage of Tr1 cells increased in patients at stage II-III compared to patients at stage I (Figure 5B), suggesting that intratumoral Tr1 cell number correlates with tumor progression.

To give clinical significance to this finding, we aimed to correlate expression of Tr1 cells with disease progression in CRC and NSCLC patients by looking for Tr1 specific transcripts. First of all, we sought to identify one or more transcripts, as revealed by single-cell RNAseq, that allow identification of Tr1 cells amongst other immune cell subsets, tumor and non-tumoral cells. To this end, we exploited single-cell transcriptomic data generated in the multicellular ecosystem of metastatic melanoma[124] that included expression data of malignant, immune, stromal, and endothelial cells. We compared the expression of Tr1 marker genes, from our single cell RNAseq data, with the profiled melanoma cell populations and found CHI3L2 which belongs to a family of mammalian chitinase-like protein coding genes with cytokine or growth factor activity, as a unique marker that discriminate Tr1 cells among the other cell populations. To confirm this, we assessed the expression of *CHI3L2* in several lymphocyte cell subsets (CD8 T cells, Tr1, NKT cells, B cells and whole $CD4^+$ T cells depleted of Tr1 and in the whole NSCLC and CRC tumor and adjacent normal tissues). *CHI3L2* is highly expressed in Tr1 cells compared to all the other cell types (Figure 5C) and is even more Tr1-specific than GZMK, because the latter is also expressed at low levels in NK cells and $CD8^+$ T-cells. Simultaneous evaluation of lineage-specific transcripts confirmed the purity of the isolated cell subsets (Figure 5C).

Finally, we asked if the expression of the Tr1-specific transcript, CHI3L2, correlates with disease progression in CRC, NSCLC and melanoma patients. For this purpose, we took advantage of the transcriptomic datasets of resected tumor tissues from a cohort of 177 CRC, 80 NSCLC and 103 melanoma patients[125, 126] and defined the survival rate in association to high and low CHI3L2 gene expression. To normalize for differences in T cell numbers within the resected tumor tissues, we used the ratio between expression of *CHI3L2* genes and CD3. Remarkably, we found that patients bearing tumors with high levels of *CHI3L2* expression had a shorter survival compared to patients whose tumors expressed low levels of *CHI3L2* (Figure 5D). Moreover, we performed a multivariate analysis to determine how expression of *CHI3L2* was associated with mortality relative to other risk factors, and, as expected, found that the hazard of death increased with tumor staging. Nevertheless, *CHI3L2* was also identified as an independent predictor of patient survival for all three tumor types.

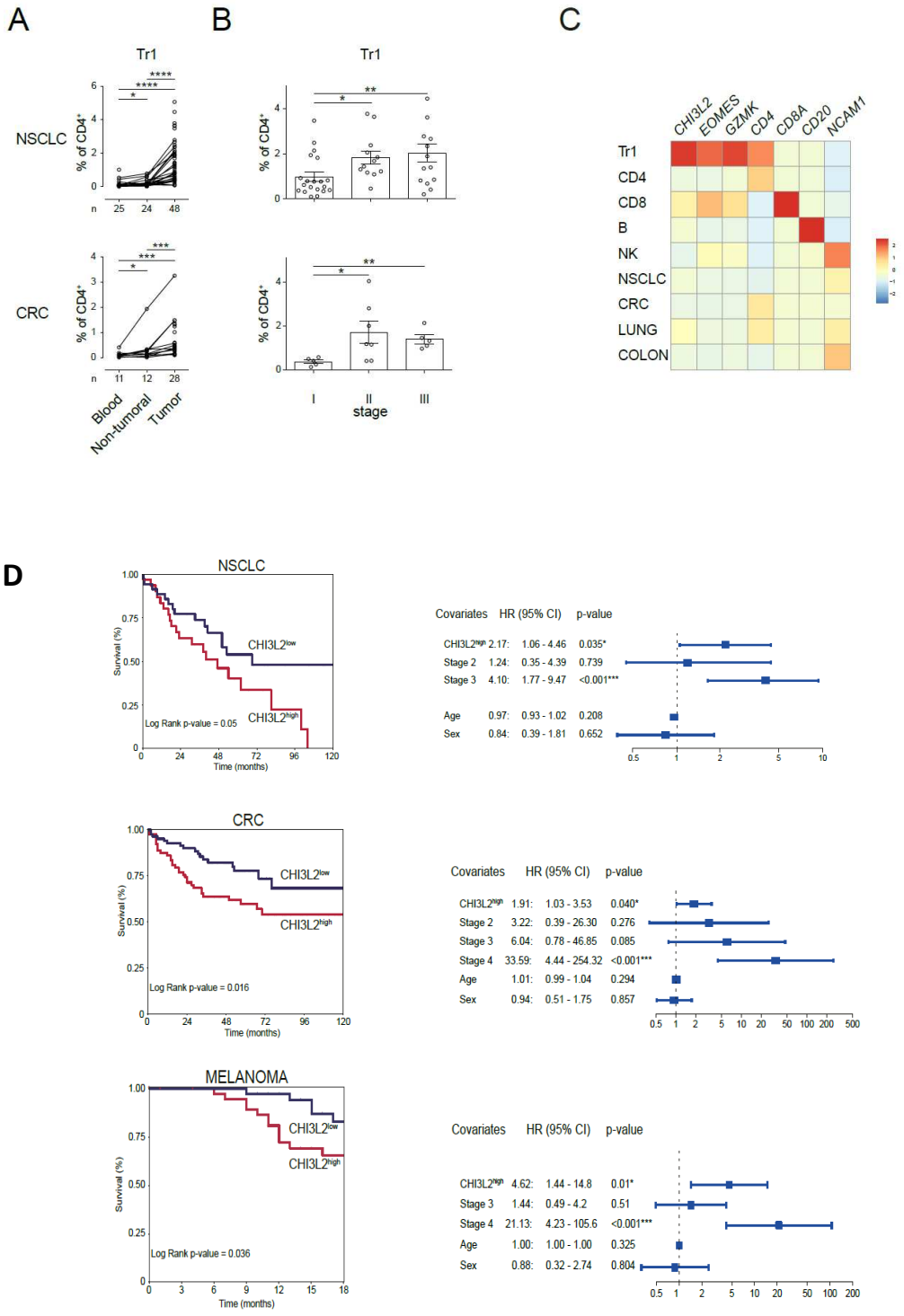

Legend on next page

Figure 5. Enrichment in intratumoral Tr1 accumulation correlates with tumor progression

A. Frequencies of $EOMES^+$ $GZMK^+$ $CD4^+$ Tr1-cells in peripheral blood, non-tumoral adjacent tissue and tumoral tissues (NSCLC or CRC) **p<0.01, *** p<0.001; ****p<0.0001; paired Wilcoxon test.
B. Bar plots represent the frequencies of $EOMES^+$ $GZMK^+$ $CD4^+$ Tr1-cells in NSCLC and CRC patients at different tumor stages. *p<0.05, **p<0.01; Mann-Whitney test
C. Heatmap represents the relative expression, measured by RT-qPCR, of *CHI3L2, EOMES*, *GZMK*, *CD4*, *CD8A*, *CD20* and *NCAM1* in various tumor infiltrating lymphocyte subsets and in the whole tumoral tisuues (NSCLC and CRC) and thw adjacent non tumoral lung and colon tissues. Data represent average of two independent experiments.
D. Kaplan-Meier plots compare survival of CRC (n=177), squamous NSCLC (n= 75) and melanoma (n=103) patients with high and low expression of *CHI3L2,* the intratumoral Tr1 signature transcript that has been normalized for the amount of T cell present (assessed as *CD3* expression levels) in the various samples. Univariate analysis confirmed a significant difference in overall survival curve comparing patients with high and low expression of *CHI3L.* Statistical significance was determined by the log-rank test (NSCLC: p = 0.05; CRC: p = 0.016; melanoma: p=0.036). Multivariate Cox regression analysis for *CHI3L2* expression has been adjusted for stage, age, and gender. Forest plots demonstrate CHI3L2 expression is an independent predictor of patient survival (NSCLC: p = 0.035; CRC: p = 0.040; melanoma: p = 0.01).

DISCUSSION AND CONCLUSIONS

In the past years a lot of effort has been put into deciphering the interplay between the immune system and cancer progression. Indeed several studies confirmed the crucial role of the immune system, which is able to shape the tumor microenvironment, through the release of inflammatory or anti-inflammatory signals, thus allowing cancer progression or preventing its formation if recognized at early stages of tumorigenesis. In this context the role of $CD4^+$ T cells in tumoral progression has been largely underestimated, at least until the discovery of intratumoral $CD4^+$ Treg cells, and more importantly their correlation with a worse prognosis in patients. Indeed new therapeutic strategies against Treg cells have been generated, but despite of several successful reported cases, still a large number of patients do not respond well to therapies. The comprehensive characterization of intratumoral Treg cells, as well as other infiltrating cell types, is essential for the development of successful immunotherapies, in order to avoid all the side effects that have been reported in current treatments, mainly autoimmune related issues.

With the aim of deeper characterizing the $CD4^+$ T cells landscape in CRC and NSCLC, in this study we performed an RNA-seq at single-cell level on tumor infiltrating $CD4^+$ T cells.

Our analysis revealed the presence of different clusters among all the tumor infiltrating $CD4^+$ T cells, but interestingly we found an enrichment in $CD4^+$ regulatory T cell subsets, Treg and Tr1 cells, that are also conserved in the two tumor types. Since Treg cells have been extensively studied and characterized, we have decided to focus our attention on the Tr1 subset. The Tr1 cluster is characterized by the predominant expression of *EOMES*, the recently identified master transcriptional factor of Tr1 cells[74, 75], and also by the expression at high levels of *GZMK*, as reported by Gruarin and collegues in human peripheral Tr1 cells*, IFN-γ* and *IL-10*, the cytokines known to be produced by Tr1 cells.

Also from the functional point of view, intratumoral Tr1 cells maintain a suppressive activity as reported for the peripheral Tr1 cells.

As happens for Treg cells, in order to give more clinical relevance to our findings, we sought to correlate Tr1 infiltration within tumors with patient prognosis; in fact we

observed an increased number of Tr1 cells in the latter stages of both tumors (stage III and IV), suggesting that the presence of Tr1 cells correlates with tumor progression, which is not so surprising if we take into account their intrinsic regulatory nature.

In addition, to extend our data to another tumoral context, we took advantage of the single-cell transcriptomic data generated in metastatic melanoma[124], where we checked for the expression of Tr1 markers identified by our single-cell analysis.

Not only we have found the cluster of Tr1 cells also in melanoma patients, but interestingly we found that *CHI3L2*, a chitinase-like protein lacking chitinase activity is univocally expressed by Tr1 cells. Although the role of CHI3L2 in Tr1 cells is still unknown, it is interesting that a close member of the chitinase like family protein, CHI3L1, has been reported to enhance inflammatory responses and to promote tumor growth[127, 128]. Finally we tried to assess *CHI3L*2 relevance as a prognostic value, by performing both an univariate analysis and a multivariate analysis, that confirmed the correlation between high expression of *CHI3L2* and worse prognosis of the patients, suggesting that Tr1 cells, as it happens for Treg cells, are at least in part responsible for the establishment of an immunosuppressive tumor microenvironment.

The other tumoral clusters delineated by our analysis are more difficult to identify, cell subset boundaries are not well defined. We identified clusters that expressed genes associated to central or effector memory $CD4^{+}$T cells (CD62L, CCR7 and IL7R) and a cluster of cells highly expressing *CXCL13,* a cytokine usually associated with T follicular helper cells (Tfh), but with no relevant expression of *BCL6*, the master transcription factor of Tfh cells. Unfortunately we were not able to define clearly effector subsets as Th1 or Th17 cells. A reason could be that effector cells are continuously shaped by changes in the tumor microenvironment (e.g., growth factors, chemokines and cytokines concentration, hypoxia), so their identification at tumor sites based on markers identified in peripheral blood, cannot always be successful. It is therefore even more striking that regulatory T cells (Treg and Tr1) are highly represented and surprisingly display conserved molecular features across tumors, suggesting that these T cell subsets are strategic to boost the anti-tumoral immune responses.

Altogether, the abundance of regulatory Tr1 cells at tumor sites and the correlation of Tr1 infiltration with a worse prognosis in several types of cancers, suggests that Tr1 cells can be effective target of novel immunotherapeutic strategies for a wide array of cancers, but still deeper characterization is needed. First of all, we have identified *CHI3L2* as a unique marker for Tr1 cells, but still we need to characterize its role and function in Tr1 cell biology. We are trying to modulate its expression in Tr1 cells and other T cell subsets, to evaluate its implication in Tr1 cell identity or their suppressive capability. Moreover we are trying to better assess Tr1 and effector T cells interaction, by performing *in vitro* cocolture assays. Our preliminary data suggest that Tr1 cells could have a role in promoting CTLs dysfunctionality, but the mechanisms that let this happen still need to be elucidated.

Finally, the molecular and functional characterization of tumor infiltrating cell populations, cannot be done without taking into account their spatial localization and organization.

One of the biggest limits of single cell approaches is that by disrupting cells and tissues in order to process the samples, all the information about spatial patterning is lost. The information about cell localization within tumors, is now becoming a central issue to provide a more detailed characterization and to infer possible cross-talks and interactions. We have successfully identified Tr1 cells in both NSCLC and CRC, using standard imaging approaches as immunofluorescence and single molecule RNA FISH. However the identification of Tr1 cells within tumors, gave us hints only about their localization and organization in the tissue, but we had no information about other cellular subsets present in the tumor, due to technical limitations of spectra overlapping.

To overcome this issue in our lab we took advantage of the latest technology advancements in fluorescent labeling and set up a protocol to visualize up to 8 targets simultaneously in the same tissue (Figure 6). Moreover, to identify more cells subsets together, we implemented out protocol in order to be able to visualize up to 48 targets, by performing sequential hybridization of multi-probe sets.

At present, we set up the technique on CRC tissues, and we are improving our knowledge in data analysis and processing, which go far from the standard imaging analysis approaches. Additionally, the setting up of the protocol on NSCLC is also on our future plans.

To sum up the integration of spatial information together with data generated by single cell RNA sequencing, will provide us a complete picture of the immune microenvironment within tumors and on how the interplay among different immune cell subsets and stromal cells contribute to the establishment and final outcome of the disease. The final goal is not a mere “count” of the immune cell types that infiltrate the tumor tissue but a reconstruction of the cellular and molecular network that define their behavior and identity in the tumor milieu.

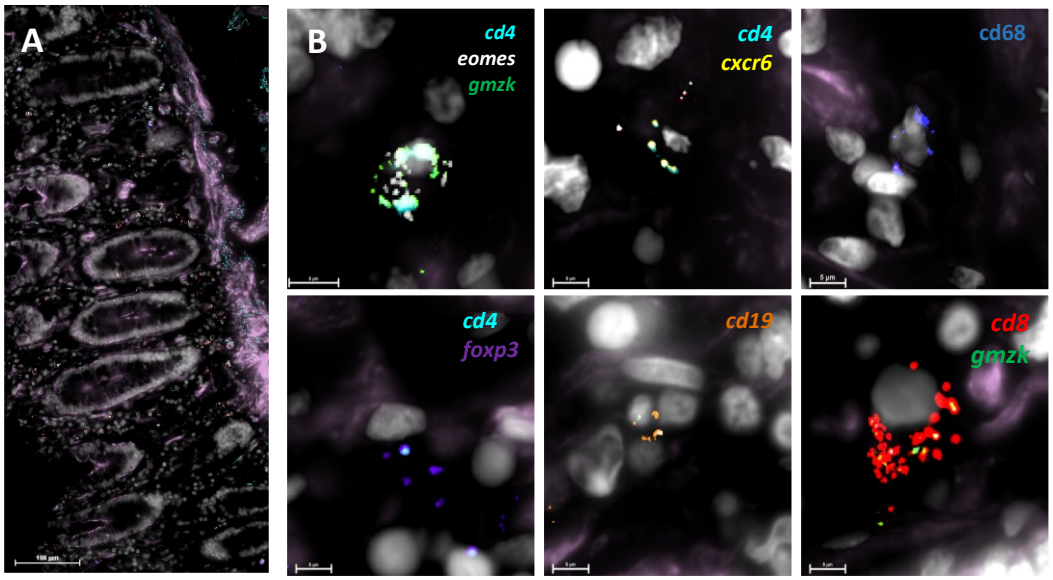

Figure 6. Multi smRNA-FISH performed with 8 probes simoultaneosly on a colorectal sample

A. Multi smRNA-FISH of a colorectal sample stained with 8 RNAfish-probes simultaneously. B. Zoom in of representative cell populations detected in A for a better visualization. Nuclei are shown in grey, Phalloidin in pink, CD4 in light blue, EOMES in white, GZMK in green, CXCR6 in yellow, CD68 in blue, FOXP3 in violet, CD19 in orange, CD8 in red.

REFERENCES

1. Janeway, C.A., Jr., *How the immune system protects the host from infection.* Microbes Infect, 2001. **3**(13): p. 1167-71.
2. Dunn, G.P., et al., *Cancer immunoediting: from immunosurveillance to tumor escape.* Nat Immunol, 2002. **3**(11): p. 991-8.
3. Thomas, L., *On immunosurveillance in human cancer.* Yale J Biol Med, 1982. **55**(3-4): p. 329-33.
4. Burnet, M., *Cancer; a biological approach. I. The processes of control.* Br Med J, 1957. **1**(5022): p. 779-86.
5. Herin, M., et al., *Production of stable cytolytic T-cell clones directed against autologous human melanoma.* Int J Cancer, 1987. **39**(3): p. 390-6.
6. Vigneron, N., *Human Tumor Antigens and Cancer Immunotherapy.* Biomed Res Int, 2015. **2015**: p. 948501.
7. Shinkai, Y., et al., *RAG-2-deficient mice lack mature lymphocytes owing to inability to initiate V(D)J rearrangement.* Cell, 1992. **68**(5): p. 855-67.
8. P, E., *Ueber den jetzigen Stand der Karzinomforschung. Ned Tijdschr Geneeskd.* 1908.
9. Folkman, J., *Tumor angiogenesis: therapeutic implications.* N Engl J Med, 1971. **285**(21): p. 1182-6.
10. Ostroumov, D., et al., *CD4 and CD8 T lymphocyte interplay in controlling tumor growth.* Cell Mol Life Sci, 2018. **75**(4): p. 689-713.
11. De Simone, M., et al., *Transcriptional Landscape of Human Tissue Lymphocytes Unveils Uniqueness of Tumor-Infiltrating T Regulatory Cells.* Immunity, 2016. **45**(5): p. 1135-1147.
12. Bubenik, J. and V. Vonka, *MHC class I status of tumours and design of immunotherapeutic strategies.* Immunol Lett, 2003. **90**(2-3): p. 177-8.
13. Campbell, K.J. and S.W.G. Tait, *Targeting BCL-2 regulated apoptosis in cancer.* Open Biol, 2018. **8**(5).
14. Shimizu, J., S. Yamazaki, and S. Sakaguchi, *Induction of tumor immunity by removing CD25+CD4+ T cells: a common basis between tumor immunity and autoimmunity.* J Immunol, 1999. **163**(10): p. 5211-8.
15. Junttila, M.R. and F.J. de Sauvage, *Influence of tumour micro-environment heterogeneity on therapeutic response.* Nature, 2013. **501**(7467): p. 346-54.
16. Wang, M., et al., *Role of tumor microenvironment in tumorigenesis.* J Cancer, 2017. **8**(5): p. 761-773.
17. Melzer, C., Y. Yang, and R. Hass, *Interaction of MSC with tumor cells.* Cell Commun Signal, 2016. **14**(1): p. 20.
18. Spurrell, E.L. and M. Lockley, *Adaptive immunity in cancer immunology and therapeutics.* Ecancermedicalscience, 2014. **8**: p. 441.
19. Roychoudhuri, R., R.L. Eil, and N.P. Restifo, *The interplay of effector and regulatory T cells in cancer.* Curr Opin Immunol, 2015. **33**: p. 101-11.
20. Dranoff, G., *Cytokines in cancer pathogenesis and cancer therapy.* Nat Rev Cancer, 2004. **4**(1): p. 11-22.

21. Gotwals, P., et al., *Prospects for combining targeted and conventional cancer therapy with immunotherapy.* Nat Rev Cancer, 2017. **17**(5): p. 286-301.
22. Borst, J., et al., *CD4(+) T cell help in cancer immunology and immunotherapy.* Nat Rev Immunol, 2018. **18**(10): p. 635-647.
23. Wang, Y., et al., *The combination of dendritic cells-cytotoxic T lymphocytes/cytokine-induced killer (DC-CTL/CIK) therapy exerts immune and clinical responses in patients with malignant tumors.* Exp Hematol Oncol, 2015. **4**: p. 32.
24. Tumeh, P.C., et al., *PD-1 blockade induces responses by inhibiting adaptive immune resistance.* Nature, 2014. **515**(7528): p. 568-71.
25. Bellone, M. and A. Calcinotto, *Ways to enhance lymphocyte trafficking into tumors and fitness of tumor infiltrating lymphocytes.* Front Oncol, 2013. **3**: p. 231.
26. Chung, A.S. and N. Ferrara, *Targeting the tumor microenvironment with SRC kinase inhibition.* Clin Cancer Res, 2010. **16**(3): p. 775-7.
27. Thomas, D.A. and J. Massague, *TGF-beta directly targets cytotoxic T cell functions during tumor evasion of immune surveillance.* Cancer Cell, 2005. **8**(5): p. 369-80.
28. Schietinger, A., et al., *Tumor-Specific T Cell Dysfunction Is a Dynamic Antigen-Driven Differentiation Program Initiated Early during Tumorigenesis.* Immunity, 2016. **45**(2): p. 389-401.
29. Baitsch, L., et al., *Exhaustion of tumor-specific CD8(+) T cells in metastases from melanoma patients.* J Clin Invest, 2011. **121**(6): p. 2350-60.
30. Gros, A., et al., *PD-1 identifies the patient-specific CD8(+) tumor-reactive repertoire infiltrating human tumors.* J Clin Invest, 2014. **124**(5): p. 2246-59.
31. Gubin, M.M., et al., *Checkpoint blockade cancer immunotherapy targets tumour-specific mutant antigens.* Nature, 2014. **515**(7528): p. 577-81.
32. Pardoll, D.M. and S.L. Topalian, *The role of CD4+ T cell responses in antitumor immunity.* Curr Opin Immunol, 1998. **10**(5): p. 588-94.
33. Zhang, M., et al., *Identification of Melanoma-reactive CD4+ T-Cell Subsets From Human Melanoma Draining Lymph Nodes.* J Immunother, 2016. **39**(1): p. 15-26.
34. O'Shea, J.J. and W.E. Paul, *Mechanisms underlying lineage commitment and plasticity of helper CD4+ T cells.* Science, 2010. **327**(5969): p. 1098-102.
35. Zhu, J., H. Yamane, and W.E. Paul, *Differentiation of effector CD4 T cell populations (*).* Annu Rev Immunol, 2010. **28**: p. 445-89.
36. Szabo, S.J., et al., *A novel transcription factor, T-bet, directs Th1 lineage commitment.* Cell, 2000. **100**(6): p. 655-69.
37. Nakajima, C., et al., *Induction of the chemokine receptor CXCR3 on TCR-stimulated T cells: dependence on the release from persistent TCR-triggering and requirement for IFN-gamma stimulation.* Eur J Immunol, 2002. **32**(6): p. 1792-801.
38. Kaplan, M.H., et al., *Impaired IL-12 responses and enhanced development of Th2 cells in Stat4-deficient mice.* Nature, 1996. **382**(6587): p. 174-7.
39. Zheng, W. and R.A. Flavell, *The transcription factor GATA-3 is necessary and sufficient for Th2 cytokine gene expression in CD4 T cells.* Cell, 1997. **89**(4): p. 587-96.

40. Kurata, H., et al., *Ectopic expression of activated Stat6 induces the expression of Th2-specific cytokines and transcription factors in developing Th1 cells.* Immunity, 1999. **11**(6): p. 677-88.
41. Zhu, J., et al., *Growth factor independent-1 induced by IL-4 regulates Th2 cell proliferation.* Immunity, 2002. **16**(5): p. 733-44.
42. Jabeen, R. and M.H. Kaplan, *The symphony of the ninth: the development and function of Th9 cells.* Curr Opin Immunol, 2012. **24**(3): p. 303-7.
43. Sakaguchi, S., et al., *T cell-mediated maintenance of natural self-tolerance: its breakdown as a possible cause of various autoimmune diseases.* J Autoimmun, 1996. **9**(2): p. 211-20.
44. Fontenot, J.D., M.A. Gavin, and A.Y. Rudensky, *Foxp3 programs the development and function of CD4+CD25+ regulatory T cells.* Nat Immunol, 2003. **4**(4): p. 330-6.
45. Hori, S., T. Nomura, and S. Sakaguchi, *Control of regulatory T cell development by the transcription factor Foxp3.* Science, 2003. **299**(5609): p. 1057-61.
46. Sharma, R., et al., *X-linked Foxp3 (Scurfy) mutation dominantly inhibits submandibular gland development and inflammation respectively through adaptive and innate immune mechanisms.* J Immunol, 2009. **183**(5): p. 3212-8.
47. Torgerson, T.R., et al., *Severe food allergy as a variant of IPEX syndrome caused by a deletion in a noncoding region of the FOXP3 gene.* Gastroenterology, 2007. **132**(5): p. 1705-17.
48. Wu, Y., et al., *FOXP3 controls regulatory T cell function through cooperation with NFAT.* Cell, 2006. **126**(2): p. 375-87.
49. Bettelli, E., M. Dastrange, and M. Oukka, *Foxp3 interacts with nuclear factor of activated T cells and NF-kappa B to repress cytokine gene expression and effector functions of T helper cells.* Proc Natl Acad Sci U S A, 2005. **102**(14): p. 5138-43.
50. Ono, M., et al., *Foxp3 controls regulatory T-cell function by interacting with AML1/Runx1.* Nature, 2007. **446**(7136): p. 685-9.
51. Du, J., et al., *Isoform-specific inhibition of ROR alpha-mediated transcriptional activation by human FOXP3.* J Immunol, 2008. **180**(7): p. 4785-92.
52. Zheng, Y., et al., *Genome-wide analysis of Foxp3 target genes in developing and mature regulatory T cells.* Nature, 2007. **445**(7130): p. 936-40.
53. Chaudhry, A., et al., *CD4+ regulatory T cells control TH17 responses in a Stat3-dependent manner.* Science, 2009. **326**(5955): p. 986-91.
54. Lee, S.M., B. Gao, and D. Fang, *FoxP3 maintains Treg unresponsiveness by selectively inhibiting the promoter DNA-binding activity of AP-1.* Blood, 2008. **111**(7): p. 3599-606.
55. Marson, A., et al., *Foxp3 occupancy and regulation of key target genes during T-cell stimulation.* Nature, 2007. **445**(7130): p. 931-5.
56. Arce-Sillas, A., et al., *Regulatory T Cells: Molecular Actions on Effector Cells in Immune Regulation.* J Immunol Res, 2016. **2016**: p. 1720827.
57. Taylor, A., et al., *Mechanisms of immune suppression by interleukin-10 and transforming growth factor-beta: the role of T regulatory cells.* Immunology, 2006. **117**(4): p. 433-42.

58. Gondek, D.C., et al., *Cutting edge: contact-mediated suppression by CD4+CD25+ regulatory cells involves a granzyme B-dependent, perforin-independent mechanism.* J Immunol, 2005. **174**(4): p. 1783-6.
59. Grossman, W.J., et al., *Human T regulatory cells can use the perforin pathway to cause autologous target cell death.* Immunity, 2004. **21**(4): p. 589-601.
60. Read, S., V. Malmstrom, and F. Powrie, *Cytotoxic T lymphocyte-associated antigen 4 plays an essential role in the function of CD25(+)CD4(+) regulatory cells that control intestinal inflammation.* J Exp Med, 2000. **192**(2): p. 295-302.
61. Schneider, H., et al., *CTLA-4 regulation of T cell function via RAP-1-mediated adhesion.* Adv Exp Med Biol, 2006. **584**: p. 115-26.
62. Soliman, H., M. Mediavilla-Varela, and S. Antonia, *Indoleamine 2,3-dioxygenase: is it an immune suppressor?* Cancer J, 2010. **16**(4): p. 354-9.
63. Liang, B., et al., *Regulatory T cells inhibit dendritic cells by lymphocyte activation gene-3 engagement of MHC class II.* J Immunol, 2008. **180**(9): p. 5916-26.
64. Klein, M. and T. Bopp, *Cyclic AMP Represents a Crucial Component of Treg Cell-Mediated Immune Regulation.* Front Immunol, 2016. **7**: p. 315.
65. Zorn, E., et al., *IL-2 regulates FOXP3 expression in human CD4+CD25+ regulatory T cells through a STAT-dependent mechanism and induces the expansion of these cells in vivo.* Blood, 2006. **108**(5): p. 1571-9.
66. Bayer, A.L., A. Pugliese, and T.R. Malek, *The IL-2/IL-2R system: from basic science to therapeutic applications to enhance immune regulation.* Immunol Res, 2013. **57**(1-3): p. 197-209.
67. Groux, H., et al., *A CD4+ T-cell subset inhibits antigen-specific T-cell responses and prevents colitis.* Nature, 1997. **389**(6652): p. 737-42.
68. Bacchetta, R., et al., *High levels of interleukin 10 production in vivo are associated with tolerance in SCID patients transplanted with HLA mismatched hematopoietic stem cells.* J Exp Med, 1994. **179**(2): p. 493-502.
69. Maynard, C.L., et al., *Regulatory T cells expressing interleukin 10 develop from Foxp3+ and Foxp3- precursor cells in the absence of interleukin 10.* Nat Immunol, 2007. **8**(9): p. 931-41.
70. Gagliani, N., et al., *Coexpression of CD49b and LAG-3 identifies human and mouse T regulatory type 1 cells.* Nat Med, 2013. **19**(6): p. 739-46.
71. Camisaschi, C., et al., *LAG-3 expression defines a subset of CD4(+)CD25(high)Foxp3(+) regulatory T cells that are expanded at tumor sites.* J Immunol, 2010. **184**(11): p. 6545-51.
72. Lino, A.C., et al., *LAG-3 Inhibitory Receptor Expression Identifies Immunosuppressive Natural Regulatory Plasma Cells.* Immunity, 2018. **49**(1): p. 120-133 e9.
73. Simonetta, F., A. Pradier, and E. Roosnek, *T-bet and Eomesodermin in NK Cell Development, Maturation, and Function.* Front Immunol, 2016. **7**: p. 241.
74. Zhang, P., et al., *Eomesodermin promotes the development of type 1 regulatory T (TR1) cells.* Sci Immunol, 2017. **2**(10).

75. Gruarin, P., et al., *Eomesodermin controls a unique differentiation program in human IL-10 and IFN-gamma coproducing regulatory T cells.* Eur J Immunol, 2019. **49**(1): p. 96-111.
76. Geginat, J., et al., *The CD4-centered universe of human T cell subsets.* Semin Immunol, 2013. **25**(4): p. 252-62.
77. Roncarolo, M.G., et al., *Interleukin-10-secreting type 1 regulatory T cells in rodents and humans.* Immunol Rev, 2006. **212**: p. 28-50.
78. de Waal Malefyt, R., et al., *Interleukin 10(IL-10) inhibits cytokine synthesis by human monocytes: an autoregulatory role of IL-10 produced by monocytes.* J Exp Med, 1991. **174**(5): p. 1209-20.
79. Fiorentino, D.F., et al., *IL-10 acts on the antigen-presenting cell to inhibit cytokine production by Th1 cells.* J Immunol, 1991. **146**(10): p. 3444-51.
80. Mosser, D.M. and X. Zhang, *Interleukin-10: new perspectives on an old cytokine.* Immunol Rev, 2008. **226**: p. 205-18.
81. Meiler, F., et al., *In vivo switch to IL-10-secreting T regulatory cells in high dose allergen exposure.* J Exp Med, 2008. **205**(12): p. 2887-98.
82. Magnani, C.F., et al., *Killing of myeloid APCs via HLA class I, CD2 and CD226 defines a novel mechanism of suppression by human Tr1 cells.* Eur J Immunol, 2011. **41**(6): p. 1652-62.
83. Hu, G., Z. Li, and S. Wang, *Tumor-infiltrating FoxP3(+) Tregs predict favorable outcome in colorectal cancer patients: A meta-analysis.* Oncotarget, 2017. **8**(43): p. 75361-75371.
84. Schaefer, C., et al., *Characteristics of CD4+CD25+ regulatory T cells in the peripheral circulation of patients with head and neck cancer.* Br J Cancer, 2005. **92**(5): p. 913-20.
85. Wolf, A.M., et al., *Increase of regulatory T cells in the peripheral blood of cancer patients.* Clin Cancer Res, 2003. **9**(2): p. 606-12.
86. Ormandy, L.A., et al., *Increased populations of regulatory T cells in peripheral blood of patients with hepatocellular carcinoma.* Cancer Res, 2005. **65**(6): p. 2457-64.
87. Sasada, T., et al., *CD4+CD25+ regulatory T cells in patients with gastrointestinal malignancies: possible involvement of regulatory T cells in disease progression.* Cancer, 2003. **98**(5): p. 1089-99.
88. Liyanage, U.K., et al., *Prevalence of regulatory T cells is increased in peripheral blood and tumor microenvironment of patients with pancreas or breast adenocarcinoma.* J Immunol, 2002. **169**(5): p. 2756-61.
89. Curiel, T.J., et al., *Specific recruitment of regulatory T cells in ovarian carcinoma fosters immune privilege and predicts reduced survival.* Nat Med, 2004. **10**(9): p. 942-9.
90. Mougiakakos, D., et al., *Intratumoral forkhead box P3-positive regulatory T cells predict poor survival in cyclooxygenase-2-positive uveal melanoma.* Cancer, 2010. **116**(9): p. 2224-33.
91. Nishikawa, H. and S. Sakaguchi, *Regulatory T cells in tumor immunity.* Int J Cancer, 2010. **127**(4): p. 759-67.

92. Varney, M.L., S.L. Johansson, and R.K. Singh, *Tumour-associated macrophage infiltration, neovascularization and aggressiveness in malignant melanoma: role of monocyte chemotactic protein-1 and vascular endothelial growth factor-A.* Melanoma Res, 2005. **15**(5): p. 417-25.
93. Yan, H., et al., *Primary Tr1 cells from metastatic melanoma eliminate tumor-promoting macrophages through granzyme B- and perforin-dependent mechanisms.* Tumour Biol, 2017. **39**(4): p. 1010428317697554.
94. Chen, J. and Z. Chen, *The effect of immune microenvironment on the progression and prognosis of colorectal cancer.* Med Oncol, 2014. **31**(8): p. 82.
95. Viehl, C.T., et al., *Depletion of CD4+CD25+ regulatory T cells promotes a tumor-specific immune response in pancreas cancer-bearing mice.* Ann Surg Oncol, 2006. **13**(9): p. 1252-8.
96. Callahan, M.K., J.D. Wolchok, and J.P. Allison, *Anti-CTLA-4 antibody therapy: immune monitoring during clinical development of a novel immunotherapy.* Semin Oncol, 2010. **37**(5): p. 473-84.
97. Brunet, J.F., et al., *A new member of the immunoglobulin superfamily--CTLA-4.* Nature, 1987. **328**(6127): p. 267-70.
98. Thompson, C.B. and J.P. Allison, *The emerging role of CTLA-4 as an immune attenuator.* Immunity, 1997. **7**(4): p. 445-50.
99. Waterhouse, P., et al., *Lymphoproliferative disorders with early lethality in mice deficient in Ctla-4.* Science, 1995. **270**(5238): p. 985-8.
100. Peggs, K.S., et al., *Blockade of CTLA-4 on both effector and regulatory T cell compartments contributes to the antitumor activity of anti-CTLA-4 antibodies.* J Exp Med, 2009. **206**(8): p. 1717-25.
101. Perkins, D., et al., *Regulation of CTLA-4 expression during T cell activation.* J Immunol, 1996. **156**(11): p. 4154-9.
102. Mahoney, K.M., G.J. Freeman, and D.F. McDermott, *The Next Immune-Checkpoint Inhibitors: PD-1/PD-L1 Blockade in Melanoma.* Clin Ther, 2015. **37**(4): p. 764-82.
103. Alsaab, H.O., et al., *PD-1 and PD-L1 Checkpoint Signaling Inhibition for Cancer Immunotherapy: Mechanism, Combinations, and Clinical Outcome.* Front Pharmacol, 2017. **8**: p. 561.
104. Callahan, M.K., M.A. Postow, and J.D. Wolchok, *CTLA-4 and PD-1 Pathway Blockade: Combinations in the Clinic.* Front Oncol, 2014. **4**: p. 385.
105. Topalian, S.L., C.G. Drake, and D.M. Pardoll, *Immune checkpoint blockade: a common denominator approach to cancer therapy.* Cancer Cell, 2015. **27**(4): p. 450-61.
106. Lee, H.T., S.H. Lee, and Y.S. Heo, *Molecular Interactions of Antibody Drugs Targeting PD-1, PD-L1, and CTLA-4 in Immuno-Oncology.* Molecules, 2019. **24**(6).
107. Mellman, I., et al., *De-Risking Immunotherapy: Report of a Consensus Workshop of the Cancer Immunotherapy Consortium of the Cancer Research Institute.* Cancer Immunol Res, 2016. **4**(4): p. 279-88.
108. Sun, X., et al., *Immune-related adverse events associated with programmed cell death protein-1 and programmed cell death ligand 1 inhibitors for non-small cell*

lung cancer: a PRISMA systematic review and meta-analysis. BMC Cancer, 2019. **19**(1): p. 558.
109. Bray, F., et al., *Global cancer statistics 2018: GLOBOCAN estimates of incidence and mortality worldwide for 36 cancers in 185 countries.* CA Cancer J Clin, 2018. **68**(6): p. 394-424.
110. Van Cutsem, E., et al., *ESMO consensus guidelines for the management of patients with metastatic colorectal cancer.* Ann Oncol, 2016. **27**(8): p. 1386-422.
111. Boland, C.R. and A. Goel, *Microsatellite instability in colorectal cancer.* Gastroenterology, 2010. **138**(6): p. 2073-2087 e3.
112. Guinney, J., et al., *The consensus molecular subtypes of colorectal cancer.* Nat Med, 2015. **21**(11): p. 1350-6.
113. Zappa, C. and S.A. Mousa, *Non-small cell lung cancer: current treatment and future advances.* Transl Lung Cancer Res, 2016. **5**(3): p. 288-300.
114. Pao, W. and V.A. Miller, *Epidermal growth factor receptor mutations, small-molecule kinase inhibitors, and non-small-cell lung cancer: current knowledge and future directions.* J Clin Oncol, 2005. **23**(11): p. 2556-68.
115. Turke, A.B., et al., *Preexistence and clonal selection of MET amplification in EGFR mutant NSCLC.* Cancer Cell, 2010. **17**(1): p. 77-88.
116. McGranahan, N., et al., *Clonal neoantigens elicit T cell immunoreactivity and sensitivity to immune checkpoint blockade.* Science, 2016. **351**(6280): p. 1463-9.
117. Holmgaard, R.B., et al., *Indoleamine 2,3-dioxygenase is a critical resistance mechanism in antitumor T cell immunotherapy targeting CTLA-4.* J Exp Med, 2013. **210**(7): p. 1389-402.
118. Gettinger, S., et al., *Impaired HLA Class I Antigen Processing and Presentation as a Mechanism of Acquired Resistance to Immune Checkpoint Inhibitors in Lung Cancer.* Cancer Discov, 2017. **7**(12): p. 1420-1435.
119. Facciotti, F., et al., *IL-10-producing forkhead box protein 3-negative regulatory T cells inhibit B-cell responses and are involved in systemic lupus erythematosus.* J Allergy Clin Immunol, 2016. **137**(1): p. 318-321 e5.
120. Alfen, J.S., et al., *Intestinal IFN-gamma-producing type 1 regulatory T cells coexpress CCR5 and programmed cell death protein 1 and downregulate IL-10 in the inflamed guts of patients with inflammatory bowel disease.* J Allergy Clin Immunol, 2018.
121. Subramanian, A., et al., *Gene set enrichment analysis: a knowledge-based approach for interpreting genome-wide expression profiles.* Proc Natl Acad Sci U S A, 2005. **102**(43): p. 15545-50.
122. Lugli, E., et al., *FACS Analysis of Memory T Lymphocytes.* Methods Mol Biol, 2017. **1514**: p. 31-47.
123. Plitas, G., et al., *Regulatory T Cells Exhibit Distinct Features in Human Breast Cancer.* Immunity, 2016. **45**(5): p. 1122-1134.
124. Tirosh, I., et al., *Dissecting the multicellular ecosystem of metastatic melanoma by single-cell RNA-seq.* Science, 2016. **352**(6282): p. 189-96.
125. Sato, M., et al., *Human lung epithelial cells progressed to malignancy through specific oncogenic manipulations.* Mol Cancer Res, 2013. **11**(6): p. 638-50.

126. Smith, J.J., et al., *Experimentally derived metastasis gene expression profile predicts recurrence and death in patients with colon cancer.* Gastroenterology, 2010. **138**(3): p. 958-68.
127. Libreros, S. and V. Iragavarapu-Charyulu, *YKL-40/CHI3L1 drives inflammation on the road of tumor progression.* J Leukoc Biol, 2015. **98**(6): p. 931-6.
128. Pouyafar, A., et al., *Angiogenic potential of YKL-40 in the dynamics of tumor niche.* Biomed Pharmacother, 2018. **100**: p. 478-485.

ACKNOWLEDGMENTS

This work was supported by the AIRC foundation (Grants n: IG 18575; Airc 5x1000 Metastatic Desease, n. 21091).

This thesis was evaluated by one reviewer: **Dr. Jens Geginat**, Fondazione Istituto Nazionale Genetica Molecolare – INGM Padiglione “Romeo ed Enrica Invernizzi”, Via Francesco Sforza, 35 – 20122 Milano, Italia

SCIENTIFIC PRODUCTS

Gruarin, P. , Maglie, S. , Simone, M. , Häringer, B. , Vasco, C. , Ranzani, V. , Bosotti, R. , Noddings, J. S., Larghi, P. , Facciotti, F. , Sarnicola, M. L., Martinovic, M. , Crosti, M. , Moro, M. , Rossi, R. L., Bernardo, M. E., Caprioli, F. , Locatelli, F. , Rossetti, G. , Abrignani, S. , Pagani, M. and Geginat, J. (2019), **Eomesodermin controls a unique differentiation program in human IL-10 and IFN-γ coproducing regulatory T cells**. Eur. J. Immunol., 49: 96-111. doi:10.1002/eji.201847722

DOI: 10.1002/eji.201847722 Eur. J. Immunol. 2019. 49: 96–111

European Journal of Immunology

Adaptive immunity

Research Article

Eomesodermin controls a unique differentiation program in human IL-10 and IFN-γ coproducing regulatory T cells

Paola Gruarin[*1], Stefano Maglie*[*1], Marco De Simone*[*1], Barbara Häringer*[*2,3], Chiara Vasco[1], Valeria Ranzani[1], Roberto Bosotti[1], Johanna S. Noddings[1], Paola Larghi[1], Federica Facciotti[1], Maria L. Sarnicola[1], Martina Martinovic[1], Mariacristina Crosti[1], Monica Moro[1], Riccardo L. Rossi[1], Maria E. Bernardo[4], Flavio Caprioli[5], Franco Locatelli[4], Grazisa Rossetti[1], Sergio Abrignani[1,6], Massimiliano Pagani[1,7] and Jens Geginat[1]*

[1] INGM-National Institute of Molecular Genetics "Romeo ed Enrica Invernizzi", Milan, Italy
[2] German Rheumatology Research Center DRFZ, Berlin, Germany
[3] Charitè Research Center for Immunosciences RCIS, Berlin, Germany
[4] Ospedale Pediatrico Bambino Gesù, Dipartimento Onco–Ematologia e Medicina Trasfusionale, Rome, Italy
[5] Unità Operativa di Gastroenterologia ed Endoscopia, Fondazione Ca' Granda Ospedale Maggiore Policlinico, Milan, Italy
[6] Department of Clinical Science and Community Health (DISCCO), University of Milan, Milan, Italy
[7] Department of Medical Biotechnology and Translational Medicine, University of Milan, Milan, Italy

Whether human IL-10-producing regulatory T cells ("Tr1") represent a distinct differentiation lineage or an unstable activation stage remains a key unsolved issue. Here, we report that Eomesodermin (Eomes) acted as a lineage-defining transcription factor in human IFN-γ/IL-10 coproducing Tr1-like cells. In vivo occurring Tr1-like cells expressed Eomes, and were clearly distinct from all other CD4$^+$ T-cell subsets, including conventional cytotoxic CD4$^+$ T cells. They expressed Granzyme (Gzm) K, but had lost CD40L and IL-7R expression. Eomes antagonized the Th17 fate, and directly controlled IFN-γ and GzmK expression. However, Eomes binding to the IL-10 promoter was not detectable in human CD4$^+$ T cells, presumably because critical Tbox binding sites of the mouse were not conserved. A precommitment to a Tr1-like fate, i.e. concominant induction of Eomes, GzmK, and IFN-γ, was promoted by IL-4 and IL-12-secreting myeloid dendritic cells. Consistently, Th1 effector memory cells contained precommitted Eomes$^+$GzmK$^+$ T cells. Stimulation with T-cell receptor (TCR) agonists and IL-27 promoted the generation of Tr1-like effector cells by inducing switching from CD40L to IL-10. Importantly, CD4$^+$Eomes$^+$ T-cell subsets were present in lymphoid and nonlymphoid tissues, and their frequencies varied systemically in patients with inflammatory bowel disease and graft-versus-host disease. We propose that Eomes$^+$ Tr1-like cells are effector cells of a unique GzmK-expressing CD4$^+$ T-cell subset.

Keywords: Differentiation · EOMES · Granzyme K · Regulatory T cells · Th17

See accompanying Commentary by Dejean et al.

Additional supporting information may be found online in the Supporting Information section at the end of the article.

Correspondence: Dr. Jens Geginat
e-mail: geginat@ingm.org

*These authors contributed equally to this work.

Introduction

Immune responses have to be tightly regulated to prevent autoimmunity or overactive immune responses against commensals or pathogens that could lead to immunopathology. Regulatory T cells are specialized cells that fulfill this task, as evidenced by the devastating autoimmune phenotype of mice and patients with genetic disorders with depleted numbers of regulatory T cells [1]. Prototypical regulatory T-cells express CD25 and the transcription factor FOXP3, which regulates several key features of Tregs and distinguishes them from conventional $CD4^+$ T cells [2]. However, it is also well-established that some $Foxp3^-$ T cells possess regulatory functions and might play a nonredundant role in several immune-mediated diseases. In particular, T cells that secrete the anti-inflammatory cytokine IL-10, so-called type 1 regulatory T cells (Tr1), have also been identified [3], and it is becoming increasingly clear that they are a second principal regulatory T-cell subset of the immune system [4, 5]. However, in contrast to $FOXP3^+$ Tregs, and other defined $CD4^+$ T-cell subsets, such as Th1, Th2, and Th17 cells, the molecular identity of Tr1 cells is still enigmatic, in particular, in humans. Features of Tr1 cells are IL-10 production and several researchers also reported GzmB expression, which endows them with suppressive and cytotoxic functions, respectively [6, 7]. Moreover, Tr1 cells express several checkpoint receptors, such as programed cell death protein 1 (PD1), T-cell immunoglobulin and mucin-domain containing-3 (TIM3), Cytotoxic T-Lymphocyte Antigen 4 (CTLA-4), and Lymphocyte-activation gene 3 (LAG3) [8, 9]. However, neither IL-10 production [10] nor GzmB or checkpoint receptor expression are unique properties of Tr1 cells [11]. Rather, IL-10 is also produced by helper T cells, including T_{FH} cells that promote B-cell responses [10]. Similarly, GzmB is expressed by the large majority of cytotoxic T cells [12], which are abundant among $CD8^+$ T cells, but are also present at low frequencies in the CD4 compartment [13, 14]. Finally, checkpoint receptors are also expressed on other $CD4^+$ T-cell subset, namely $FOXP3^+$Tregs and follicular helper T (T_{FH}) cells that express high levels of CTLA-4 and PD1, respectively. Several transcription factors that regulate IL-10 production in helper and Tr1 cells have been described [7, 15–18], including c-Maf, AHR, and Blimp-1, yet they are not unique to Tr1 cells and are, therefore, insufficient to define Tr1-cells. Indeed, it is still debated if Tr1 cells are only a transient and unstable activation stage of conventional $CD4^+$ T cells [19], or if they represent a unique differentiation stage similar to $Foxp3^+$Tregs [4]. Moreover, while it was originally assumed that Tr1 cells express little or no IFN-γ, it is now clear that IL-10 and IFN-γ coproducing regulatory T cells exist [19, 20], consistent with the findings that IFN-γ can have anti-inflammatory functions under certain conditions. Several protocols to induce Tr1 cells in vitro have been published, including cytokines, such as IL-10 and IFN-α [21] or IL-27 [15] and APCs such as immature DC, IL-10 secreting monocyte-derived DC [22], or plasmacytoid DC (pDC) [23, 24]. In mice, Tr1 cells can be easily identified in IL-10 and Foxp3 reporter mice, or by CD49b and/or LAG-3 expression [8]. LAG3 was also proposed to be a useful surface marker for Tr1 cells in humans [8, 9], but in vivo occurring humans Tr1 cells are still poorly characterized. We have published an alternative strategy to identify human IL-10 and IFN-γ coproducing Tr1-like cells directly ex vivo. These Tr1-like cells are strongly enriched among $CD4^+CD25^-IL\text{-}7R^-$ effector T cells [25, 26], and coexpress CCR5 and PD-1 in lymphoid and nonlymphoid human tissues [26]. They showed selective functional defects in systemic lupus erythematosus [26] and inflammatory bowel diseases (IBDs) [27]. Here, we performed a genome-wide gene expression analysis to provide a molecular blueprint of these in vivo occurring Tr1-like cells. We identified the Tbox transcription factor Eomes as a key regulator, which induced a unique cytotoxic differentiation program that unequivocally distinguishes them from all other $CD4^+$ T cells.

Results

Human IL-10 and IFN-γ coproducing Tr1-like cells express the transcription factor Eomes

We previously showed that IL-10 and IFN-γ coproducing effector cells with Tr1-like regulatory function are present among $CD4^+IL\text{-}7R^-CD25^-$ T-cells ("$IL\text{-}7R^-$") in human peripheral blood of healthy individuals [25]. To provide a molecular blueprint of these in vivo occurring Tr1-like cells, we performed a genome-wide gene expression analysis of $IL\text{-}7R^-$ T cells that secreted IL-10 following brief polyclonal stimulation ex vivo (Supporting Information Fig. 1A). As control, we purified the abundant $CD4^+IL\text{-}7R^+CD25^{lo}$helper T cells ("$IL\text{-}7R^+$") according to IL-10 secretion (Supporting Information Fig. 1A and B). A total of 83 genes were selectively and significantly upregualted and 81 downregulated in IL-10-secreting $IL\text{-}7R^-$ T cells as compared to IL-10-secreting $IL\text{-}7R^+$ T cells and to control populations that failed to produce IL-10 (Supporting Information Table 1). Strikingly, the strongest upregulated gene was Eomesodermin (Eomes, Fig. 1A and Supporting Information Fig. 1C), a Tbox transcription factor that controls cytotoxic functions of $CD8^+$ T cells and NK cells. In addition, among the most strongly upregulated genes there were two cytotoxic molecules, Granzyme (Gzm) A and GzmK, and several surface receptors, including CD27, LAG3, TIM3 (HAVCR2), and 4-1BB (TNFRSF9, Fig. 1A and Supporting Information Table 1). Among the most downregulated genes, we identified several proinflammatory cytokines and chemokines, including IL-22, GM-CSF (CSF2), IL-17F, IL-8, as well as the transcription factors RAR-related orphan nuclear receptor (ROR)α (HS_560343, Fig. 1A and Supporting Information Table 1). Of note, only a low number of genes were specifically up- or downregulated in IL-10 producing $IL\text{-}7R^+$ control T cells (Supporting Information Fig. 1B). The selective expression of Eomes in Tr1-like cells was confirmed at the protein level by intracellular staining. Thus, the majority of IL-10-producing $IL\text{-}7R^-$ T cells expressed Eomes, whereas $IL\text{-}10^+IL\text{-}7R^+$ control cells expressed only low levels (Fig. 1B). Moreover, among $IL\text{-}7R^-$ T cells, Eomes was expressed in the large majority of IL-10 and IFN-γ coproducing cells, but was largely undetectable in cells that lacked IL-10 and IFN-γ producing capacities (Fig. 1C

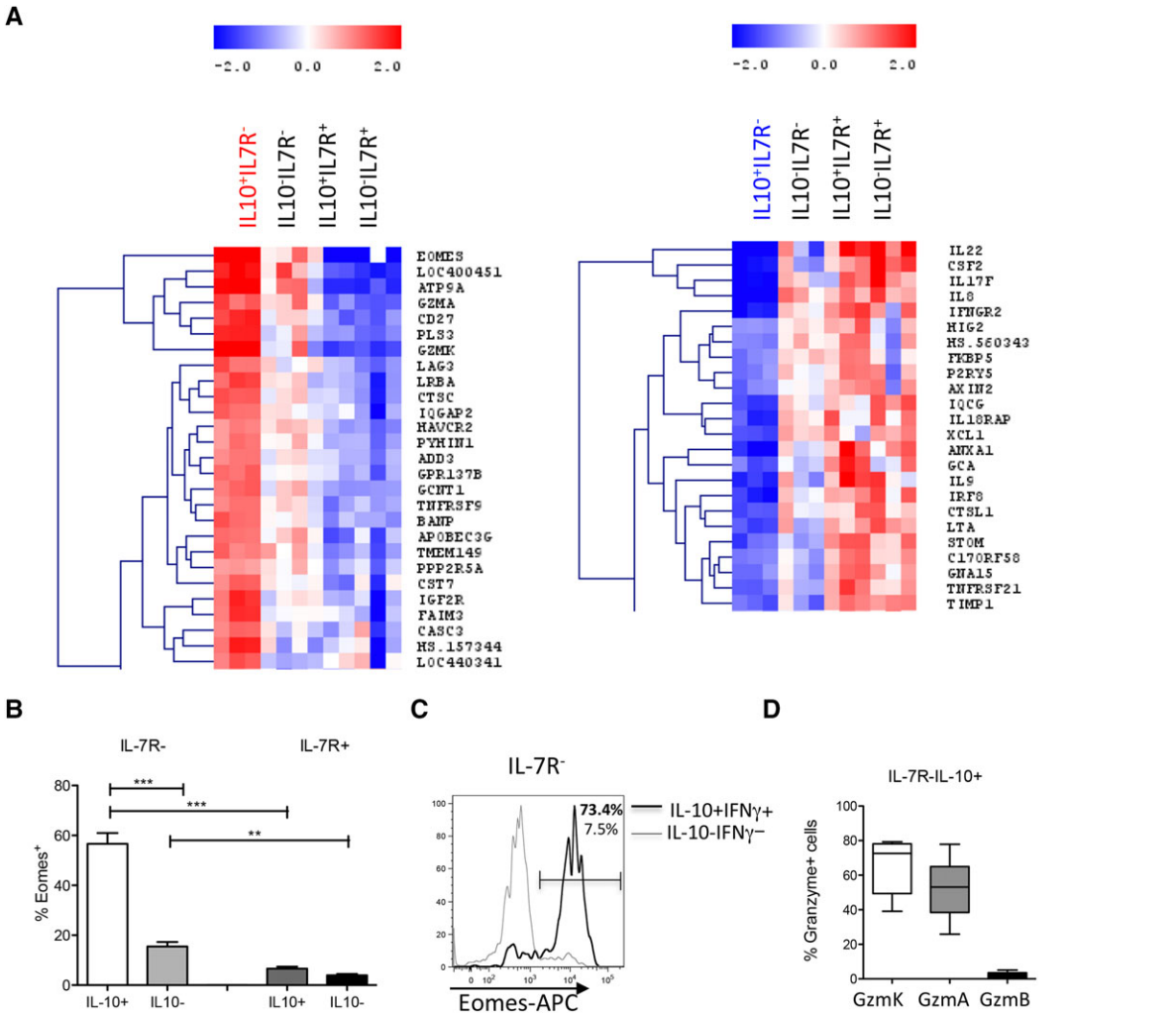

Figure 1. Eomes is highly expressed in human IL-10/IFN-γ coproducing Tr1-like cells. (A) Gene expression analysis of presorted CD4$^+$IL-7R$^+$ and IL-7R$^-$CD25$^-$ T-cell subsets purified from human peripheral blood according to IL-10 secretion, following brief stimulation with PdBu and Ionomycin (Supporting Information Fig. 1A). Heat Map of selectively up- (red, left panel) and downregulated (blue, right panel) genes in IL-7R-IL-10$^+$ Tr1-like cells from peripheral blood as compared to the indicated control populations. Data are from the three donors who were analyzed in the same experiment. (B) Percentages of Eomes$^+$ cells among CD4$^+$IL-7R$^+$ and IL-7R$^-$ T-cell subsets that did or did not produce IL-10 (cells from 16 different donors analyzed in eight experiments) were analyzed by flow cytometry. (C) Eomes protein expression in gated IL-10$^-$IFN-γ$^-$ (dotted line) and IL-10$^+$IFN-γ$^+$ (bold line) cells in purified CD4$^+$IL-7R$^-$ T cells. Numbers indicate the percentage of Eomes$^+$ cells. (D) Intracellular GzmK, A, and B expression in gated IL-10$^+$cells among purified CD4$^+$IL-7R$^-$ T cells (cells from five (GzmB), six (GzmA), or eight (GzmK) donors analyzed in three (GzmB/A) or four (GzmK) experiments). Data from different experiments were pooled and shown as mean + SEM, **/***$p < 0.005/0.00005$ according to statistical analysis with One-way ANOVA.

and Supporting Information Fig. 1D). IL-10$^+$ IL-7R$^-$ Tr1-like cells expressed also high levels of GzmK and GzmA proteins, while GzmB was hardly detectable (Fig. 1D).

In summary, the gene expression analysis revealed that IL-10 and IFN-γ coproducing Tr1-like cells had a unique gene signature, and expressed in particular high levels of the transcription factor Eomes and selected cytotoxic proteins.

Eomes$^+$ Tr1-like cells are distinct from conventional helper and regulatory T cells

Genes of proinflammatory Th17 cells were strongly downregulated in IL-7R$^-$ Tr1 cells (Fig. 1A), suggesting that they were distinct from Th17 cells. Consistently, Eomes$^+$ CD4$^+$ T cells produced high levels of IFN-γ upon stimulation, while IL-17A protein was hardly detectable (Fig. 2A). This was also true for IL-7R$^-$CD4$^+$Eomes$^+$ T cells, which were also negative for the Th17-associated chemokine receptor CCR6 (Supporting Information Fig. 2A) and failed to produce IL-17F, GM-CSF, and IL-22 (data not shown). We then asked how Eomes$^+$ Tr1-like cells were related to conventional regulatory T cells, i.e. CD25$^+$IL-7R^{lo}Tregs ("CD25$^+$"), which express FOXP3. Among total CD4$^+$ T cells, there were two distinct populations of FOXP3$^+$ and Eomes$^+$ cells, while Eomes and FOXP3 co-expressing cells were hardly detectable (Supporting Information Fig. 2B). Furthermore, CD25$^+$Tregs expressed, as expected, high levels of FOXP3, but

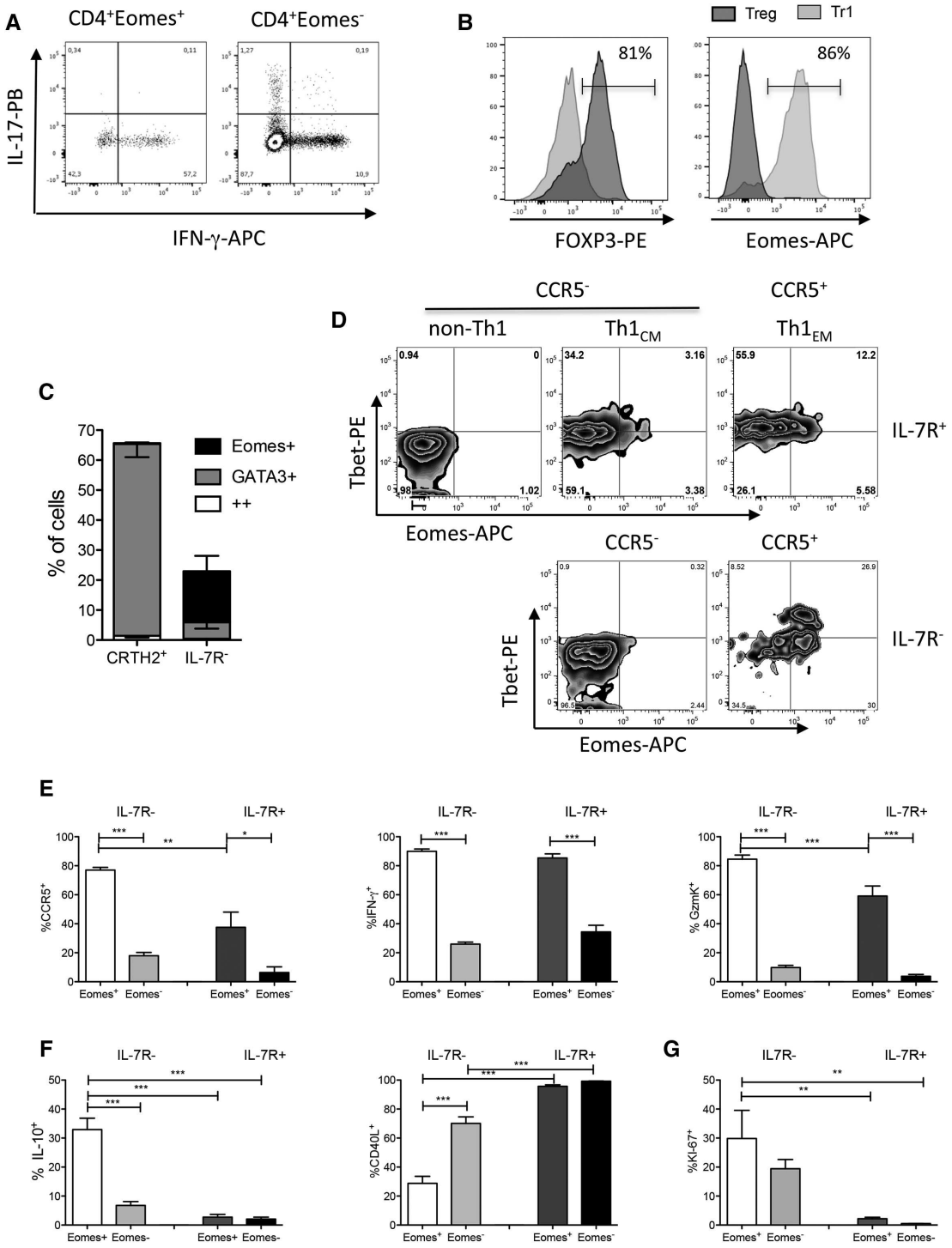

Figure 2. Eomes$^+$Tr1-like cells in human blood are distinct from established CD4$^+$ T-cell subsets. CD4$^+$ T cells from human PBMC were analyzed by flow cytometry. (A) IFN-γ versus IL-17 production in gated CD4$^+$Eomes$^+$ (upper panel) and CD4$^+$Eomes$^-$ T cells (lower panel) was analyzed by flow cytometry. (B) Histogram overlays showing Foxp3 (left) and Eomes (right) expression in CD25$^+$IL-7R^{lo}Tregs (dark grey) and CCR5$^+$CCR6$^-$PD1$^+$IL-7R$^-$Tr1-like cells (light grey). Percentages indicate Foxp3 expression in Tregs and Eomes expression in Tr1 cells. (C) Intracellular GATA3 or Eomes protein expression in gated CRTH2$^+$Th2-cells and Tr1-containing IL-7R$^-$ T cells (four experiments with four different donors). (D) Ex vivo Eomes versus T-bet protein expression in CXCR3$^-$IL-7R$^+$ non-Th1" cells, in CXCR3$^+$IL-7R$^+$Th1 subsets (CCR5$^-$:Th1$_{CM}$/CCR5$^+$:Th1$_{EM}$), and in IL-7R$^-$ cells gated according to CCR5 expression. (E–G) Analysis of CD4$^+$CD25$^-$ T-cells according to Eomes and IL-7R expression. (E) CCR5 expression (cells from four different donors analyzed in three experiments), IFN-γ production (middle, cells from 17 different donors analyzed in nine experiments), and GzmK expression (right, cells from eight different donors analyzed in four experiments). (F) IL-10 production (left, cells from 15 donors analyzed in nine experiments) and CD40L upregulation (right, cells from seven donors analyzed in four experiments) (G) Ex vivo Ki-67 expression (cells from six donors analyzed in two experiments). Data from different experiments were pooled and shown as mean + SEM, */**/***$p < 0.05/0.005/0.00005$ according to statistical analysis with One-way ANOVA.

not Eomes (Supporting Information Fig. 2C and D). Importantly, when all surface receptors that are associated with IL-10 and IFN-γ coproduction [25–27] were combined, a very efficient enrichment for Eomes-expressing cells was achieved, and Foxp3$^+$ cells were excluded (Fig. 2B and Supporting Information Fig. 2C and D). Tr1-like cells were also distinct from Th2 cells, since circulating CRTH2$^+$ Th2 cells [28] expressed high levels of the lineage-defining transcription factor GATA3, but little or no Eomes (Fig. 2C). Moreover, although some Eomes$^+$IL-7R$^-$ Tr1-like cells coproduced IL-4 and IFN-γ ([25] and data not shown), there were virtually no IL-7R$^-$ T cells that coexpressed Eomes and GATA-3 (Fig. 2C). We then analyzed how Eomes$^+$ Tr1-like cells were related to Th1 cells, which also secrete IFN-γ, but express the related Tbox transcription factor T-bet and the chemokine receptor CXCR3 [29]. Of note, CCR5 is expressed on both Th1 effector memory cells ("Th1$_{EM}$") and by Tr1-like cells [26], but these two subsets can be distinguished by IL-7R expression [13]. CXCR3$^-$ "non-Th1" cells and CXCR3$^+$CCR5$^-$Th1 central memory cells ("Th1$_{CM}$") expressed respectively no and low levels of T-bet and Eomes (Fig. 2D). Conversely, CCR5$^+$Th1$_{EM}$ cells expressed intermediate levels of T-bet, and a minor fraction was Eomes$^+$. Furthermore, among IL-7R$^-$T-cells, the Tr1-containing CCR5$^+$ subset expressed high levels of Eomes, while CCR5$^-$ cells did not. Notably, among Eomes$^+$ IL-7R$^-$ T cells two distinct populations with high and low expression of T-bet could be distinguished (Fig. 2D), suggesting cellular heterogeneity (see below).

We next compared Eomes$^+$ IL-7R$^+$ T cells to Eomes$^+$IL-7R$^-$ Tr1-like cells. Both Eomes$^+$ subsets expressed elevated levels of CCR5, IFN-γ, and GzmK (Fig. 2E). Conversely, Eomes$^-$ subsets, including CD25$^+$Tregs (data not shown), expressed only low levels of these proteins and other cytotoxic molecules (Supporting Information Fig. 2E). Notably, Eomes$^+$ Th1 cells expressed low amounts of IL-10 and high levels of CD40L (Fig. 2F), similar to conventional CD4$^+$Eomes$^-$ T cells. In contrast, Eomes$^+$ Tr1-like cells produced high amounts of IL-10 and low levels of CD40L (Fig. 2F). Furthermore, IL-7R$^-$Eomes$^+$ Tr1-like cells expressed the proliferation marker Ki67, indicating that they had recently divided in vivo, while Eomes$^+$ Th1 cells were largely Ki67$^-$ and, thus, in a resting state (Fig. 2G).

In conclusion, Eomes$^+$ Tr1-like cells are distinct from other established CD4$^+$ T-cell subsets in peripheral blood, including Th17 cells, Th2 cells, and Foxp3$^+$Tregs. Intriguingly, a fraction of Th1$_{EM}$ cells also expressed Eomes and GzmK. They lacked, however, some key characteristics of Tr1-like cells, but might represent precommitted Tr1-like precursors.

Eomes$^+$ Tr1-like cells are distinct from conventional CTL

Eomes controls cytotoxic functions of CD8$^+$ T cells [30], but there are also rare cytotoxic T cells in the CD4 compartment [13, 14]. We, therefore, asked how Eomes$^+$ Tr1-like cells were related to these CD4$^+$ CTL. As CD27 was among the most upregulated genes in Tr1-like cells (Fig. 1A), and is absent on CTL [12], we subdivided IL-7R$^-$CCR5$^+$ T cells into putative CD27$^+$ Tr1-like cells and CD27$^-$CTL (Supporting Information Fig. 3A). Both subsets expressed high levels of Eomes (Fig. 3A). However, GzmK was selectively expressed in CD27$^+$Eomes$^+$ Tr1-like cells, while GzmB was preferentially expressed by CD27$^-$CTL (Fig. 3B and Supporting Information Fig. 3B). GzmA and perforin were expressed in both subsets, but CTL expressed higher levels of perforin (data not shown). Both Tr1-like cells and CTL degranulated upon TCR stimulation by CD1c$^+$DC and induced cell death of monocytes ex vivo, (Fig. 3C). However, Tr1 cells required higher effector–target ratios to kill efficiently, suggesting that conventional CTL had superior cytotoxic capabilities. Of note, CTL expressed high levels of T-bet, whereas Tr1-like cells expressed only low levels (Fig. 3D and Supporting Information Fig. 3A), explaining the observed heterogeneity among total Eomes$^+$ IL-7R$^-$ T cells (Fig. 2D). Moreover, while conventional Eomes$^-$ Th1 cells rapidly upregulated T-bet expression following TCR stimulation, Eomes$^+$ Tr1-like cells failed to do so and remained T-bet^{lo}. Eomes$^+$ CTL, which expressed already high levels of T-bet ex vivo, did not further upregulate T-bet expression upon stimulation (Fig. 3D). Importantly, CD27$^+$ Tr1-like cells produced high levels of IL-10 together with IFN-γ, while CD27$^-$CTL did not (Fig. 3E). Intriguingly, also CD8$^+$Eomes$^+$ T cells with a IL-7R$^-$CCR5$^+$CD27$^+$ Tr1-like phenotype produced some IL-10 and expressed high levels of GzmK, while the corresponding CD27$^-$ subset failed to produce IL-10 and expressed mainly GzmB (Supporting Information Fig. 3C). Finally, while Tr1-like cells and CD25$^+$Tregs consistently suppressed DC-induced naïve CD4$^+$ T-cell proliferation, CD4$^+$CTL had no consistent suppressive effects (Fig. 3F). Suppression by Tr1-like cells was, as expected, dose dependent (Supporting Information Fig. 3D) and decreased upon IL-10 neutralization (Fig. 3G).

We conclude that CD27 expression distinguishes Eomes$^+$ Tr1-like cells from conventional CTL. These two Eomes$^+$ T-cell subsets differ in IL-10 production, suppressive capacities, T-bet expression levels, and their GzmK/B expression profiles, and populations with similar characteristics are present in the CD8$^+$ T-cell pool.

Myeloid DC, IL-12, and IL-4 promote a precommitment to a Tr1-like fate

In other T-cells, IL-12 and, paradoxically, IL-4 were shown to regulate Eomes expression [31–34], but the factors that induce Eomes in human CD4$^+$ T cells are unknown. We screened, thus, for cytokines that could upregulate Eomes expression in anti-CD3 stimulated naïve CD4$^+$ T cells. IL-4 efficiently induced Eomes expression, while all other tested cytokines, including IL-12, IL-27, with or without TGF-β, IL-10, IFN-γ, and IL-13, were inefficient (Fig. 4A and data not shown). Of note, IL-4 induced Eomes also in naïve CD8$^+$ T cells and in CD4$^+$ memory T cells (Supporting Information Fig. 4A). Naïve CD4$^+$ T cells that were stimulated with anti-CD3 stimulation and IL-4 expressed some GzmK (Supporting Information Fig. 4B), but failed to produce IFN-γ (data not shown). We therefore assessed if naïve T cells that upregulated Eomes upon more physiological priming by DCs coexpressed

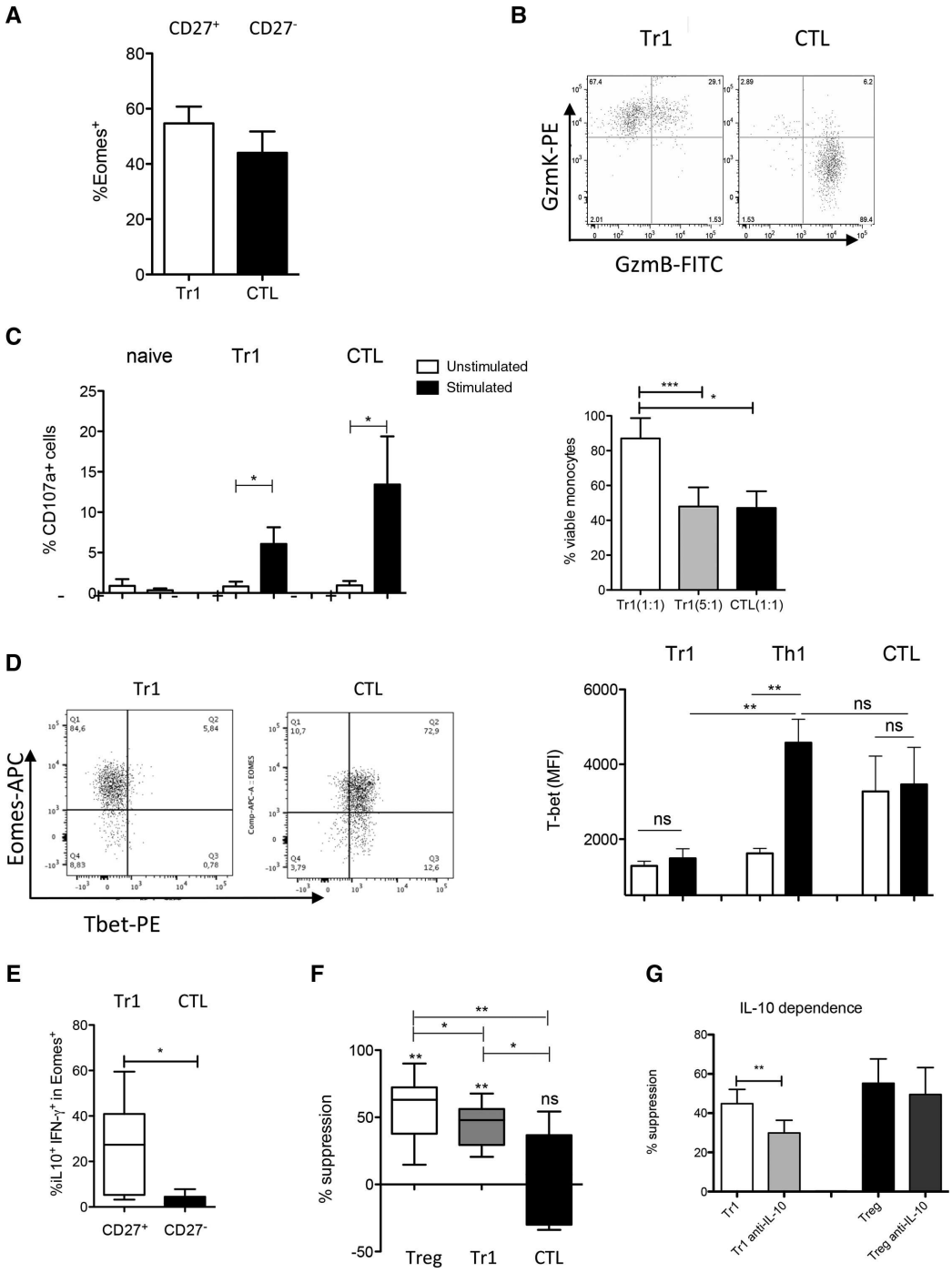

Figure 3. Tr1-like cells and conventional CTL are two distinct Eomes$^+$ T-cell subsets. Shown is an analysis of CD4$^+$ T-cells among mononuclear cells of human peripheral blood mononuclear cells (PBMC). (A) Eomes expression in gated CD27$^+$(Tr1) and CD27$^-$(CTL) subsets among CD4$^+$CCR5$^+$IL-7R$^-$T cells (six experiments with cells from different donors). (B) Intracellular GzmK versus GzmB protein expression in gated Eomes$^+$CD27$^+$Tr1-like cells and Eomes$^+$CD27$^-$CTL. (C) Left: degranulation of Tr1-like cells and CTL following TCR stimulation with SEB (+) presented by CD1c$^+$ DC as compared to naïve control cells was measured by CD107a surface exposure (five experiments with FACS-purified DC and T cells from five different donors). Right: Ex vivo killing of purified monocytes by Tr1 cells and CTL at a Effector–Target ratio of 1.1 or 5:1 as indicated. Percentages are calculated on viable monocytes in the absence of killer cells (100%, three experiments analyzing cells from five different donors). (D) Left: Eomes versus T-bet expression in gated Tr1-like cells and CTL. Right: T-bet expression by Eomes$^-$Th1 cells, Eomes$^+$Tr1-like cells, or CTL before (white bars, "–") or after (black bars, "+") TCR stimulation with anti-CD3 and anti-CD28 antibodies for 24 h (five experiments with cells from five different donors). (E) Percentages of IL-10$^+$IFN-γ$^+$ cells in gated Eomes$^+$ cells in purified IL-7R$^-$CCR5$^+$T-cells were sorted according to CD27 expression. (F) Suppression of DC-induced naïve CD4$^+$ T-cell proliferation by FACS-purified Tregs, Tr1-like cells, and CTL. Proliferation of responder cells in the presence of unlabeled naïve control cells was set to 0% suppression. (G) Suppression by Tregs and Tr1-like cells in the absence or presence of neutralizing anti-IL-10 antibodies. (F/G) (six experiments with cells from six different donors). Data were pooled from different experiments and the mean + SEM is shown; */**/***$p < 0.05/0.005/0.00005$ according to statistical analysis with paired student's *t*-test.

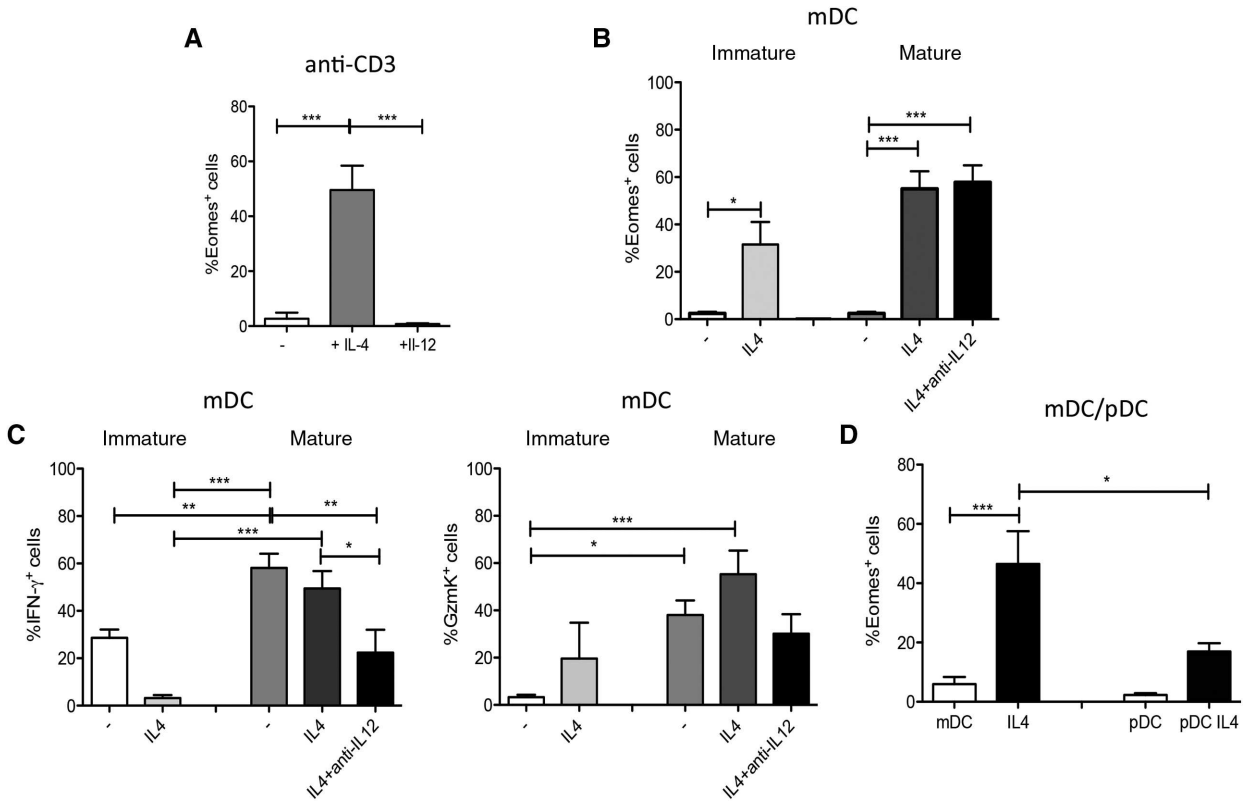

Figure 4. Tr1-like commitment is induced by IL-12-secreting myeloid DC and IL-4. (A) Purified naïve human CD4$^+$ T cells were stimulated with anti-CD3 antibodies in the absence or presence of IL-4 or IL-12. Shown is the mean percentage of Eomes$^+$ cells (nine donors analyzed in nine experiments). (B/C) Naive human CD4$^+$ T cells were stimulated with allogenic CD1c$^+$ DC that were either left unstimulated (immature) or stimulated with LPS and R848 to induce IL-12 (mature). Recombinant IL-4 or neutralizing anti-IL-12 antibodies were added as indicated. Induction of Eomes (B), IFN-γ (C, left), and GzmK (C, right) were assessed (six donors analyzed in six experiments). (D) Eomes induction by CpG-matured pDC or LPS/R848-matured CD1c$^+$ DC in the absence and presence of IL-4 (cells from five donors analyzed in five experiments). Data from different experiments were pooled and is shown as mean + SEM, */**/***$p < 0.05/0.005/0.00005$ according to statistical analysis with One-way ANOVA.

IFN-γ and GzmK, as do in vivo occurring Eomes$^+$ CD4$^+$ T cells. CD1c$^+$ myeloid DCs were matured with a combination of LPS and R848, which induces high levels of IL-12 [35]. IL-4 consistently induced Eomes also in DC-primed CD4$^+$ (Fig. 4B) and CD8$^+$ T cells (data not shown). It inhibited IFN-γ production as expected, but DC maturation abrogated this inhibitory effect in an IL-12-ependent manner (Fig. 4C). IL-4 also inhibited GzmB and T-bet induction (data not shown). Conversely, IL-4 increased GzmK expression, and the highest levels of GzmK were induced when both IL-4 and IL-12 were available (Fig. 4C). However, IL-4 failed to downregulate CD40L (Supporting Information Fig. 4C), and CD1c$^+$DC-primed T cells also produced low levels of IL-10 (Supporting Information Fig. 4D). CpG-matured pDC induced higher levels of IL-10 (Supporting Information Fig. 4D), as expected [24, 36, 37]. However, T cells primed with pDC and IL-4 expressed only low amounts of Eomes (Fig. 4D), as well as of GzmK and IFN-γ (Supporting Information Fig. 4D). This was true for pDC matured either with CpG-B or -C (data not shown), which differ in their capacity to induce type 1 interferon.

In summary, IL-4 induces Eomes expression in human T cells, and IL-4 and IL-12 surprisingly cooperated to induce T cells that expressed Eomes, GzmK, and IFN-γ upon priming with myeloid DC. These in vitro-generated Eomes$^+$ T cells lacked, however, some key properties of Tr1-like cells, but had the same characteristics as the in vivo occurring Eomes$^+$ Th1 cells.

Eomes regulates Tr1 effector molecules jointly with IL-27

To understand if Eomes could regulate effector molecules of Tr1-like cells, we forced the expression of Eomes in in vitro-stimulated naïve CD4$^+$ T cells with lentiviral vectors. The cultures were either supplemented with IL-12 or IL-27, which did not induces Eomes (Fig. 3A and data not shown), but promoted CTL and Tr1 differentiation, respectively. Eomes was induced in the majority of cells by a lentiviral vector encoding full-length human Eomes, but was undetectable in cells transduced with a control vector (Fig. 5A). Of note, T-bet was only transiently upregulated by IL-12, and was undetectable at the analyzed late time points (>d6, data not shown).

Eomes induced a moderate but significant increase of IL-10 production, and cooperated with IL-27, but not with IL-12, to induce high levels of IL-10 (Fig. 5A). Eomes had, however, no

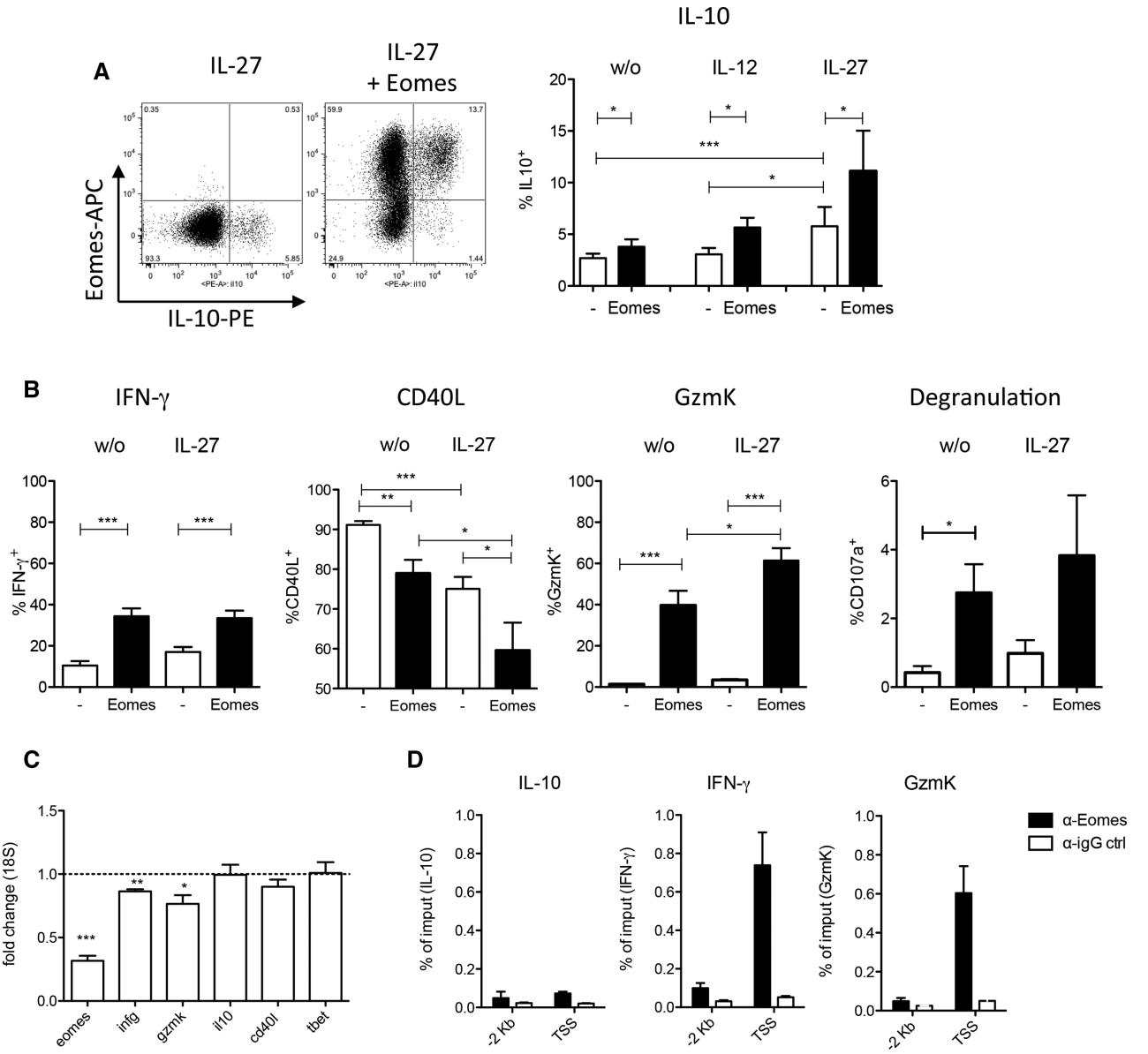

Figure 5. An Eomes controls GzmK and IFN-γ expression, and cooperates with IL-27 to promote Tr1-like properties. (A/B) Naïve human CD4$^+$ T cells were activated with anti-CD3 and -CD28 antibodies with or without IL-12 or IL-27, and viral vectors coding for either GFP and Eomes ("Eomes," black bars) or for GFP only ("–," white bars). Expression of indicated markers was analyzed by flow cytometry (A) Left panel: Eomes versus IL-10 expression in the presence of IL-27. Right panel. Mean percentage of IL-10$^+$ cells in the absence or presence of Eomes and IL-12 or IL-27 (seven experiments with cells from different donors). (B) IFN-γ production, CD40L upregulation, and GzmK expression (six experiments with cells from different donors) or degranulation (CD107a surface exposure; five experiments with cells from different donors) in the absence or presence of Eomes and IL-27 as indicated. (C) Eomes was downregulated with siRNAs in human CCR5$^+$CD4$^+$ T cells and mRNAs for Eomes, IFN-γ, GzmK, IL-10, CD40L, and T-bet measured by RT-PCR (six experiments with cells from different donors). mRNA levels were normalized and the foldchange to scrambled control siRNA was calculated. (D) CHIP analysis of Eomes binding to proximal ("TSS") and distal ("−2kb") regulatory regions (see Supporting Information Fig. 5) of the IL-10, IFN-γ, and GzmK genes in human Tr1 clones (three experiments with the same clone). Data from different experiments were pooled and shown as mean + SEM, */**/***$p < 0.05/0.005/0.00005$ according to statistical analysis with One-way ANOVA.

clear effect on the expression of Blimp-1, AHR, and c-Maf mRNAs (Supporting Information Fig. 5A), transcription factors that promote IL-10 production in IL-27-induced Tr1 cells [7, 15, 16]. IFN-γ production was also induced by Eomes (Fig 5B) or by IL-12 (data not shown), and to a lesser degree by IL-27. Importantly, Eomes significantly inhibited CD40L expression and cooperated with IL-27 to efficiently downregulate CD40L (Fig. 5B), while IL-12 was inefficient (data not shown). In addition, Eomes was sufficient to induce high levels of GzmK, while IL-27 (Fig. 5B) and IL-12 (data not shown) alone induced only low levels. Eomes had also a weak positive effect on GzmB, but GzmB expression was low unless IL-12 was added (Supporting Information Fig. 5B). Finally, Eomes-expressing CD4$^+$ T cells also degranulated (Fig. 5B). Overall, these results show that Eomes regulates the expression of

several effector molecules that are characteristic for in vivo occurring Tr1-like cells, and is sufficient to induce IFN-γ and GzmK. In addition, Eomes promoted a switch from CD40L to IL-10 in cooperation with IL-27.

To understand if Eomes was necessary for the expression of Tr1-associated genes, we downregulated Eomes expression with siRNAs in $CD4^+$ $CCR5^+$ T cells, and measured the expression of the most relevant mRNAs by qRT-PCR. Eomes expression was reduced to approximately 30% by specific siRNAs [33], and both IFN-γ and GzmK mRNAs were also significantly reduced (Fig. 5C). In contrast, the levels of CD40L, IL-10, and T-bet control mRNAs were not affected by Eomes downregulation. To understand if Eomes could directly regulate these genes by binding to their promoter regions, we searched for predicted Eomes/Tbox binding sites in the relevant regulatory elements. We identified predicted binding sites in the proximal promoter regions of IFN-γ and GzmK (Supporting Information Fig. 5C). Conversely, the CD40L promoter contained no potential binding sites for Eomes (data not shown). Notably, only the proximal, but not the distal part of the IL-10 promoter was conserved in humans and mice (Supporting Information Fig. 5D). Consequently, two T-box binding sites in the distal part of the murine IL-10 promoter [17] were not conserved in humans. Nevertheless, we also identified a predicted, partially altered Eomes/Tbox binding site in the distal part of the human IL-10 promoter (Supporting Information Fig. 5C). CHIP analysis in cloned Tr1 cells with high IL-10 production (Supporting Information Fig. 5E) revealed that Eomes bound to the proximal promoter regions of IFN-γ and GzmK, but neither to the proximal nor to the distal analyzed promoter regions of IL-10 (Fig. 5D). Similar results were obtained with naïve $CD4^+$ T cells that were forced to express Eomes (data not shown).

Overall these results indicate that IFN-γ and GzmK are directly controlled by Eomes in human $CD4^+$ T cells. Conversely, IL-10 and CD40L are probably not regulated in a direct manner, which could explain why their expression depends more heavily on IL-27.

Eomes regulates chemokine receptor expression and antagonizes the Th17 fate

Since $Eomes^+$ Tr1-like cells had a characteristic IL-$7R^-CCR5^+PD1^+CCR6^-$ phenotype (Fig. 2B), we analyzed whether the expression of these membrane proteins was regulated by Eomes or by IL-27. Eomes induced CCR5 in $CD4^+$ T cells, and collaborated with IL-27 (Fig. 6A) and with IL-12 (data not shown) to induce high levels of CCR5. In contrast, IL-7R expression was not affected by Eomes expression, whereas IL-27 had a significant inhibitory effect (Fig. 6A). Although $Eomes^+$Tr1-like cells expressed high levels of PD1 (Supporting Information Fig. 6A), forced expression of Eomes actually inhibited PD1 expression (Fig. 6B), while IL-12 or IL-27 had no effect (data not shown). Similar results were obtained for CTLA-4 (data not shown), another checkpoint receptor that is highly expressed by Tr1-like cells [25, 26]. Conversely, surface expression of LAG3 was low on $Eomes^+$Tr1-like cells (Supporting Information Fig. 6B), despite of the fact that LAG3 was among the most upregulated genes in Tr1-like cells (Fig. 1A). This was not unexpected, since $IL\text{-}7R^-$ Tr1-like cells express LAG-3 mRNA, but they barely express LAG3 protein on the cell surface [27]. Of note, the large majority of $LAG3^+$ $CD4^+$ T cells were $IL\text{-}7R^+$ (Supporting Information Fig. 6C), and only a small fraction expressed Eomes (data not shown). Thus, $LAG3^+CD4^+$T-cells contain some $Eomes^+$ Th1-cells, but they show virtually no overlap with $Eomes^+IL\text{-}7R^-$ Tr1-like cells.

As Tr1-like cells expressed neither IL-17 nor CCR6, we analyzed if Eomes could antagonize human Th17 differentiation. Since in vitro human Th17 differentiation is inefficient [38] and CCR6 upregulation is unstable [39], we assessed if forced expression of Eomes could suppress Th17 signature genes in ex vivo isolated $CCR6^+IL\text{-}7R^+$T-cells, which contain in vivo differentiated Th17 cells [40]. Indeed, Eomes strongly inhibited CCR6 expression (Fig. 6C), as well as production of IL-17A/F (Fig. 6C) and IL-22 (data not shown). Moreover, Eomes significantly reduced the expression of RORC and RORA mRNAs (Fig. 6D), which code for the lineage-defining transcription factors of Th17 cells. Finally, even under optimal Th17 polarizing conditions [38], Tr1-like failed to acquire IL-17 producing capacities, and maintained Eomes and GzmK expression (data not shown).

In conclusion, Eomes induces CCR5 and inhibits CCR6 expression, consistent with the $CCR5^+CCR6^-$ phenotype of in vivo occurring $Eomes^+$Tr1-like cells. In addition, Eomes blocks the RORA/C transcription factors and the production of Th17 cytokines, explaining why Th17-associated genes are strongly downregulated in $Eomes^+$Tr1-like cells.

$Eomes^+$ Tr1-like subsets are present in human tissues and are modulated in immune-mediated diseases

We previously identified Tr1-like cells also in human lymphoid [26] and nonlymphoid tissues [27], and we, therefore, assessed if these tissue-derived Tr1 cells also expressed Eomes. Indeed, Eomes was highly expressed by IL-10 producing $IL\text{-}7R^-$T cells in human tonsils, but was hardly detectable in tonsillar $IL\text{-}10^-IL\text{-}7R^-$, $IL\text{-}7R^+$, or $CD25^+$ control populations (Fig. 7A). These tonsillar Tr1-like cells also expressed GzmK and IFN-γ (Supporting Information Fig. 7B). A caveat in human tonsils is, however, that they contain activated follicular helper T cells ("T_{FH}"), which have also downregulated IL-7R expression [41] and produce IL-10. However, analyzing T_{FH}- and Tr1-like cells according to their specific surface markers (Supporting Information Fig. 7B) revealed that Eomes was expressed selectively in tonsillar Tr1-like cells, but not in T_{FH} cells (Fig. 7B). Moreover, BCL6 was as expected expressed by T_{FH}-cells, but was hardly detectable in tonsillar Tr1-like cells (Supporting Information Fig. 7C). In the intestinal lamina propria, $CD4^+IL\text{-}7R^-$ T cells expressed high amounts of Eomes (Fig. 7C). As observed in the blood (Fig. 2D), both in the lamina propria (Fig. 7C) and in intestinal lymph nodes (Supporting Information Fig. 7D), two subsets of $Eomes^+$T-bet^{lo}Tr1-like cells and of $Eomes^+Tbet^{hi}$CTL were distinguishable. Intestinal

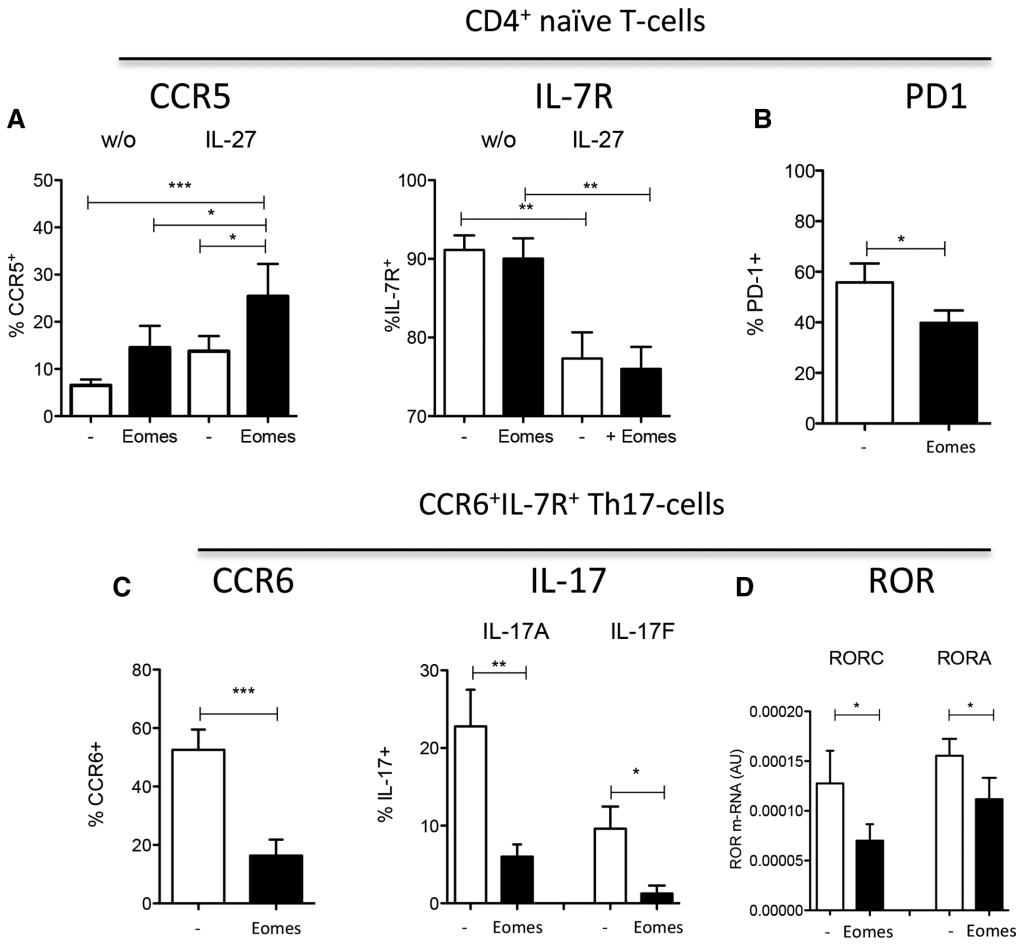

Figure 6. Eomes induces CCR5, but not PD1, and inhibits Th17 signature genes. (A/B) Human naïve CD4$^+$ T cells were transduced with Eomes- and/or GFP- encoding lentiviral vectors and analyzed for phenotypic markers of Tr1-like cells. (A) CCR5 and IL-7R expression in the absence (–) or presence of Eomes or IL-27 (eight for CCR5 and six for IL-7R) experiments with cells from different donors. */**/***$p < 0.05/0.005/0.00005$ according to statistical analysis with One-way ANOVA. (B) Effects of forced Eomes expression on PD1 (five experiments with cells from different donors). *$p < 0.05$ according to statistical analysis with paired student's *t*-test. (C/D) Human CCR6$^+$IL-7R$^+$ T cells were stimulated and transduced with lentiviral vectors coding for Eomes and/or GFP and analyzed for features of Th17 cells. Left: CCR6 surface expression and Right: production of IL-17A/F in the absence (–) or presence of Eomes. (D) Expressions of RORC and RORA transcription factors were measured by qRT-PCR. (C/D) Five experiments with cells from different donors. Data from different experiments were pooled and shown as mean + SEM; */**/***$p < 0.05/0.005/0.00005$ according to statistical analysis with paired student's *t*-test.

Eomes$^+$Tr1-like cells expressed also high levels of GzmK (Supporting Information Fig. 7E).

Since Eomes$^+$ Tr1-like cells were present in tissues, we analyzed whether the frequencies of Eomes$^+$ subsets in the CD4 compartment were altered locally or systemically in immune-mediated diseases where Tr1 cells are of therapeutic relevance, namely IBDs and graft-versus-host disease (GvHD) [42, 43]. In the inflamed gut of IBD patients, but also in the healthy control mucosa obtained from colorectal cancer patients (CRC), Eomes$^+$Tr1-like cells were strongly enriched as compared to peripheral blood (Fig. 7D). Intriguingly, IBD patients had significantly lower frequencies of Eomes$^+$IL-7R$^+$ T-cells than healthy individuals, suggesting that Tr1-like precommitment might be compromised. FOXP3$^+$Tregs were, in contrast, increased in the blood of CRC patients (Fig. 7D). Finally, we analyzed Eomes$^+$ and FOXP3$^+$T-cell subsets also in the blood of patients that develop a new immune system following allogenic stem cell transplantation. This is a peculiar clinical condition where Tr1 cells were first described, are increased and could potentially inhibit GvHD [43]. In these patients, Eomes$^+$ Tr1-like cells were indeed significantly increased (Fig. 7E). In a smaller cohort of patients, we also observed an increase of GzmK$^+$CD4$^+$ T cells (Supporting Information Fig. 7F). Notably, we detected highly variable frequencies of IL-7R$^+$Eomes$^+$ T cells, which were very abundant in some patients. Foxp3$^+$Tregs showed much less variability and were only moderately increased (Fig. 7E).

We conclude that Eomes$^+$Tr1-like cells are present in human lymphoid and nonlymphoid tissues, and are enriched in the gut. Moreover, the frequencies of Eomes$^+$ Tr1-like cells or their potential precursors were systemically altered in two prototypical clinical conditions where Tr1 cells play a critical role. Finally, the strong variability of Eomes$^+$ Tr1-like subsets in patients suggests that their in vivo homeostasis is highly dynamic, and that they should thus be included in monitoring strategies to assess the equilibrium between regulatory and effector T cells in diseases.

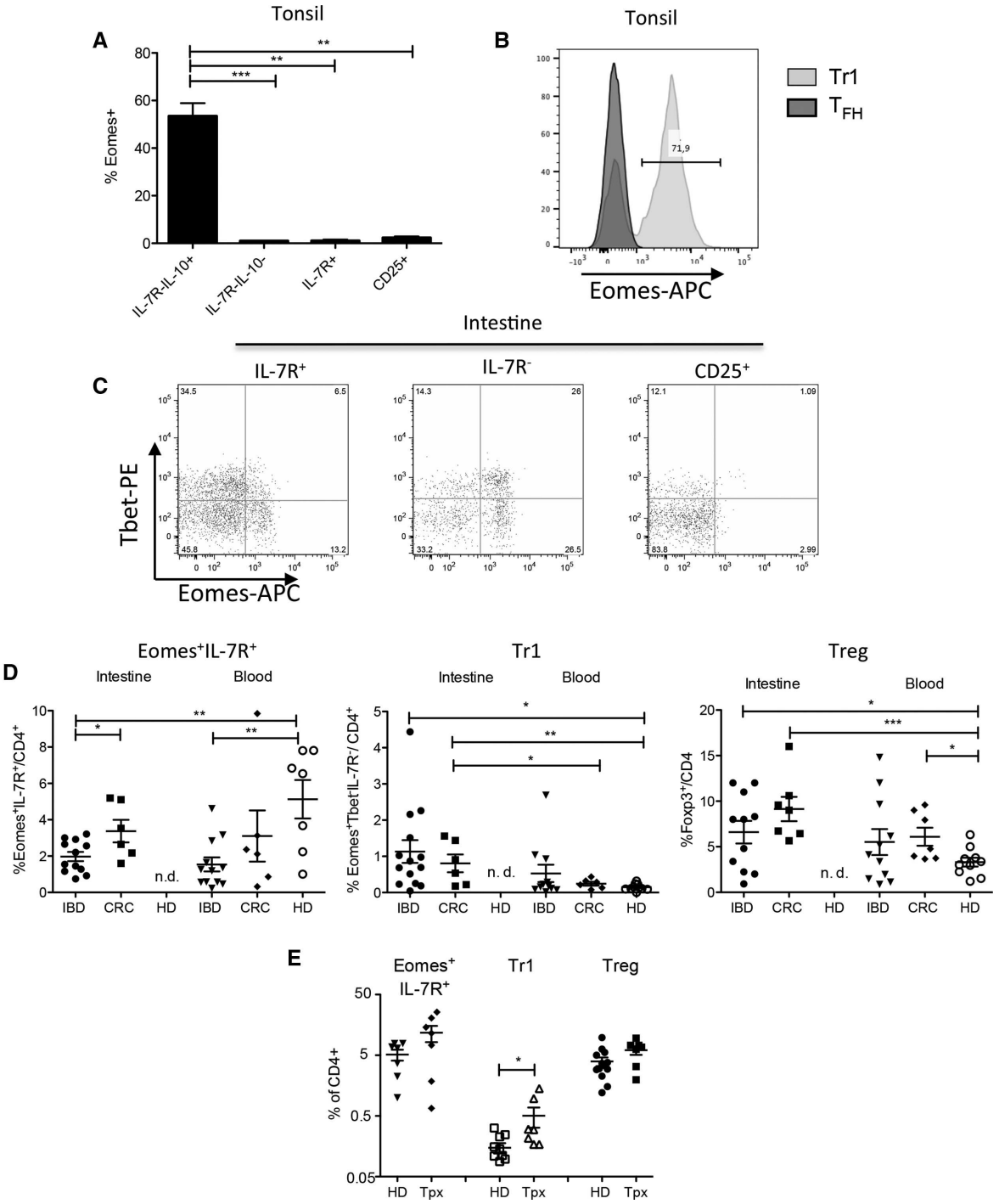

Figure 7. Eomes$^+$ T-cell subsets are present in human solid tissues and are modulated in Tr1-relevant clinical settings. (A) Purified tonsillar CD4$^+$IL-7R$^+$, CD25$^+$IL-7R^{lo}, and IL-7R$^-$CD25$^-$ subsets gated according to IL-10 expression were analyzed for the expression of Eomes (five experiments with cells from different patients). (B) Tonsillar IL-7R$^-$CCR5$^+$CXCR5$^-$ICOS$^-$Tr1-like cells and IL-7R$^-$CCR5$^-$CXCR5$^+$ICOS$^+$T$_{FH}$-cells were analyzed for Eomes expression. (C) CD4$^+$ T-cell subsets gated according to the expression of IL-7R and CD25 from the intestinal lamina propria were analyzed for T-bet and Eomes expression. (D) Frequencies of IL-7R$^+$Eomes$^+$ T-cells (left panel), Tr1-like cells (central panel), and FOXP3$^+$Tregs (right panel) among CD4$^+$ T cells in the inflamed intestinal lamina propria (intestine) of IBD patients ("IBD", 14 (Tr1), 12 (Eomes+IL-7R$^+$), or 11 (FOXP3$^+$Tregs) patients analyzed in different experiments) or the healthy, noninflamed lamina propria of CRC control patients ("CRC", six experiments with cells from different patients). Eomes$^+$ and FOXP3$^+$ T-cell subsets were also analyzed in peripheral blood ("blood") of the same patients and compared to healthy donors (HD, seven experiments with cells from different donors); n.d., not determined. (E) Eomes$^+$ and Foxp3$^+$ subsets among CD4$^+$ T cells in healthy donors ("HD", five experiments analyzing cells from nine donors) and in patients who received stem cell transplantation ("Tpx," seven experiments with cells from seven different patients). Frequencies of Eomes$^+$IL-7R$^+$ cells, of Eomes$^+$T-bet$^-$IL-7R$^-$Tr1-like cells ("Tr1"), and of Foxp3$^+$Tregs ("Treg") are shown. Data from different experiments were pooled and shown as mean + SEM; */**/***$p < 0.05/0.005/0.00005$ according to statistical analysis with One-way ANOVA.

Discussion

Regulatory T-cell subsets are required to prevent overshooting immune responses. It is increasingly recognized that, besides, Foxp3$^+$Tregs, also Tr1-cells play a crucial and sometimes nonredundant role [4, 5]. However, while the molecular identity of Foxp3$^+$Tregs is well established, the biology of in vivo occurring human Tr1 cells is poorly understood. We showed here that Eomes acted as a lineage-defining transcription factor in human Tr1-like cells. Moreover, we identified putative precursor cells and identified the APC and cytokine conditions that could induce Eomes$^+$ precursor and effector Tr1-like cells.

Several transcription factors have been proposed to regulate IL-10 production in murine Tr1 cells, but the transcriptional regulation of in vivo occurring human Tr1-like cells remains an understudied area. We performed here the first detailed molecular characterization of in vivo occurring IFN-γ and IL-10 coproducing Tr1-like cells, allowing their unequivocal identification and their distinction from all other CD4$^+$ T cells. Key to their biology is Eomes, the lineage-defining transcription factor of cytotoxic lymphocytes. Consistent with a recent report in mice [17], our results suggest that Eomes acted as a lineage-defining transcription factor in human Tr1 cells. The induction of cytotoxicity and the suppression of Th17 differentiation by Eomes [44], as well as the expression of Eomes in IL-10 and IFN-γ coproducing regulatory T cells appear to be conserved between humans and mice [17]. Conversely, our results suggest that the regulation of IL-10 by T-box transcription factors differs in humans and mice, and whether murine Tr1 cells also express GzmK remains to be shown. In human Tr1-like cells, Eomes establishes a unique cytotoxic differentiation program, which is characterized by the expression of GzmK, IFN-γ, and CCR5. In the CD4 compartment Eomes, CCR5 and IFN-γ are also expressed by conventional CTL. Conversely, GzmK expression was characteristic for Tr1-like cells and their putative precursor cells in humans, and is, thus, the most powerful single marker to identify in vivo occurring Tr1-like cells. Surprisingly, GzmB was not expressed in human Tr1-like cells in vivo, but was selectively expressed in conventional CD4$^+$CTL. Thus, GzmB is not only not a marker of in vivo occurring Eomes$^+$Tr1-like cells, but is on the contrary useful to distinguish them from conventional CTL.

Besides IL-10 and GzmB, also checkpoint receptors are characteristic for Tr1 cells. Since they are expressed on the cell surface they could be exploited to purify viable Tr1 cells [8, 26]. Checkpoint receptors are, however, also expressed on other activated T-cell subsets, and Eomes neither induce PD1 nor CTLA4. LAG3 was proposed to be more specific for Tr1 cells [8, 9], but a limitation in humans is that LAG3 protein has to be induced on the surface of Eomes$^+$Tr1-like cells by in vitro TCR stimulation [27]. The fact that human LAG3$^+$T-cells possess regulatory functions [8], but are distinct from Eomes$^+$Tr1-like cells, suggests that additional Tr1-like populations might exist. However, since they lack Eomes they are expected to have a different biology. Importantly, the Tr1-associated chemokine receptor pattern CCR5$^+$CCR6$^-$ [26] was determined by Eomes, consistent with the notion that chemokine receptors are powerful in vivo differentiation markers of human T-cells [13, 29]. Together with IL-7R, CD25 [25], and CD27, these chemokine receptors allow to sort unstimulated Eomes$^+$Tr1-like cells with high purity.

In mice, Tr1-cells could be generated in vivo with nanoparticles from precommitted precursors, possibly Th1 cells [45]. Consistently, the potential Tr1 precursor cells that we identified in humans had a $Th1_{EM}$ phenotype, produced IFN-γ and expressed Eomes and GzmK. Unlike Tr1-like cells, however, they were resting and expressed IL-7R and CD40L, but not IL-10. Intriguingly, all these missing features of Tr1-like effector cells could be induced by TCR stimulation in the presence of IL-27, a well-known condition to induce Tr1-cells. However, IL-27 failed to induce Eomes in human T cells, suggesting that it induces Eomes$^+$ Tr1-like cells from Eomes$^+$ Th1 precursors rather than from naive T cells [29]. It seems likely that the putative IL-7R$^+$ Tr1 precursors express not only Eomes and GzmK, but have also the same phenotype as Eomes$^+$ Tr1-like cells, i.e. expression of CCR5, CD27, and PD1, but not of CCR6. Notably, an accompanying article by Mazzoni et al. shows that Th17-derived "nonconventional" Th1 cells that coexpress Eomes and CCR6 possess proinflammatory properties [46], suggesting that CCR6$^+$Eomes$^+$Th1-cells are indeed more distantly related to anti-inflammatory Tr1 cells. Nevertheless, since they already express Eomes, they could transdifferentiate more efficiently to Eomes$^+$ Tr1-like cells upon resolution of inflammation [47]. Cells with characteristics of Eomes$^+$ Tr1-like precursor cells could be induced by IL-4 and mature DC, IL-12 secreting myeloid DC, consistent with the view that Eomes$^+$ Tr1-like cells are generated in immune responses against pathogens [23, 25]. IL-4 and IL-12 are known to act antagonistically to induce Th2 and Th1 differentiation, respectively, and IL-4 blocks, in addition, the induction of conventional CTL. However, IL-4 was previously shown to induce Eomes in other T-cell subsets, including human CD8$^+$ and γ/δ T cells [31–34], suggesting that the induction of Eomes is similarly regulated in all human T-cell subsets. In addition, CD56^{bright} NK cells, which possess regulatory properties, express high levels of GzmK [48] (and data not shown), suggesting that GzmK might be a universal marker of lymphocytes with regulatory functions. IL-4 can be induced upon tissue damage via IL-33, in particular in the gut [49]. Thus, IL-4 and IL-12 could collaborate to induce Tr1-like commitment in response to tissue damage induced by pathogens. Interestingly, IBD patients had reduced frequencies of Eomes$^+$ Th1 cells, suggesting that Tr1 commmittment might be affected. In addition, Tr1-like cells downregulate IL-10 production in the inflamed gut of IBD patients [27], and the Tr1 response in IBD might, thus, be affected at multiple levels.

In conclusion, we provided here a molecular blueprint of human IL-10 and IFN-γ coproducing Tr1-like cells. The identification of Eomes and GzmK as Tr1-associated markers in humans will greatly facilitate their study in immune-mediated diseases in the future.

Materials and methods

Human samples and patients

Buffy-coated blood of healthy donors and tonsils specimens were obtained from the IRCCS Policlinico Ospedale Maggiore, Milan, Italy and the Deutsches Rotes Kreuz (DRK), Germany), as described [26]. The ethical committee approved the use of tonsil specimen for research purposes (permission EA1/107/10). Intestinal specimens were obtained from IBD or CRC patients undergoing therapeutic resection as described [27]. The ethical committee approved the use of specimens for research purposes (permission n. 2476) and informed consent was obtained from patients. The cohort of IBD was composed of 12 severe patients, six with Crohn's Disease and six with ulcerative colitis who were not treated with anti-TNF antibodies. The cohort of transplanted pediatric patients was composed of 7 patients, 3 were transplanted with cord-blood derived stem cells and 4 with mobilized, circulating $CD34^+$ stem cells from a first-degree relative. Five patients developed GvHD, one chronic GvHD and four acute GvHD of grade I or II. Three patients experienced viral reactivations, two with CMV and one with HHV6.

Cell isolation

Mononuclear cells from PBMCs, tonsils, and the intestinal lamina propria molecular cells were isolated as described [26, 27]. $CD4^+$T-cell subsets were purified by cell sorting on a FACSAria (BD Biosciences) based on CD25 and IL-7R marker expression into IL-$7R^+CD25^{-/lo}$ helper T cells, IL-$7R^-CD25^-$ Tr1-containing cells, and IL-$7R^{lo}CD25^+$Tregs. IL-$7R^-$ cells were further subdivided into $CCR5^+CCR6^-CD27^+$Tr1-like cells and $CCR5^+CCR6^-CD27^-$CTL. $CD1c^+$DC and pDC were enriched with magnetic beads (Miltenyi) and purified by cell sorting as described [37].

Flow cytometry

Flow cytometry was performed according to the published guidelines [50]. T cells were stained at the cell surface with the following antibodies: CD4 (RPA-T4, BD), CCR5 (27D, BD), PD-1 (MIH4, Biolegend, San Diego, CA), CD25 (M-A251, Biolegend), CD127 (eBioRDR5, eBioscience), LAG3 (REA351, Miltenyi), CXCR3 (1C6, BD), CCR6 (R6H1 Ebioscience), CRTH2 (BM16, Miltenyi), CD27 (L128, BD), and CD45RA (HI100, BD). For the analysis of intracellular proteins, cells were fixed and permeabilized and stained intracellularly for GzmA (Cb9, BD), GzmB (GB11, BD), GzmK (GM6C3, Santa Cruz), Eomes (WD 1928, Ebioscience), FOXP3 (PCH101, Ebioscience), GATA3 (L50-823, BD), T-bet (O4-46, BD), BCL6 (K112-91, BD), or the proliferation marker KI67. Cytokine production was assessed by intracellular staining after stimulation with 0.1 μM phorbole ester (PMA) and 1 μg/mL ionomycin (both from Sigma–Aldrich) in the presence of 10 μg/mL Brefeldin A (Sigma). Cells were fixed, permeabilized, stained, and analyzed by flow cytometry for intracellular IL-17A (BL168, Biolegend), IL-17F (SHLR17, Ebioscience), IL-22 (22 URTI; Ebioscience), IFN-γ (B27, Biolegend), IL-10 (JES-19F1, Biolegend), as well as CD40L (2431, Biolegend) and CTLA-4 (BNI3, BD) expression.

T-cell stimulation

Naïve $CD4^+CD45RA^+$T-cells, $CD4^+CD45RA^-$ memory T-cells, and naive $CD8^+CD45RA^+CD27^+$T-cells were labeled with CellTrace and 10^5 cells per well activated by plate-bound anti-CD3 antibodies (UCHT1, BD; 2 μg/ml) in the absence or presence of 10 ng/mL recombinant IL-12or IL-4 (R&D systems). Cells were analyzed by flow cytometry after 5 days. For priming with DC, $CD1c^+$DC or BDCA-4^+pDC was isolated and either left untreated or matured with a combination of LPS and R848 to induce IL-12 ($CD1c^+$DC) or CpGB/C (pDC) as described [37]. Naïve $CD4^+$ and $CD8^+$ T cells were cocultured with DC at a 1:5 ratio in the absence or presence of 10 ng/mL recombinant IL-4 and 10 μg/mL neutralizing anti-IL-12 antibodies.

Suppression assay

Naïve $CD4^+$ T cells were sorted as $CD4^+CD45RA^+$ and labeled with CellTrace Violet (Life Technologies). A total of 2.5×10^4 naive T cells were cocultured at different ratios with sorted Tregs, Tr1-like cells, or CTL. A total of 5×10^3 allogenic $CD1c^+$DCs were added as stimulators. Unlabeled naive cells were used as a negative control to assess specific suppression. After 4–5 days, cells were stained and analyzed for CellTrace Violet dilution by FACS.

Generation of T-cell lines and clones

Tr1-like cells were isolated according to phenotypic markers (single cells were positioned with a FACSAria in wells containing 10^6/mL PBMC from five different donors and 2×10^5/mL Rosi-EBV cells as feeder cells, 1 μg/mL anti-CD3 antibodies (OKT3) and 200 U/mL IL-2 in RPMI 10% FCS. Fresh medium was added every 3 days. Clones were used after 3–4 weeks and restimulated with the same protocol every 4–6 weeks.

Cytotoxicity assays

Ex vivo isolated or cloned Tr1-like cells were incubated with $CD1c^+$DC as target cells in the absence or presence of Staphylococcus enterotoxin B (SEB) at a 1:1 ratio. Degranulation was assessed by surface exposure of the lysosomal protein CD107a after 16 h. Cytotoxicity of Tr1 clones was assessed by staining of $CD1c^+$DC with AnnexinV and propidium iodide. To assess cytotoxicity of Tr1 cells ex vivo, $CD14^+$ monocytes were isolated with anti-CD14

beads (Miltenyi) from peripheral blood. They were either incubated alone, or with *ex vivo* isolated Tr1-like cells and SEB at a 1:1 and 5:1 Effector–Target ratio for 16 h. UV irradiation was used as a positive control (data not shown). Percentage of viable $CD14^+$monocytes that were negative for DAPI and LIVE/DEAD dye (Invitrogen) in the absence of T cells was set to 100%.

Lentivirus-mediated EOMES gene transfer in primary T cells

Purified $CD4^+$ naive or Th17-enriched $CCR6^+IL\text{-}7R^+$ T-cells were activated at a density of 10^5 cells per well in 96-well MaxiSorp plates (Nunc) coated with anti-CD3 (0.1 μg/mL; UCHT1; BD) and anti-CD28 (6 μg/mL; CD28.2; BD) and IL-2 (20 IU/mL; Novartis). In some cases, 10 ng/mL IL-12 or IL-27 was added. Lentiviral particles were produced according to a standard protocol (System Biosciences User Manual). T cells were simultaneously activated and transduced with either GFP control lentiviral vector or a lentiviral vector encoding whole length wildtype EOMES at a multiplicity of infection of 1×10^7 transducing units/mL. Cells were detached on day 3, and transduction efficiency was assessed by flow cytometry on day 4 as the frequency of GFP^+ cells (normally >50%). Transduced cells were then transferred to uncoated wells and were cultured in complete RPMI medium. After 7–14 days cells were analyzed by flow cytometry for various proteins according to Eomes expression.

Eomes downregulation in primary $CD4^+$T cells

A total of 10^6 FACS-purified $CD4^+CCR5^+$T-cells were transfected with Eomes siRNA [33] or scrambled control siRNA. Cells were activated with PMA and Ionomycin for 5 h, and RT-PCR for Tr1-associated genes was performed.

In silico prediction of Eomes binding sites

Prediction of Tbox binding sites in the regulatory elements of the human IL-10, GzmK, IFN-γ, and CD40L was done with two different softwares, Jaspar and Matinspector. Sequences with a score >0.85 were considered as candidates.

Chromatin immune precipitation analysis

A total of 10^7 cloned Tr1 cells or lentiviral-transduced $CD4^+$ T cells were activated with PMA and Ionomycin, lysed and DNA shredded. Eomes was immune precipitated and bound DNA revealed with primers was located in the proximal or distal part of the promoters of IL-10 (distal fw 5′-CCCTGTTGGGACAGATGAAAA-3′; distal rev 5′-TTGGCCCTGCCACTCTATAGTC-3′; proximal fw 5′-TGAGAACA GCTGCACCCACTT-3′; proximal rev 5′-TCGGAGATCTCGAAGCAT GTTA-3′), GzmK (distal fw 5′-GCATTCTGATGCGTGATCTG-3′; distal rev 5′-GCCAGGCCTTCAATACAAAA-3′; proximal fw 5′-CC TGAAAGTCCCCAAACTGA-3′; proximal rev 5′-CCACAGGTGCTCT AGGGGTA-3′), or IFN-γ (distal fw 5′-TGCCCCATAACTGCAATA CTG-3′; distal rev 5′- CCTCCACTCTTTGGTTCAAACC-3′; proximal fw 5′-CCAACCACAAGCAAATGATCA-3′; proximal rev 5′-TGGCCCTGGTAAAATGTTGA-3′). Primers specifc for the promoter region of GAPDH (fw 5′-ACAGTCAGCCGCATCTTCTT-3′; rev 5′- TGACTCCGACCTTCACCTTC-3′), as well as isotype control antibodies were used to control specificity of binding.

RNA isolation and mRNA expression profiling

Total RNA Integrity Number (RNA) was isolated using mirVana miRNA Isolation Kit (Ambion) following the standard protocol. Briefly, the lysates were extracted once with acid — phenol chloroform and further purified to yield total RNA with specific miRNA retention. Extracted RNA was quantified with RiboGreen Quantitation Kit (Molecular Probes) on an Infinite F200 plate reader (Tecan Trading AG). All extracted RNA samples were quality controlled for integrity with 2100 Bioanalyzer (Agilent Technologies) and samples with RNA Integrity Number (RIN) lower than eight were discarded. The standard Megaplex protocol (Applied Biosystems) was performed starting from 10 ng of total RNA for each sample with preamplification. Gene expression of whole transcriptome was performed on $CD4^+$ T-cells subsets isolated as described in Supporting Information Fig. 1A, with Illumina Direct Hybridization Assays according to the standard protocol (Illumina Inc.).

Gene expression profiling

Gene expression arrays were quantile normalized, with background subtraction, and average signals were calculated on gene-level data for genes whose detection p value was lower than 0.001 in at least one of the cohorts considered. Normalized data were log2 transformed and presented as z-scores. A one-way analysis of variance (ANOVA) (p value < 0.001) was used to select selectively expressed genes. Statistical tests were performed on MeV software version 4.5.

TaqMan gene expression assays

For assessment of gene expression levels, TaqMan gene expression assays (Thermo Fisher Scientific) were used. 200 ng of total RNA was used for reverse transcription with VILO Reverse Transctiptase (Thermo Fisher Scientific). 1 ng of diluted cDNA was then used as input for RT-qPCR to assess the expression of *EOMES* (Hs 00172872_m1), *IL10* (Hs 00961622_m1), *GZMK* (Hs 00157878_m1), *PRDM1* (Hs 01068508_m1), *AHR* (Hs 00169233_m1), *CD40LG* (Hs 00163934_m1), *TBX21* (Hs 00203436_m1), *FOXP3* (Hs 03987537_m1), and *IFNG* (Hs 00989291_m1). Gene expression levels were normalized on 18s rRNA (Hs 99999901_s1) and reported as arbitrary units.

Statistics

Statistical significance for two variables was calculated using paired two-tailed Student's *t*-test. In the case of multiple comparisons, one-way ANOVA with Tukey's post-test was used. $p < 0.05$(*), $p < 0.005$(**), and $p < 0.0005$(***) were regarded as statistically significant. Error bars reflect ±SEM.

Acknowledgments: This work was supported by the Cariplo and AIRC foundations (Grants nos. 2013-0937 and IG 2015 Id17448).

Conflicts of interest: The authors declare no financial or commercial conflicts of interest.

References

1 **Ochs, H. D., Gambineri, E. and Torgerson, T. R.**, IPEX, FOXP3 and regulatory T-cells: a model for autoimmunity. *Immunol. Res.* 2007. **38**: 112–121.

2 **Sakaguchi, S., Ono, M., Setoguchi, R., Yagi, H., Hori, S., Fehervari, Z., Shimizu, J. et al.**, Foxp3$^+$ CD25$^+$ CD4$^+$ natural regulatory T cells in dominant self-tolerance and autoimmune disease. *Immunol. Rev.* 2006. **212**: 8–27.

3 **Groux, H., O'Garra, A., Bigler, M., Rouleau, M., Antonenko, S., de Vries, J. E. and Roncarolo, M. G.**, A CD4$^+$ T-cell subset inhibits antigen-specific T-cell responses and prevents colitis. *Nature* 1997. **389**: 737–742.

4 **Roncarolo, M. G., Gregori, S., Battaglia, M., Bacchetta, R., Fleischhauer, K. and Levings, M. K.**, Interleukin-10-secreting type 1 regulatory T cells in rodents and humans. *Immunol. Rev.* 2006. **212**: 28–50.

5 **O'Garra, A., Vieira, P. L., Vieira, P. and Goldfeld, A. E.**, IL-10-producing and naturally occurring CD4$^+$ Tregs: limiting collateral damage. *J. Clin. Invest.* 2004. **114**: 1372–1378.

6 **Grossman, W. J., Verbsky, J. W., Tollefsen, B. L., Kemper, C., Atkinson, J. P. and Ley, T. J.**, Differential expression of granzymes A and B in human cytotoxic lymphocyte subsets and T regulatory cells. *Blood* 2004. **104**: 2840–2848.

7 **Gandhi, R., Kumar, D., Burns, E. J., Nadeau, M., Dake, B., Laroni, A., Kozoriz, D. et al.**, Activation of the aryl hydrocarbon receptor induces human type 1 regulatory T cell-like and Foxp3(+) regulatory T cells. *Nat. Immunol.* 2010. **11**: 846–853.

8 **Gagliani, N., Magnani, C. F., Huber, S., Gianolini, M. E., Pala, M., Licona-Limon, P., Guo, B. et al.**, Coexpression of CD49b and LAG-3 identifies human and mouse T regulatory type 1 cells. *Nat. Med.* 2013. **19**: 739–746.

9 **Okamura, T., Sumitomo, S., Morita, K., Iwasaki, Y., Inoue, M., Nakachi, S., Komai, T. et al.**, TGF-beta3-expressing CD4$^+$CD25(-)LAG3+ regulatory T cells control humoral immune responses. *Nat. Commun.* 2015. **6**: 6329. https://doi.org/10.1038/ncomms7329

10 **Geginat, J., Larghi, P., Paroni, M., Nizzoli, G., Penatti, A., Pagani, M., Gagliani, N. et al.**, The light and the dark sides of Interleukin-10 in immune-mediated diseases and cancer. *CytokineGrowth Factor Rev* 2016. **30**: 87–93.

11 **Cao, X., Cai, S. F., Fehniger, T. A., Song, J., Collins, L. I., Piwnica-Worms, D. R. and Ley, T. J.**, Granzyme B and perforin are important for regulatory T cell-mediated suppression of tumor clearance. *Immunity* 2007. **27**: 635–646.

12 **Hamann, D., Baars, P. A., Rep, M. H., Hooibrink, B., Kerkhof-Garde, S. R., Klein, M. R. and van Lier, R. A.**, Phenotypic and functional separation of memory and effector human CD8+ T cells. *J. Exp. Med.* 1997. **186**: 1407–1418.

13 **Geginat, J., Paroni, M., Facciotti, F., Gruarin, P., Kastirr, I., Caprioli, F., Pagani, M. et al.**, The CD4-centered universe of human T cell subsets. *Semin. Immunol.* 2013. **25**: 252–262.

14 **Cheroutre, H. and Husain, M. M.**, CD4 CTL: living up to the challenge. *Semin. Immunol.* 2013. **25**: 273–281.

15 **Neumann, C., Heinrich, F., Neumann, K., Junghans, V., Mashreghi, M. F., Ahlers, J., Janke, M. et al.**, Role of Blimp-1 in programing Th effector cells into IL-10 producers. *J. Exp. Med.* 2014. **211**: 1807–1819.

16 **Pot, C., Jin, H., Awasthi, A., Liu, S. M., Lai, C. Y., Madan, R., Sharpe, A. H. et al.**, Cutting edge: IL-27 induces the transcription factor c-Maf, cytokine IL-21, and the costimulatory receptor ICOS that coordinately act together to promote differentiation of IL-10-producing Tr1 cells. *J. Immunol.* 2009. **183**: 797–801.

17 **Zhang, P., Lee, J. S., Gartlan, K. H., Schuster, I. S., Comerford, I., Varelias, A., Ullah, M. A. et al.**, Eomesodermin promotes the development of type 1 regulatory T (TR1) cells. *Sci. Immunol.* 2017. **2**. pii: eaah7152. https://doi.org/10.1126/sciimmunol.aah7152

18 **Karwacz, K., Miraldi, E. R., Pokrovskii, M., Madi, A., Yosef, N., Wortman, I., Chen, X. et al.**, Critical role of IRF1 and BATF in forming chromatin landscape during type 1 regulatory cell differentiation. *Nat. Immunol.* 2017. **18**: 412–421.

19 **Jankovic, D., Kullberg, M. C., Feng, C. G., Goldszmid, R. S., Collazo, C. M., Wilson, M., Wynn, T. A. et al.**, Conventional T-bet(+)Foxp3(-) Th1 cells are the major source of host-protective regulatory IL-10 during intracellular protozoan infection. *J. Exp. Med.* 2007. **204**: 273–283.

20 **O'Garra, A. and Vieira, P.**, T(H)1 cells control themselves by producing interleukin-10. *Nat. Rev. Immunol.* 2007. **7**: 425–428.

21 **Levings, M. K., Sangregorio, R., Galbiati, F., Squadrone, S., de Waal Malefyt, R. and Roncarolo, M. G.**, IFN-alpha and IL-10 induce the differentiation of human type 1T regulatory cells. *J. Immunol.* 2001. **166**: 5530–5539.

22 **Levings, M. K., Gregori, S., Tresoldi, E., Cazzaniga, S., Bonini, C. and Roncarolo, M. G.**, Differentiation of Tr1 cells by immature dendritic cells requires IL-10 but not CD25+CD4+ Tr cells. *Blood* 2005. **105**: 1162–1169.

23 **Geginat, J., Nizzoli, G., Paroni, M., Maglie, S., Larghi, P., Pascolo, S. and Abrignani, S.**, Immunity to pathogens taught by specialized human dendritic cell subsets. *Front. Immunol.* 2015. **6**: 527. https://doi.org/10.3389/fimmu.2015.00527

24 **Ito, T., Yang, M., Wang, Y. H., Lande, R., Gregorio, J., Perng, O. A., Qin, X. F. et al.**, Plasmacytoid dendritic cells prime IL-10-producing T regulatory cells by inducible costimulator ligand. *J. Exp. Med.* 2007. **204**: 105–115.

25 **Haringer, B., Lozza, L., Steckel, B. and Geginat, J.**, Identification and characterization of IL-10/IFN-gamma-producing effector-like T cells with regulatory function in human blood. *J. Exp. Med.* 2009. **206**: 1009–1017.

26 **Facciotti, F., Gagliani, N., Haringer, B., Alfen, J. S., Penatti, A., Maglie, S., Paroni, M. et al.**, IL-10-producing forkhead box protein 3-negative regulatory T cells inhibit B-cell responses and are involved in systemic lupus erythematosus. *J. Allergy Clin. Immunol.* 2016. **137**: 318–321 e5.

27 **Alfen, J. S., Larghi, P., Facciotti, F., Gagliani, N., Bosotti, R., Paroni, M., Maglie, S. et al.**, Intestinal IFN-gamma-producing Tr1-cells co-express CCR5 and PD-1, and down-regulate IL-10 in the inflamed gut of IBD patients. *J. Allergy Clin. Immunol.* 2018. **142**:1537–1547.

28 **Cosmi, L., Annunziato, F., Galli, M. I. G., Maggi, R. M. E., Nagata, K. and Romagnani, S.**, CRTH2 is the most reliable marker for the detection of circulating human type 2 Th and type 2T cytotoxic cells in health and disease. *Eur. J. Immunol.* 2000. **30**: 2972–2979.

29 **Rivino, L., Messi, M., Jarrossay, D., Lanzavecchia, A., Sallusto, F. and Geginat, J**, Chemokine receptor expression identifies Pre-T helper (Th)1, Pre-Th2, and nonpolarized cells among human CD4+ central memory T cells. *J. Exp. Med.* 2004. **200**: 725–735.

30 **Pearce, E. L., Mullen, A. C., Martins, G. A., Krawczyk, C. M., Hutchins, A. S., Zediak, V. P., Banica, M. et al.**, Control of effector $CD8^+$ T cell function by the transcription factor Eomesodermin. *Science* 2003. **302**: 1041–1043.

31 **Lino, C. N. R., Barros-Martins, J., Oberdorfer, L., Walzer, T. and Prinz, I.**, Eomes expression reports the progressive differentiation of IFN-gamma-producing Th1-like gammadelta T cells. *Eur. J. Immunol.* 2017. **47**: 970–981.

32 **Carty, S. A., Koretzky, G. A. and Jordan, M. S.**, Interleukin-4 regulates eomesodermin in $CD8^+$ T cell development and differentiation. *PLoS One* 2014. **9**: e106659.

33 **Atreya, I., Schimanski, C. C., Becker, C., Wirtz, S., Dornhoff, H., Schnurer, E., Berger, M. R. et al.**, The T-box transcription factor eomesodermin controls CD8T cell activity and lymph node metastasis in human colorectal cancer. *Gut* 2007. **56**: 1572–1578.

34 **Takemoto, N., Intlekofer, A. M., Northrup, J. T., Wherry, E. J. and Reiner, S. L.**, Cutting Edge: IL-12 inversely regulates T-bet and eomesodermin expression during pathogen-induced $CD8^+$ T cell differentiation. *J. Immunol.* 2006. **177**: 7515–7519.

35 **Nizzoli, G., Krietsch, J., Weick, A., Steinfelder, S., Facciotti, F., Gruarin, P., Bianco, A. et al.**, Human $CD1c^+$ dendritic cells secrete high levels of IL-12 and potently prime cytotoxic T cell responses. *Blood* 2013. **122**: 932–942.

36 **Kassner, N., Krueger, M., Yagita, H., Dzionek, A., Hutloff, A., Kroczek, R., Scheffold, A. et al.**, Cutting edge: plasmacytoid dendritic cells induce IL-10 production in T cells via the Delta-like-4/Notch axis. *J. Immunol.* 2010. **184**: 550–554.

37 **Nizzoli, G., Larghi, P., Paroni, M., Crosti, M. C., Moro, M., Neddermann, P., Caprioli, F. et al.**, IL-10 promotes homeostatic proliferation of human CD8(+) memory T cells and, when produced by CD1c(+) DCs, shapes naive CD8(+) T-cell priming. *Eur. J. Immunol.* 2016. **46**: 1622–1632.

38 **Kastirr, I., Crosti, M., Maglie, S., Paroni, M., Steckel, B., Moro, M., Pagani, M. et al.**, Signal strength and metabolic requirements control cytokine-induced Th17 differentiation of uncommitted human T Cells. *J. Immunol.* 2015. **195**: 3617–3627.

39 **Steinfelder, S., Floess, S., Engelbert, D., Haeringer, B., Baron, U., Rivino, L., Steckel, B. et al.**, Epigenetic modification of the human CCR6 gene is associated with stable CCR6 expression in T cells. *Blood* 2011. **117**: 2839–2846.

40 **Rivino, L., Gruarin, P., Haringer, B., Steinfelder, S., Lozza, L., Steckel, B., Weick, A. et al.**, CCR6 is expressed on an IL-10-producing, autoreactive memory T cell population with context-dependent regulatory function. *J. Exp. Med.* 2010. **207**: 565–577.

41 **Lim, H. W. and Kim, C. H.**, Loss of IL-7 receptor alpha on $CD4^+$ T cells defines terminally differentiated B cell-helping effector T cells in a B cell-rich lymphoid tissue. *J. Immunol.* 2007. **179**: 7448–7456.

42 **Desreumaux, P., Foussat, A., Allez, M., Beaugerie, L., Hebuterne, X., Bouhnik, Y., Nachury, M. et al.**, Safety and efficacy of antigen-specific regulatory T-cell therapy for patients with refractory Crohn's disease. *Gastroenterology* 2012. **143**: 1207–1217 e1–e2.

43 **Bacchetta, R, Lucarelli, B, Sartirana, C, Gregori, S, Lupo Stanghellini M. T., Miqueu P, Tomiuk, S. et al.**, Immunological outcome in haploidentical-HSC transplanted patients treated with IL-10-anergized donor T Cells. *Front. Immunol.* 2014. **5**: 16. https://doi.org/10.3389/fimmu.2014.00016

44 **Ichiyama, K., Sekiya, T., Inoue, N., Tamiya, T., Kashiwagi, I., Kimura, A., Morita, R. et al.**, Transcription factor Smad-independent T helper 17 cell induction by transforming-growth factor-beta is mediated by suppression of eomesodermin. *Immunity* 2011. **34**: 741–754.

45 **Clemente-Casares, X., Blanco, J., Ambalavanan, P., Yamanouchi, J., Singha, S., Fandos, C., Tsai, S. et al.**, Expanding antigen-specific regulatory networks to treat autoimmunity. *Nature* 2016. **530**: 434–440.

46 **Mazzoni, A., Maggi, L., Siracusa, F., Ramazzotti, M., Rossi, M. C., Santarlasci, V., Montaini, G. et al.**, Eomes controls the development of Th17-derived (non-classic) Th1 cells during chronic inflammation. *Eur. J. Immunol.* 2018. https://doi.org/10.1002/eji.201847677

47 **Gagliani, N., Vesely, M. C., Iseppon, A., Brockmann, L., Xu, H., Palm, N. W., de Zoete, M. R. et al.**, Th17 cells transdifferentiate into regulatory T cells during resolution of inflammation. *Nature* 2015. **523**: 221–225.

48 **Jiang, W., Chai, N. R., Maric, D. and Bielekova, B.**, Unexpected role for granzyme K in CD56bright NK cell-mediated immunoregulation of multiple sclerosis. *J. Immunol.* 2011. **187**: 781–790.

49 **Humphreys, N. E., Xu, D., Hepworth, M. R., Liew, F. Y. and Grencis, R. K.**, IL-33, a potent inducer of adaptive immunity to intestinal nematodes. *J. Immunol.* 2008. **180**: 2443–2449.

50 **Cossarizza, A., Chang, H. D., Radbruch, A., Akdis, M., Andra, I., Annunziato, F., Bacher, P. et al.**, Guidelines for the use of flow cytometry and cell sorting in immunological studies. *Eur. J. Immunol.* 2017. **47**: 1584–1797.

Abbreviations: **GvHD**: graft-versus-host disease · **IBDs**: inflammatory bowel diseases

Full correspondence: Dr. Jens Geginat 1INGM-National Institute of Molecular Genetics "Romeo ed Enrica Invernizzi", Milan, Italy
e-mail: geginat@ingm.org

See accompanying Commentary:
https://onlinelibrary.wiley.com/doi/10.1002/eji.201848000

Received: 28/5/2018
Revised: 28/9/2018
Accepted: 9/11/2018
Accepted article online: 15/11/2018

Ringraziamenti

Oggi si conclude una piccola parte della mia vita.
Giunta al traguardo finale, non posso che ripercorrere mentalmente gli anni passati.
Il PhD è una costante sfida con sé stessi, che comporta sacrificio e dedizione; durante questi anni ci sono stati momenti difficili, che mi hanno insegnato ad andare avanti senza perdere la forza di volontà. Non arrendersi, non abbattersi, non lasciarsi sopraffare dalle sconfitte sono le cose che ho effettivamente imparato, quasi senza accorgermene.
Il dottorato forma il carattere oltre che la mente, mai una frase è stata più vera di questa.
Nonostante ci siano stati diversi momenti in cui mi sono sentita sola, mentirei se dicessi che quei sentimenti ripecchiavano la realtà. Non sarei qui oggi se non ci fossero state al mio fianco le persone che ad oggi posso effettivamente considerare una parte fondamentale di tutto il mio percorso.
Prima di tutti, la mia famiglia, da sempre un supporto costante e sicuro. Sono fortunata ad avervi e lo so.
Voi ragazzi del 113, un insostituibile sostegno: Tanya, mia amica fidata e costante ormai da anni, non penso di dover aggiungere altro; Maria Lucia, la prima che ho conosciuto ormai quasi 4 anni fa. Mi hai sempre difeso e mi sei sempre stata vicina; Ramona, quella buona e sempre pronta a spendere una buona parola per me anche, forse, quando non me lo meritavo; Mariangela, una continua fonte di sapere e di sostegno; Valeria, un' incredibile scoperta professionale e soprattutto personale; Federica, una 113 acquisita, il tuo aiuto e il confronto con te sono stati preziosi; Chiara, anche se la vita ti ha portato a fare scelte diverse, sono contenta di questi ultimi mesi passati insieme, sei stata di un supporto fondamentale; l'ultimo, ma non per importanza: Stefano, un fratello e un uomo d'altri tempi, pronto ad aiutarmi in qualsiasi momento. Ragazzi, siete tutti favolosi!
Alessia e Claudia che pur intraprendendo strade diverse, siete sempre rimaste nello spirito del laboratorio, anche da lontano siete presenti e siete state una mia certezza durante questi anni.
Paola, mia tutor e anche amica ormai; grazie per avermi sempre sostenuta e difesa, sempre.
Tutti gli altri membri del laboratorio e dell'istituto che in un modo o nell'altro mi hanno aiutata a crescere e a sopravvivere questi anni: Stefania, Chiara, Sabrina, Lorenzo, Marco, Serena. A voi, grazie.

Ilaria, come una sorella ormai, che mi sopporta da anni tutte le sere senza lamentarsi mai.
Infine, niente sarebbe stato possibile senza le mie persone, che da sempre mi sostengono e fanno il tifo per me: Giulia, Anna, Stefania, Valentina, Michela, Lorenzo, Mattia, Gabriele e Umberto.

A tutti voi,
Grazie